Faculty of Mechanical Engineering
Department of Automotive, Combustion Engine and Railway Engineering

Master's Thesis

TWO-LEVEL ENERGY MANAGEMENT STRATEGY FOR HYBRID ELECTRIC VEHICLE USING PLANNED-TRIP INFORMATION

Dvouúrovňová řídící strategie pro hybridní vozidlo s využitím informací o plánované trase

Jan Soukup

Study programme
(N2301) Mechanical Engineering

Branch of study
(2301T047) Transportation, Aerospace and Handling Technology

Supervisor
Ing. Rastislav Toman

Prague, July 2021

MASTER'S THESIS ASSIGNMENT

I. Personal and study details

Student's name: **Soukup Jan** Personal ID number: **459619**

Faculty / Institute: **Faculty of Mechanical Engineering**

Department / Institute: **Department of Automotive, Combustion Engine and Railway Engineering**

Study program: **Mechanical Engineering**

Branch of study: **Transportation, Aerospace and Handling Technology**

II. Master's thesis details

Master's thesis title in English:

Two-Level Energy Management Strategy for Hybrid Electric Vehicle Using Planned-Trip Information

Master's thesis title in Czech:

Dvouúrovňová řídící strategie pro hybridní vozidlo s využitím informací o plánované trase

Guidelines:

1. Analyse the current state of hybrid electric vehicle control and energy management strategies.
2. Focus on parallel HEV configuration.
3. Design an energy management strategy with close-to-optimal results using trip information.
4. Validate the strategy on a created vehicle model.
(Thesis will be submitted in English language)

Bibliography / sources:

Name and workplace of master's thesis supervisor:

Ing. Rastislav Toman, Department of Automotive, Combustion Engine and Railway Engineering, FME

Name and workplace of second master's thesis supervisor or consultant:

Date of master's thesis assignment: **14.04.2021** Deadline for master's thesis submission: **14.07.2021**

Assignment valid until: **19.09.2021**

Ing. Rastislav Toman	doc. Ing. Oldřich Vítek, Ph.D.	prof. Ing. Michael Valášek, DrSc.
Supervisor's signature	Head of department's signature	Dean's signature

III. Assignment receipt

The student acknowledges that the master's thesis is an individual work. The student must produce his thesis without the assistance of others, with the exception of provided consultations. Within the master's thesis, the author must state the names of consultants and include a list of references.

. | Date of assignment receipt

Student's signature

Declaration

I declare that the following work has not been previously submitted for the award of any other degree. The entirety of the research and work has been carried out by me under the supervision and guidance of Rastislav Toman and, to the best of my knowledge, does not contain any material previously published or written by another person, except where due reference has been made in the text.

July 8, 2021

_____

Jan Soukup

Acknowledgements

Thanks to my supervisor, Rastislav Toman, for his guidance, prompt support and useful advice in the past two years, and for giving me freedom to pursue different ideas that ultimately resulted in the following work.

Abstract

Hybrid electric vehicles are currently used as a way of improving fuel consumption and consequent carbon dioxide emissions of conventional vehicles powered by an internal combustion engine and as means for paving the way for fully electric vehicles. To exploit their potential to the biggest extent by using energy more efficiently, energy management strategies are employed to control whether a torque request will be met by the internal combustion engine, the electric motor, or their combination. Numerous smart strategies have been proposed in literature to improve on strategies based on heuristics used in passenger vehicles today. Strategies based on optimisation taking into account characteristics of the current trip tend to perform better than others. According to this, a strategy taking into account predicted or past information about planned trip has been designed. The strategy is composed of two levels, where the higher level generates reference battery-state-of-charge trajectory before a trip, which is subsequently tracked by the lower level in real-time. The reference is generated from predicted speed and elevation profile of the planned trip using Pontryagin's minimum principle optimisation on a simplified vehicle model. This optimisation also results in a reference equivalence factor trajectory, which is then used for real-time control. The strategy was tested on several routes and vehicles with three levels of electrification. The results were then compared to a common heuristic strategy and optimal solution using dynamic programming. Improvements ranging between 1-5 % were achieved in full hybrid vehicle application and 3-4 % in plug-in hybrid vehicle application. Mild hybrid vehicle achieved only negligible improvements around 1 %.

Keywords: *Energy Management Strategy*, *Hybrid Electric Vehicle*, *Prediction*, *Optimisation*, *Pontryagin's Minimum Principle*

Anotace

Hybridní pohon slouží ke snížení spotřeby paliva a výsledných emisí oxidu uhličitého u konvenčních vozidel poháněných spalovacím motorem a jako cesta k jejich úplné elektrifikaci. Aby byl co nejlépe využit potenciál tohoto pohonu co nejefektivnějším využitím energie, je nutné implementovat řídící strategii, která rozhoduje, zda požadovaný točivý moment bude vyprodukován spalovacím motorem, elektromotorem, nebo jejich kombinací. V literatuře jsou uváděny nejrůznější strategie, které mají dosahovat lepších výsledků než heuristické strategie běžně užívané v osobních automobilech, založené na intuitivních pravidlech. Strategie založené na optimalizaci, využívající charakteristické rysy jízdy, obecně dosahují lepších výsledků než ostatní. Na základě těchto poznatků byla navržena řídící strategie využívající informace o plánované trase. Skládá se ze dvou úrovní, kde vyšší úroveň před jízdou vygeneruje referenční průběh stavu nabití baterie, který je pak nižší úrovní sledován během jízdy. Tento průběh je vygenerován z předpokládaného rychlostního profilu a výškového profilu trasy optimalizačním algoritmem na základě Pontryaginova principu minima aplikovaného na zjednodušený model vozidla. Výsledkem je zároveň průběh součinitele ekvivalence, pomocí kterého je uskutečněno real-time řízení při jízdě. Strategie byla otestována na několika trasách a vozidlech se třemi úrovněmi elektrifikace. Výsledky byly následně porovnány s běžnou heuristickou řídící strategií a optimálním řešením dynamického programování. Implementací na full hybrid vozidle bylo dosaženo zlepšení 1-5 % a na plug-in hybrid vozidle 3-4 %. U mild hybrid vozidla pak bylo dosaženo pouze zanedbatelných zlepšení kolem 1 %.

Klíčová slova: *Řídicí strategie*, *Hybridní vozidlo*, *Predikce*, *Optimalizace*, *Pontryaginův princip minima*

CONTENTS

Chapter 1

INTRODUCTION

Due to the steep increase of cumulative carbon dioxide (CO_2) emissions contributing to the greenhouse effect in the past decades, extensive changes in human mobility and transportation are underway. Because carbon dioxide emissions are directly dependent on fuel consumption, one of the main efforts in ground-vehicle development to combat this is in the form of making the powertrain more efficient. The general trend is using electric machines (EM) in lieu of internal combustion engines (ICE), allowing higher well-to-wheel efficiency and usage of other energy sources than fossil fuels. This, however, creates a challenge with onboard energy storage, as most vehicles cannot be permanently connected to the grid. Since electricity storage is a costly and resource-demanding matter on its own, not all applications are a suitable subject to electrification.

Hybrid electric vehicles (HEV)—vehicles combining internal combustion engine system with electric propulsion system—are supposed to incorporate the best of both worlds to improve conventional ICE powertrain efficiency while reducing the amount of electric energy that needs to be stored, most commonly electrochemically in the form of batteries. One of the main problems of the internal combustion engine is its inability to recuperate acquired kinetic energy instead of dissipating it when a vehicle needs to be braked. This makes hybrid vehicles even with small battery capacity effective, as they require minimal additional cost and weight while attaining noticeable fuel savings thanks to energy recuperation. Because the efficiency of an EM does not vary as much over its operating range, an additional benefit is using it in place of the ICE at operating points where the efficiency of the ICE would be very low.

Two propulsion systems however result in increased complexity in powertrain control, adding another degree of freedom in terms of power delivery. Naturally, deciding when to shift from one energy source to the other cannot be left to the driver, and therefore an automatic control strategy needs to be implemented to achieve optimal fuel savings while keeping the battery charge within desired bounds.

As the first mass-produced HEV was released in 1997 [1], these *energy management strategies* (EMS) began as a simple control logic based on rules, taking into account only the instantaneous vehicle state—such as required torque, *state of charge* (SOC) and vehicle speed—to decide how to divide the torque request from the driver between EM and ICE [2]. As technology advanced, EMSs have gradually grown to be more complex, incorporating not only the current state of the vehicle, but also past, present and predicted future data about the current trip.

Ideally, to optimally split work between the EM and the ICE over an entire vehicle trip,

the exact speed and route elevation profile as a function of time would have to be known in advance. In other words, knowing the exact operating points of the engine along with route sections, where recuperation is possible, to assess how much electrical energy can be utilised and when it is the best moment to do so. Naturally, this is not possible to know exactly, as every driver controls the speed of a vehicle with a certain level of unpredictability. This issue can be minimised with autonomous vehicles which track a predefined route and speed profile. However, a predefined profile is still subject to ad hoc modifications conforming to real-time road conditions.

Even with potential perfect knowledge of a driving trip in advance, an optimal power split at every point cannot be computed with currently available technology in a reasonable time to be used in real driving conditions. Tasks like these are usually calculated when there are no time constraints, to be used as a benchmark for a real-time control strategy from past trip data, or as a tool to get insight into how changing certain vehicle parameters affects its performance.

The thesis aims to explore the potential of efficiently using available information about the whole trip to attain close-to-optimal results in real-time, attempting to address the aforementioned challenges. A predefined route with its elevation profile and a predicted speed profile, which can be obtained from past data, or constraints such as legal speed limits, traction limits and current traffic conditions, will be used. The generation of this speed profile prediction is not part of the work presented in this thesis.

The main approach is dividing the control logic into two levels, where the higher level analyses the whole trip from the prediction to generate reference values of SOC for the lower level to adhere to and track in real-time. All of the simulations are written using *Python*.

The structure of the thesis is as follows; Chapter 2 lays the foundation for the issues addressed over the entire thesis–Section 2.1 is devoted to a brief introduction to the topic of hybrid electric vehicles in general. Afterwards, in Section 2.2, HEV energy management strategies are discussed in more detail to expand on the objective and the contribution of this thesis, which is then finally formulated in Section 2.3. After that, in Chapter 3, the main part containing the actual control strategy design is presented, followed by results in Chapter 4 and conclusions and future work suggestions in Chapter 5.

Chapter 2

BACKGROUND

The definition of a *hybrid vehicle* is a vehicle with multiple sources of energy. Most often two, in the form of an ICE-propulsion system complemented by an alternative source of energy. Noteworthy representatives of these are electricity stored in a battery or a supercapacitor, kinetic energy stored in a flywheel, or potential energy stored in compressed air.

Even though fossil fuels as the main energy source are most often used, fuel-cell-based hybrid vehicles with batteries or supercapacitors also exist. For more information about types of hybrid propulsion systems, the reader is directed to Chapter 4, 5 and 6 of [3].

As this thesis deals with control of hybrid *electric* vehicles, from now on, only the ICE-battery combination—which is also the most common—will be discussed. In the following section, HEV principles will be described along with nomenclature to create a basis for the rest of the thesis. After that, methods of HEV energy management control and the current state will be explored in more detail, focusing especially on parallel hybrid vehicles.

2.1 HYBRID ELECTRIC VEHICLES

The main components of a HEV powertrain are the ICE and the EM to deliver power; a fuel tank for the ICE and a battery for the EM as an energy storage. Then, similarly as a conventional ICE needs a fuel management system to deliver the correct amount of fuel according to the required output, an electric powertrain needs a control system in the form of a power inverter to, simply put, manage current flowing between the battery and electric motor. Naturally, there are numerous other components to facilitate the proper function of the powertrain, however, these are out of scope for the purposes of this thesis.

Based on the specifications and configuration of the aforementioned components, there are several ways to classify hybrid electric vehicles. The classes are however purely conventional, because their boundaries are not clearly distinct or normalized in any way. One can therefore come across different nomenclature depending on the source.

The two main ways of classifying HEVs are based on:

- how much energy or power is provided by the electric part of the powertrain compared to the ICE, also known as *degree of electrification*,
- configuration of the powertrain, also known as *topology*.

Both of these will be discussed more in-depth in the following sections.

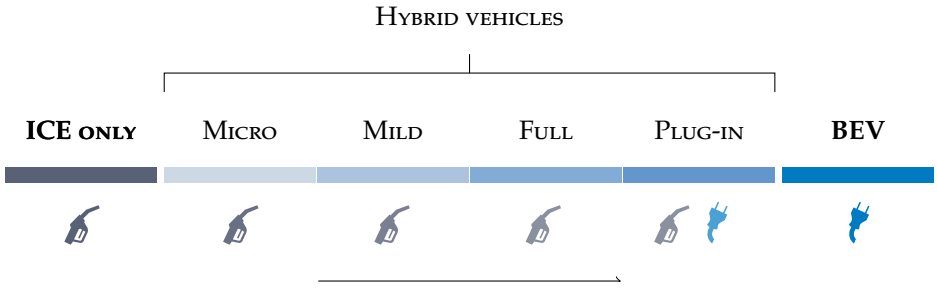

Figure 2.1 Degree of electrification

2.1.1 Degree of Electrification

The approximate electrification spectrum is illustrated in Figure 2.1. At the opposite ends are two extremes – ICE powertrain, using fossil fuel only, and *battery electric vehicle* (BEV), using electricity only. Anything inbetween is a hybrid electric vehicle using both energy sources to a certain extent. Based on the share of electricity usage, HEVs are conventionally divided into four following groups:

1. *Micro* hybrid vehicle,
2. *Mild* hybrid vehicle, usually regarded as *MHEV*,
3. *Full* hybrid vehicle, usually regarded as *HEV*,
4. *Plug-in* hybrid vehicle, usually regarded as *PHEV*[1].

Of these, only a plug-in hybrid vehicle can be charged from the grid. The other types rely on the ICE or energy recuperation to keep the battery charged. In general, the further a vehicle is on this spectrum, the larger battery and the more powerful electric motor it has.

Micro Hybrid

Micro hybrid vehicle is a conventional ICE vehicle augmented with a *Start & Stop* system, allowing to shut down the ICE automatically when idling at a stop (or at very low speed before stopping), and rapidly restart it again before accelerating, thereby technically saving fuel that would otherwise be wasted by engine operating without load. In this case, the label *hybrid* might be counterintuitive, as these vehicles are not capable of providing electric driving torque, but only have an adapted electric system to facilitate frequent engine starts.

There are clear fuel-saving improvements in simulations and dynamometer tests, however, the effectiveness of this system decreases significantly in real-world driving, especially with the operation of air-conditioning, reducing the time the engine is actually off [4, 5].

Mild Hybrid

Mild hybrid vehicles are also generally not capable of pure electric driving, as the EM does not have sufficient power. However, it can both provide drive torque to assist the ICE and recuperate energy. These vehicles usually have a higher voltage 48 V system alongside

[1]The abbreviation PHEV is sometimes used to refer to a *parallel* hybrid electric vehicle (classification based on topology; further information in Section 2.1.2).

or instead of the regular 12 V one. The EM acts as a starter-generator, either belt-driven (BSG) or crankshaft-mounted (CSG). Since the starter-generator allows switching off the engine even during higher-speed coasting, essential systems such as power steering, brake boosting and air-conditioning have to be powered by an electric motor instead of the ICE.

Even with small battery capacity and EMs with limited power, mild hybrid vehicles can achieve significant fuel consumption reduction, generally in the range of 8-25 % [6]—depending on the driving conditions—at little additional weight and cost.

Full Hybrid

Unlike micro and mild hybrid vehicles, full hybrid vehicles are able to use electric power for pure electric driving. Their batteries are still relatively small and therefore pure electric range is only several kilometres. Because of this and the fact that the battery cannot be charged from the grid, the EM driving is mostly used just to take over operation from the ICE at lower speeds and loads, where the thermal efficiency is very low.

Depending on the trip type and driving style, fuel savings in the range of 20-50 % [7, 8, 9] can be typically achieved. The higher savings correspond to city driving, where the low-speed EM operation combined with regenerative braking is particularly effective, while the additional weight to the conventional vehicle counterpart is only around 100 kg.

Plug-in Hybrid

In terms of electric power, plug-in hybrid vehicles are very similar to full hybrid vehicles, being capable of fully electric driving. However, their battery is several times larger, allowing them to cover a driving range usually around 30 km [10]. This means that plug-in hybrid vehicles can be operated as a purely-electric vehicle in short-distance driving, such as around the city. Using a plug-in hybrid solely for this type of driving is not ideal, because the vehicle has effectively two powertrains, making it rather heavy. This is amplified by the fact that hybrid vehicles aren't usually designed and optimised from the ground up, but as a modification to an existing ICE powertrain.

Whereas previous hybrid vehicle configurations used electric power as a way of making the conventional powertrain more efficient, because any electric charge consumed must be either recuperated or created by the ICE, plug-in hybrids can be recharged from the grid, effectively introducing new energy source into the system. Fuel savings are therefore greatly dependent on the frequency of recharging.

Non-plug-in hybrid vehicles—which cannot be charged from the grid—are therefore driven in a *charge-sustaining* mode (Fig. 2.2a), where the battery SOC is allowed to only fluctuate around a certain value, usually 70 %, which means that SOC at the end of the trip should be ideally the same as at the beginning. Whereas plug-in hybrid vehicles may use up a larger part of the battery – from full charge at around 90 % to 30 %. Typically[2], the vehicle is driven as a BEV until the battery is depleted, known as *charge-depleting* mode, after which they are either recharged from the grid, or driven in charge-sustaining mode, before being charged from the grid again (Fig. 2.2b).

[2]Because the fuel economy of a plug-in hybrid being driven in CD/CS mode is not ideal in terms of its full potential, the efforts in PHEV are to avoid battery depletion until the very end of the trip, to take full advantage of available battery charge, but avoid charge-sustaining mode at a low SOC value. This type of battery discharging is known as *blended mode* [11, 12].

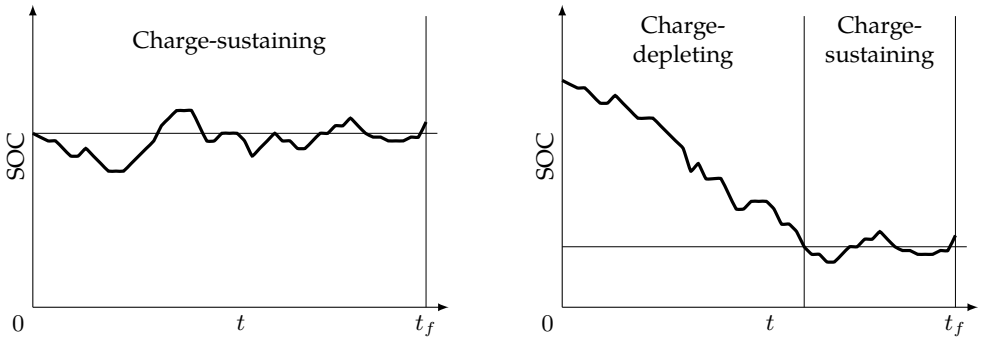

A Mild/Full hybrid

B Plug-in hybrid

Figure 2.2 Typical state of charge (SOC) trajectories along a trip

2.1.2 Topology

Another possible way of classifying HEVs is based on their powertrain configuration. In other words, how power flows from the energy source to wheels. A conventional ICE powertrain has mechanical linkages (shafts) from the engine, in the most common form, through clutch, gearbox and differential, to the wheels.

To take advantage of electric energy for propulsion, EMs have to be coupled to the powertrain alongside the ICE in a manner that allows simultaneous cooperation between these two systems. Based on the way this is achieved, the main HEV categories are:

- *Series* hybrid vehicles,
- *Parallel* hybrid vehicles,
- *Series-parallel* or *combined* hybrid vehicles.

Each of these is schematically illustrated in Figure 2.3.

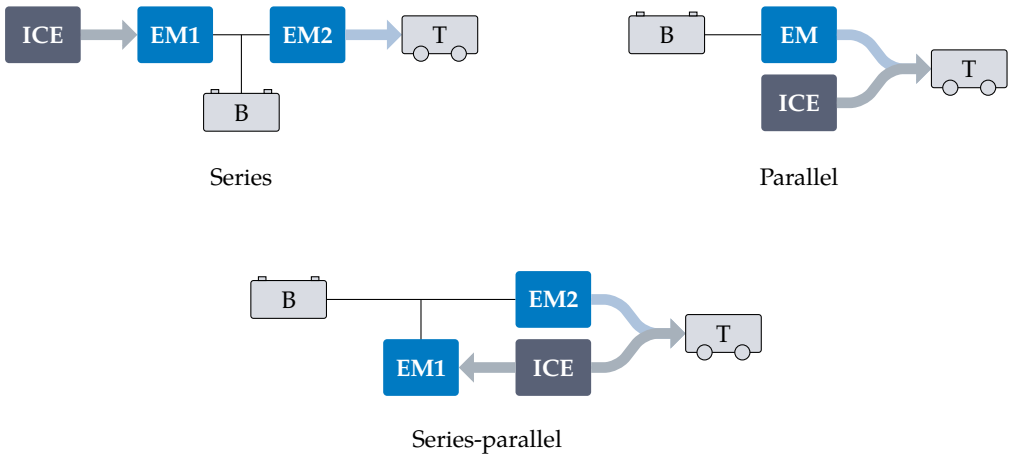

Figure 2.3 HEV topologies; thick lines: mechanical connection, thin lines: electrical connection, B: battery, T: traction. Fuel tank, inverters, clutches and gearboxes are not displayed for clarity.

Series

A series hybrid vehicle does not have a mechanical linkage between the ICE and the wheels, which means that traction power is facilitated by the EMs only. The ICE is connected to a generator, recharging the battery or directly providing energy for the traction motor. The traction motor can also recharge the battery during regenerative braking. Decoupling the ICE from the wheels is advantageous, as it can operate at a high-efficiency point, regardless of wheel speed and demanded power. This is to a certain extent negated by the efficiency of mechanical-electrical and subsequent electrical-mechanical energy conversion. This extent is determined by the operating point the ICE would be operating at during regular driving. In low-speed and low-sload driving—such as city driving—the efficiency would be low, and therefore even with double energy conversion, the efficiency of the series hybrid would still be higher than of the conventional powertrain. On the other hand, in other types of driving, the efficiency of the HEV becomes similar or even smaller than the one with a conventional powertrain, negating the benefits by having added cost and weight compared to an ICE-only powertrain.

Series hybrid vehicles are therefore mostly in the form of a plug-in hybrid vehicle with a small internal combustion engine acting as a *range-extender*, providing additional electricity if battery capacity isn't sufficient for a longer trip.

Parallel

In parallel hybrid vehicles, the EM or set of EMs is mechanically coupled to the ICE powertrain, thereby providing traction torque (power) in parallel with the ICE. The EM generally works both as a motor and a generator. Since both the ICE and the EM are linked to the speed of the wheels, neither can always operate at a point with their optimal efficiency. However, the drivetrain[3] efficiency is much higher than the series configuration counterpart, as there are fewer energy conversions – the coupling of EM and ICE is purely mechanical.

Depending on the position of the EM-coupling in the powertrain, there are several categories of parallel HEVs. These are illustrated in Figure 2.4. Longitudinal engine configuration in the schematic is used just for clarity – both longitudinal and transverse hybrid versions exist.

P0 hybrid, generally used only as a mild hybrid, uses a belt drive to connect the EM to the ICE. It is a cost-effective solution for hybridisation of an existing ICE-only powertrain, replacing the classic alternator. However, the belt drive has limited torque capacity and rotation of the EM cannot be decoupled from the ICE, reducing the efficiency of EM operation.

P1 hybrid has an EM directly mounted to the crankshaft. This configuration is also aimed at the lower end of the electrification spectrum (MHEV) as the power of the motor is limited by the installation dimensions, although it eliminates the belt drive torque issue. Similarly to P0, EM rotation cannot be decoupled from the ICE rotation. This configuration is rarely used, because the architecture changes needed are substantial, with little fuel efficiency improvement in return.

P2 hybrid has an EM connected between the ICE and transmission and, unlike in the previous two topologies, can be decoupled from the ICE using the clutch, thereby significantly improving purely-electric operation efficiency. Sometimes it is used before a dual-

[3] not including the engine combustion process

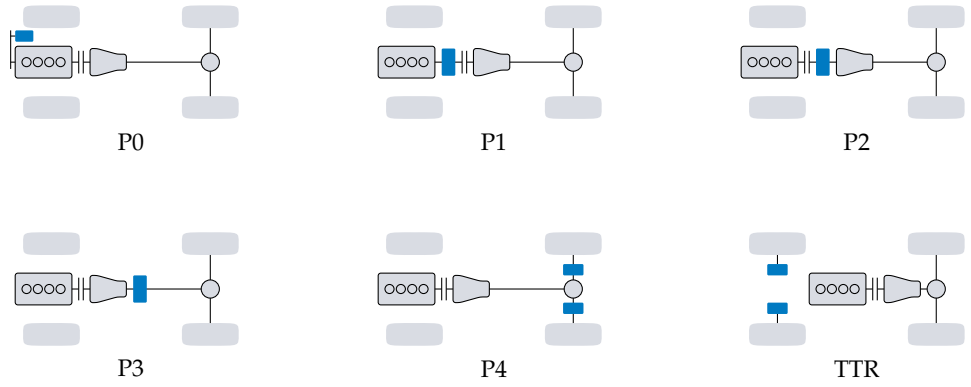

Figure 2.4 Parallel hybrid configurations; showing ICE, clutch, gearbox, differential and location of EM (in blue).

clutch transmission, making the EM decoupled from the gearbox as well. If that is not the case, the P2 (and subsequent P3 and P4) layout cannot provide the start-stop function of the engine, since it is coupled to the rotation of wheels, and another electric machine is required.

P3 hybrid has an EM connected to the output shaft of the gearbox or the differential. This means that the EM needs to cover a wide range of speed and torque and therefore is usually coupled through a single or planetary gear set. While this topology provides slightly better electric driveline efficiency than P2, generally, a more powerful EM is required to cover high torque requests.

P4 hybrid uses EMs mounted either on the axles or directly in wheels, meaning the electric driveline efficiency is the highest of all topologies. The in-wheel version especially also has a very large bandwidth in terms of torque-distribution control due to the minimum number of elastic members in the torque path, making it effective for performance and safety improvements using torque vectoring. This advantage is to some extent negated by the additional unsprung mass, which increases vertical load fluctuations, reducing road contact [13]. Similarly to the P3 configuration, the EMs need to cover wide speed and torque ranges. While versions with EMs coupled with ICE drivetrain are possible, this configuration is usually used as a separate unit, driving the other axle that is not connected to the ICE powertrain, also known as *through-the-road* (TTR) hybrid.

TTR (Through-the-road) hybrid is a configuration, in which one axle is powered by the ICE and the other by EM(s). In other words, this configuration decouples the two powertrains and uses the road as a torque coupler. Variations with ICE-driven front or rear axle exist. Motors can be in P3 or P4 configuration. The decoupling of powertrains makes it particularly effective for hybridisation of an existing conventional ICE-only vehicle. Resulting all-wheel-drive (AWD) capability can also improve safety and performance. However, the lack of mechanical connection between the ICE and EM reduces the operating mode possibilities, especially in terms of battery charging with the ICE [14].

Series-parallel

Also known as combined or power-split hybrid vehicles, these combine characteristics of both series and parallel hybrid configurations. Naturally, the intent is to preserve the advantageous characteristics (such as operating the engine at an arbitrary point irrespective

of instantaneous wheel speed and torque requirement) and suppress the disadvantageous (such as not having a direct mechanical link between ICE and the wheels when the operation efficiency is high).

This layout has two EMs, both able to act as a motor or a generator, however, one is primarily used as a motor-generator as in the parallel configuration and the other as a generator in the series configuration. The simultaneous connection of the ICE and these two EMs is in practice most often achieved with a planetary gear set, splitting torque between them according to the type of driving. Even though this configuration is a combination of the previous two, thanks to the planetary gearset, the powertrain can be made very simple, in its basic form without the need for clutches[4] or a gearbox. There are however some limits to the possibilities of power flow and not all characteristics of series and parallel HEVs can be achieved.

2.2 ENERGY MANAGEMENT STRATEGIES

In terms of finding the most fuel-efficient way of getting from a starting location to an end location with a HEV, there are technically three stages. The first is choosing the most energy-efficient route, also known as *eco-routing*. The second is finding the most energy efficient driving strategy (speed profile) along the route, also known as *eco-driving*. The required power at each instant is then defined by the vehicle speed and driving resistances. The last stage is splitting this power between the EM and the ICE to achieve optimal fuel consumption over the entire trip while keeping the battery SOC within predefined admissible bounds, also known as an *energy management strategy* (EMS).

While in the most ideal scenario, these three tasks would be coupled to obtain the absolute optimum, due to the complexity of such optimization[5], they are almost always—at least to some extent—decoupled. The focus of the following sections and this entire thesis is the last stage – energy management strategy.

Each of the topologies mentioned in Section 2.1.2 has slightly different possibilities and problems in terms of driving modes and splitting power, therefore their control strategies are different. In parallel hybrid vehicles, the only degree of freedom in terms of power delivery is torque-split between the ICE and the EM, as their angular speed is determined by the vehicle speed and cannot be controlled separately. Since this thesis deals with the parallel configuration, strategies in the following sections will be discussed mainly in terms of parallel HEVs. Nevertheless, a lot of principles and findings are universal.

An energy management controller in a HEV refers to a high-level supervisory powertrain controller determining operation of its individual components. In a conventional ICE vehicle, the torque requested by the driver (through the accelerator pedal) is provided by the ICE. In a HEV, this request can be met by either the EM, the ICE, or their combination. The aim of the controller is to determine, which power to use at each instant using an EMS. A block diagram of an energy management control loop in its most basic form is illustrated in Figure 2.5. It takes an input from the driver (or another higher-level controller) in the form of demanded torque T_d and based on available information such as the state of the vehicle x (battery SOC, vehicle speed, coolant temperature) outputs control signals u for lower-level controllers. These signals can be a combination of ICE torque, EM

[4] However, adding clutches can enable more driving modes. [15]

[5] Or due to the existence of constraints imposed by other factors than fuel consumption (predefined route, legal speed limits, traffic, driveability, comfort).

torque, engine on/off, clutch engagement, gear shift command, etc.

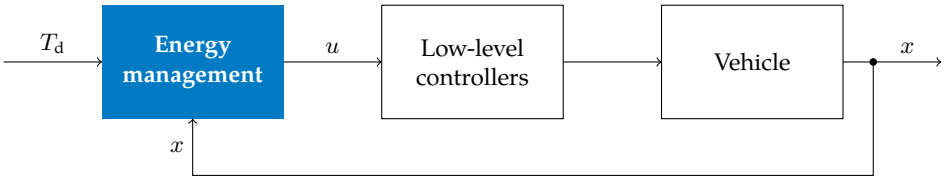

Figure 2.5 HEV supervisory controller block diagram

The arbitrary torque request is however decoupled from the EMS, making this basic form of HEV control *causal*, reacting only to past and current inputs. The problem is that there is no information about the total length of the trip or about future driving conditions (such as recuperation possibilities) to take into account, making the control suboptimal. Such control is referred to as *online* – implemented in real-time.

Noncausal control, on the other side of the spectrum, deals with actual optimisation based on the information of the entire trip (speed and elevation profiles). However, because it is too computationally demanding to be implemented in real-time and a speed profile is never perfectly known in advance, this type of optimisation is done *offline*, as a benchmark for online control strategies or another type of analysis[6].

Another possible criterion for EMS classification, loosely linked to the previous, is optimality. The simplest and most easy to implement (and therefore good candidates to be used online) strategies are based on predefined rules, derived from human intuition, experience or analyses results. The rules are generally formulated as which power is preferred for instantaneous propulsion based on the requested torque and current state of battery charge. These strategies are categorized as *heuristic*. While they are robust and easy to implement online, they are not optimisation techniques and therefore do not exploit the full potential of the system configuration.

The other category is optimisation-based strategies, where the control law is based on a mathematical model of the system, minimising defined performance measure (usually fuel consumption) subject to constraints (such as battery SOC) over a certain time interval. Therefore, to be used online, these strategies need more information about the trip than just instantaneous state of the vehicle – to find optimal control policy over a known or predicted time period. When the optimisation interval assumed is the whole trip, the control is noncausal and the optimisation typically takes place offline.

A tree structure of EMS classification is depicted in Figure 2.6. The two main classifications are loosely connected, because heuristic control is used only in causal cases and optimal solution can be obtained only in noncausal cases. However, using simplifications and predictions makes optimisation-based strategies applicable for causal online control as well, albeit with suboptimal results. The following sections will go over heuristic and optimization method principles and review the current state of research.

2.2.1 Heuristic Methods

This type of EMS is based on rules, hence also known as *rule-based*. The rules generally follow intuition, such as that the engine should be operated only when its efficiency is relatively high. Therefore during low speed and torque operation, electric-only propulsion

[6]Some online control strategies use patterns obtained from offline optimisation results as their basis.

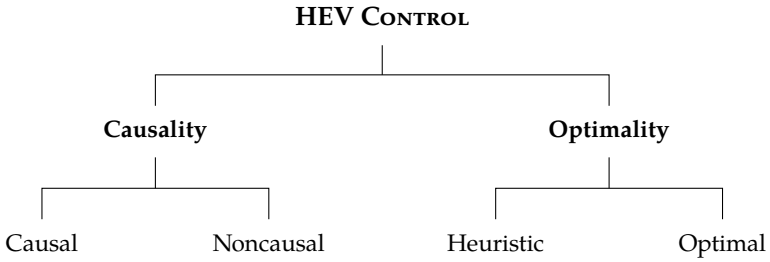

Figure 2.6 Tree structure showing EMS categorisation

is favoured, or the engine provides excess torque than it is demanded, with the rest of the generated power going into charging the battery. These strategies are either, in the most basic form, *deterministic* rule-based or, in the slightly more sophisticated form, *fuzzy logic* (FL) rule-based.

Deterministic methods are only composed of boolean expressions (true-false statements), whether variables such as demanded torque, battery SOC or vehicle speed are higher/lower than a certain threshold to determine which type of driving mode should be selected. The rules are in the IF-THEN form:

$$\textbf{If } x_1 \text{ is } A_1 \text{ and } x_2 \text{ is } A_2, \textbf{ then } u \text{ is } B. \tag{2.1}$$

where x_i are the input variables, A_i are their values and u are the output control signals and B their values. The first part before 'then' is called the *antecedent* and the second part the *consequent*. An example rule can be: "*If* SOC *is higher than* 60 % *and demanded torque lower than* 50 N m*, then electric-only propulsion is selected.*" No vehicle model or complex computations are therefore required. This makes the control fast and robust, which is the reason why such EMSs have been used since the beginning of HEVs for online control.

The aim is to attain desired vehicle behaviour (minimse fuel consumption, prevent excessive battery-ageing or ensure vehicle driveability) using an intuitive set of rules (hence heuristic methods), rather than explicit optimisation performance measure applied to a mathematical model. These rules are derived from acquired knowledge, experiments or results from optimisation analyses. Even though the resulting rules can be simple and easy to implement, their derivation and calibration procedure is usually a complex task.

However, the lack of optimisation character means that such methods cannot achieve optimal results, even with perfect knowledge of a trip, as the rules are predetermined. While a set of rules can be optimised to perform the best at specific driving conditions, it usually results in poor performance in other cases.

Fuzzy Logic

Rule-based control strategies can be made more flexible by using fuzzy logic in lieu of boolean logic, where instead of true (1) or false (0) values, a statement can have a truth value anywhere between 0 and 1 (hence the name *fuzzy*), which is more consistent with human reasoning and allows more flexibility in both control inputs and outputs.

Similarly as deterministic strategies, variables like battery SOC and demanded torque are taken as an input to a rule in the same form as in 2.1, however—in simple terms—instead of true-false only, each of the statements can have a value between 0 and 1 and the consequent is applied in an amount according to how true the statements are.

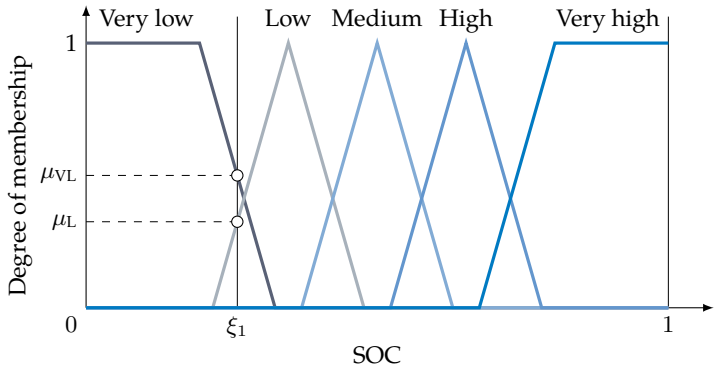

Figure 2.7 Fuzzification of a variable; showing degrees of membership μ of an arbitrary battery charge value ξ_1 to *Very low* and *Low* membership functions.

As an example: "*If a battery is high and the demanded torque is medium-high, torque supplied by the ICE is medium*". This linguistic classification of the magnitude of input variables, referred to as *fuzzification* process, is achieved using *membership functions* distributed along the admissible range of the variable. Each value of the variable then belongs to some extent (called *degree of membership* and ranging from 0 to 1) to each function. These functions are depicted in Figure 2.7 and are usually in the form of trapezoidal or triangular function.

There are two main fuzzy logic methods for how an output control signal is obtained from fuzzified inputs, also known as *defuzzification* – the Mamdani method [16] and the Takagi-Sugeno method [17]. Mamdani method uses membership functions for the output variable to get to a crisp number value, whereas Takagi-Sugeno directly calculates a crisp output number as a function of the degree of membership of the inputs. Both methods have been previously used for HEV EMS design. As an example, [18] uses Mamdani and [19] uses Takagi-Sugeno.

As a result, compared to deterministic rule-based control's binary character, fuzzy logic rule-based control can be more continuous. As an example, instead of switching to engine-only driving at a predefined SOC level, the ICE can gradually provide more torque (compared to the EM) as the SOC decreases. While using fuzzy logic this way can make the EMS more flexible and perform better, the rules are still based on intuition and do not follow optimal behaviour.

2.2.2 Optimisation Methods

As opposed to heuristic rule-based methods, optimisation methods are based on optimal control theory, minimising a predefined *performance measure*, with respect to the control variable $\mathbf{u}$, according to a mathematical model of the system described by state variables $\mathbf{x}$ and its constraints. The aim is to obtain *optimal control* $\mathbf{u^*}$ that minimises the performance measure, achieving optimal performance over a certain period. This is known as an optimal control problem.

The performance measure J, is in the general form

$$J(\mathbf{u}) = \int_{t_0}^{t_f} g(\mathbf{x}(t), \mathbf{u}(t), t)\, \mathrm{d}t \tag{2.2}$$

where g is a general penalty function up to the designer of the controller to define. In HEV

control, this can be simply the fuel-mass flow $\dot{m}_f$, minimising fuel consumption over a specified time interval. However, additional emissions [20], drivability (such as reducing frequent gear shifting or engine startups) [21] or battery-aging [22] behaviour can be implemented as well. The control variable **u** can be a combination of signals such as torque split between ICE and EM, gear shift signal or engine start/stop.

Because optimal behaviour does not equal minimising a performance measure at each instant, but over a predefined time interval, trip information has to be known to some extent for the strategy to perform well. In offline energy management control, the time t_0 in (2.2) is the initial time and t_f is the duration of the entire trip, minimising the performance globally. In online control strategies, t_0 is the current time and t_f the value of prediction horizon, optimising performance locally.

Once an optimal control problem is set up, numerous algorithms can be used to obtain solution. Some of the algorithms that have been used in the past in the field of HEV control are:

1. *Dynamic programming* (DP) [23, 24],
2. *Pontryagin's minimum princple* (PMP) [25, 24],
3. *Convex optimisation* (CO) [26, 27]
4. *Particle swarm optimisation* (PSO) [28],
5. *Genetic algorithm* (GA) [29].

The first three are used the most frequently, as their advantages (in terms of computational effort, introducing constraints and ease of modelling) make them suitable for HEV application and their analytical simplification can be used online with a reasonable amount of effort and accuracy.

Thanks to the discrete nature of dynamic programming, constraints and nonlinear behaviour are easily implemented. However, it requires large computational effort, especially when increasing the dimensions of the system. The nature of PMP and CO is analytical, which results in a more computationally-effective solution. However, simplifictions of the system usually have to be made, for example when introducing discrete behaviour such as gear shifting or engine on/off. This is especially true for CO, where the model has to be approximated by convex functions. *Equivalent consumption minimisation strategy* (ECMS), which is widely used in HEV control, along with its numerous variations, is also derived from PMP.

PSO and GA can both be considered evolutionary algorithms, as they use generated population to find the optimum. These algorithms are derivative-free, hence suitable to solve highly nonlinear, non-continuously-differentiable problems. While they can be used for solving the optimal control problem, their application for HEV EMS is limited, as they are not very suitable for online control, requiring a high number of iterations (and therefore longer computation time) for acceptable solution accuracy.

Dynamic programming and Pontryagin's minimum principle will be described in more detail in the following sections, as they are used later in this thesis.

Dynamic Programming

Dynamic programming is an optimisation method for obtaining optimal policy of a multi-stage decision process. The original derivation from 1954 is based on the intuition that no

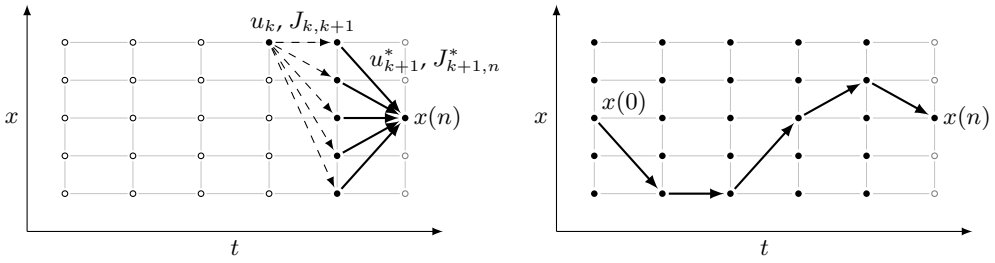

A Backward recursion

B Forward recursion

Figure 2.8 Dynamic programming procedure; bold arrows: optimal control, dashed arrows: admissible control.

matter what the current stage of the process is, there is an optimal policy (control), to reach the end stage from the current one. The exact formulation of this *principle of optimality* by the inventor, R. E. Bellman is:

> *An optimal policy has the property that whatever the initial state and initial decisions are, the remaining decisions must constitute an optimal policy with regard to the state resulting from the first decisions.* [30]

This means, that instead of starting from the beginning and calculating every possible state trajectory, starting at the end and going backwards, always calculating the optimal control from the current stage to the end, dramatically reduces the number of calculations.

This can be applied to HEV energy management, where each stage represents an instant of a driving trip where an optimal split is being decided and the goal is to reach a predefined value of state variable (such as SOC) in the final time. Each decision (control) at each stage has a certain cost associated with it (value of the performance measure function) and leads to a change of state in the next stage. The optimal control of this next stage and its cost have already been calculated in the previous step. This means that the decision with the lowest sum of the value of the performance measure corresponding to this decision and the value of the optimal performance measure required to reach the end from the following stage is the optimal control for this stage. The algorithmisation is schematically shown in Figure 2.8.

The time and state are discretised into a $n \times m$ grid where n is the number of stages (time of a trip) and m are the discretised state levels. Final level of state $x(n)$ that needs to be reached at the final time is determined and for each point of the grid, starting at the second to last stage, every admissible control u and its cost is calculated. If the control has a continuous nature, it needs to be discretised as well. The control u can be the torque of the EM, which then affects the SOC level at the next stage, as using EM will either charge or recharge the battery. The optimal decision u^* at each point is the control with the lowest value of the sum of its cost $J_{k,k+1}$ to get to the next stage $k+1$ and the optimal cost $J^*_{k+1,n}$ associated with getting from the point from the following stage $k+1$ to reach the end state $x(n)$. The mathematical formulation of this procedure can be written as

$$u^*_k(k) = \arg J^*_{k,n} = \arg\left(\min_u \left(J_{k,k+1}\left(x(k), u(k)\right) + J^*_{k+1,n}\left(x(k+1)\right)\right)\right) \tag{2.3}$$

and is called the *backward recursion* (Figure 2.8a). This procedure is gradually done for each point of the grid, resulting in a $n \times m$ matrix containing information about the optimal

control at each point and the cost to get to the final state $x(n)$. The optimal state trajectory x^* is subsequently computed starting at a selected stage k and state level x and following optimal control which has been calculated during backward recursion at each stage. This is called the *forward recursion* (Figure 2.8b).

The example above used only a one-dimensional state representing the battery SOC for illustration. However, when an additional state quantity, such as gear shifting, is added, the grid becomes three-dimensional, exponentially increasing the already high computation effort required. This adverse property of dynamic programming has been named the *curse of dimensionality*.

As the optimisation procedure starts at the end of the optimised time interval, it is clear that the future conditions have to be known beforehand, making it unsuitable for online control. Its usage is therefore limited for offline benchmark computations for other EMSs, heuristic strategy design, or training data for machine learning algorithms.

This online implementability issue is however addressed by *stochastic dynamic programming*, which uses Markov chain process probability distribution to define expected future cost [31, 32]. The result is however clearly suboptimal.

Pontryagin's Minimum Principle

This method of finding an optimum is based on calculus of variations, with the aim to find the global extremum of a functional, in this case, a minimum of the performance measure in (2.2), to obtain optimal control.

A functional called the *Hamiltonian* is derived [33] by analytically searching for necessary conditions for finding an extremal maximising (minimising) the original functional using the *Langrange multiplier* method. The Hamiltonian is defined as:

$$\mathscr{H}(\mathbf{x}(t), \mathbf{u}(t), \mathbf{p}(t), t) \triangleq g(\mathbf{x}(t), \mathbf{u}(t), t) + \mathbf{p}^T(t)[\mathbf{a}(\mathbf{x}(t), \mathbf{u}(t), t)] \tag{2.4}$$

where g is the penalty function from (2.2), $\mathbf{p}$ are the Lagrange multipliers, also called the *costates* and $\mathbf{a}$ are the system equality constraints:

$$\dot{\mathbf{x}}(t) = \mathbf{a}(\mathbf{x}(t), \mathbf{u}(t), t)\,. \tag{2.5}$$

The Hamiltonian is then minimised at each instant to obtain optimal control according to the *Pontryagin's minimum principle*, which says that *an optimal control must minimise the Hamiltonian*:

$$\mathscr{H}(\mathbf{x}^*(t), \mathbf{u}^*(t), \mathbf{p}^*(t), t) \leq \mathscr{H}(\mathbf{x}^*(t), \mathbf{u}(t), \mathbf{p}^*(t), t) \tag{2.6}$$

for all $t \in [t_0, t_f]$ and *for all admissible controls*, which is one of the neccessary conditions

$$\left.\begin{aligned} \dot{\mathbf{x}}(t) &= \frac{\partial \mathscr{H}}{\partial \mathbf{p}}(\mathbf{x}^*(t), \mathbf{u}^*(t), \mathbf{p}^*(t), t) && \text{(2.7a)} \\ \dot{\mathbf{p}}(t) &= -\frac{\partial \mathscr{H}}{\partial \mathbf{x}}(\mathbf{x}^*(t), \mathbf{u}^*(t), \mathbf{p}^*(t), t) && \text{(2.7b)} \\ \mathscr{H}(\mathbf{x}^*(t), \mathbf{u}^*(t), \mathbf{p}^*(t), t) &\leq \mathscr{H}(\mathbf{x}^*(t), \mathbf{u}(t), \mathbf{p}^*(t), t) && \text{(2.7c)} \end{aligned}\right\} \forall t \in [t_0, t_f]$$

for $\mathbf{u}^*$ to be optimal control, minimising the performance measure. To be exact, in a general

problem, an additional neccessary condition

$$\left[\frac{\partial h}{\partial \mathbf{x}}(\mathbf{x}^*(t_f), t_f) - \mathbf{p}^*(t_f)\right]^T \delta\mathbf{x}_f + \left[\mathscr{H}(\mathbf{x}^*(t_f), \mathbf{u}^*(t_f), \mathbf{p}^*(t_f), t_f) + \frac{\partial h}{\partial t}(\mathbf{x}^*(t_f), t_f)\right] \delta t_f = 0 \tag{2.8}$$

where h is the cost of the final state (which is in the general form present in the performance measure), needs to be satisfied. However, in HEV control, final time and final state are usually specified, as the time is fixed and not part of the optimisation and the aim is to reach a predefined level of SOC at the end of the trip (or prediction horizon). Therefore $\delta\mathbf{x}_f$ and δt_f are zero and the condition (2.8) is always satisfied.

This method, thanks to its analytical nature, is less computationally demanding than dynamic programming. Nevertheless, some numerical methods must be employed anyway, because the problem is almost always nonlinear and the optimal control cannot be obtained analytically.

The disadvantage is that state or control inequality constraints—such as range of available torque, or range of admissible SOC—have to be incorporated into the Hamiltonian by additional Lagrange multipliers, increasing the dimension of the system and computational effort required to solve the problem.

Equivalent consumption minimisation strategy (ECMS), a widely used control method with numerous variations [20, 34, 35, 36, 37], is derived from PMP, applying it to a vehicle model with certain simplifying assumptions[7]. The resulting Hamiltonian is in the form:

$$\mathscr{H}(x(t), u(t), p, t) = \dot{m}_\mathrm{f}(u(t), t) + p\,\dot{\xi}(u(t), t) \tag{2.9}$$

where $\dot{m}_\mathrm{f}$ is the fuel mass flow and $\dot{\xi}$ is the change of SOC with respect to time. The Hamiltonian is now effectively the sum of instantaneous fuel power and electric power converted to an equivalent fuel power by the Lagrange multiplier p acting as a dimensionless scaling constant, called the *equivalence factor*. The value of p is unique for a given trip and depends on recuperation possibilities, efficiency of the ICE, efficiency of the energy transformation, etc. of such trip. The challenge of implementing ECMS is to accurately predict this value for the current trip. The Hamiltonian can then be minimised in real-time, obtaining optimal[8] control at each instant.

The effect of different equivalence factor values is illustrated in Figure 2.9. Choosing a higher value p_1 than a charge-sustaining mode requires will make the theoretical cost of electric power higher, therefore the control will prioritise the thermal energy of the ICE more frequently, resulting in unnecessarily higher SOC at the end of the trip. Similarly, choosing a lower value will make the control use electricity more than is available for charge-sustaining operation, eventually depleting the battery.

2.2.3 State of the Art

The trend in HEV EMSs has been combining the aforementioned methods – using their positive aspects and addressing their shortcomings to obtain close-to-optimal results with online control, where low computational effort is needed and future conditions uncer-

[7] More detailed derivation will be shown in Chapter 3 to be used for the proposed control strategy.

[8] The optimal control is naturally optimal only with respect to the simplified model, making the control strategy itself suboptimal.

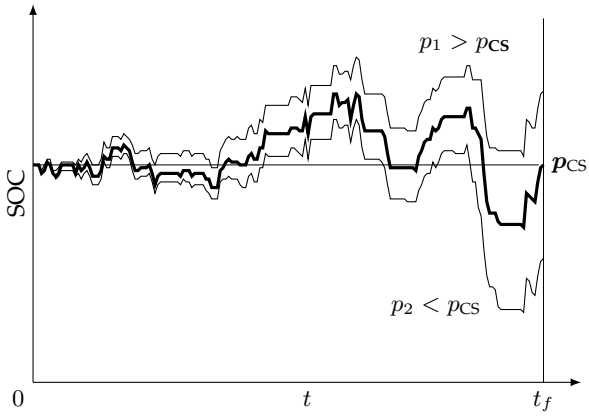

Figure 2.9 SOC trajectory using different equivalence factor values.

tainty is present. Research can therefore be loosely categorised into two branches:

- making heuristic strategies smarter,
- simplifying the scope of optimisation-based strategies,

both of which can achieve good results.

Variations of heuristic methods have been used in production vehicles for their robustness and simplicity of implementation, however, there is little insight on specific methods used by car manufacturers. Most of the researched control strategies and algorithms have not been applied in the industry yet and are limited to simulations. This also makes direct comparison of reported fuel savings amongst different studies complicated, as different vehicle models and solving methods used by individual authors yield disparate results.

Heuristic Methods

Rule-based methods have been improved by using optimal methods to derive their rules or use neural networks to make them adaptive to the current driving cycle. Large scale simulation was used to select rule-based control parameters in [38] to obtain the best results in selected driving cycles. Similarly, [39] used GA to optimise rules of FL-based control that were originally created from expertise.

In [18] and [40], the inflexibility of rule-based methods across different driving cycles was addressed by using neural networks (NN), making the FL rule-based strategy adaptive online, based on driving cycle recognition. [18], employing the Mamdani FL model, adapts the output membership functions, while [40], employing the Takagi-Sugeno FL model, adapts the inference output function parameters. A pure neural-network approach was chosen in [41], using deep reinforcement learning. The input layer of the network is just instantaneous SOC and torque demand, which then outputs ICE torque as the action value. The learning process can be done both offline and online from a heuristically defined reward function.

Optimisation Methods

In online control, optimisation methods are usually used in connection with model predictive control (MPC), to optimise power-split over a predicted horizon. MPC consists of

predicting a velocity profile at each instant some time into the future using a certain system model. Afterwards, optimal control sequence for this time interval is calculated and the first element of this sequence is applied. The process starts again at the next instant. The prediction horizon is hence continuously being shifted forward in time and is therefore known as *receding horizon*.

Various methods of predicting velocity are used, usually a combination of probability and GPS data. Stochastic Markov-chain prediction is used in [42], which is then solved using DP. In [43], velocity prediction is synthesised from macroscopic traffic data and microscopic stochastic disturbations. This prediction is then solved using linear programming.

With the advent of connected vehicles, algorithms using GPS data, radars and *Vehicle-to-everything* (V2X) communication are used. Prediction based on the information obtained from V2X, including historical driving data, traffic light information and leading vehicle trajectories is made in [44]. A combination of an optimal and heuristic method is then used for finding a control policy. Bi-Level MPC is used in [45] to generate an optimal speed trajectory from GPS data in the outer loop and the inner loop optimises torque split and gear shift using PMP.

ECMS-based control relies upon correctly selecting the equivalence factor (EF)—which is dependent on driving conditions—for instantaneous minimisation of the Hamiltonian, which generally does not need to consider receding horizon for optimisation. Inaccurate values however result in deviations of SOC at the end of the trip, either failing to be charge-sustainable or not fully exploiting its electric energy potential.

[46] uses maps to select the equivalence factor online based on current SOC and demanded power. The maps are created offline using DP from known driving cycles (NEDC, UDDS and 10-15). However, usage of the algorithm outside of these cycles will likely yield poor performance. Similarly, in [35], the EF is estimated from past and predicted driving conditions. Instead of adaptation based on driving conditions, [37], [47] and [48] update the EF in real-time for the SOC to follow reference trajectory generated from available trip information.

Results from recent algorithms and strategies (both heuristic and optimisation) were compared to classic rule-based methods used in commercial vehicles in [49], showing that smarter algorithms are indeed much closer to the global optimum. Of these, MPC and ECMS-based methods having the highest potential, which can be attributed to the fact that they use future trip information to some extent and do not rely solely on pattern recognition.

2.3 MOTIVATION AND CONTRIBUTIONS

Since an algorithm's optimality largely relies upon the extent of knowledge of the entire trip, the clear direction of HEV control strategies is towards incorporating trip information obtained through various ways, such as using GPS, built-in radar and V2X. Whole-trip knowledge plays a role especially for PHEVs, which should ideally deplete their battery just before the end of the trip for optimal fuel efficiency [11, 12]. Therefore, EMS using information about the whole trip is proposed, studying the effects of global trip data on fuel consumption of HEVs with different degree of electrification, including PHEVs.

It is assumed that a starting point and an endpoint of a trip will be defined before a trip, from which a route with an approximate speed profile will be generated. The determination of speed profile is not part of this thesis. Previous route data or eco-driving

algorithms [50] along with traffic information can be used. An accurate elevation profile can be obtained from an onboard navigation system.

The proposed EMS is composed of two levels. The high-level calculates a reference SOC trajectory from elevation and speed profiles. To achieve acceptable computation time with reasonable accuracy, a simplified optimisation algorithm has to be developed. This will be done by simplifying both the vehicle model and PMP optimisation algorithm. Apart from the reference SOC trajectory, the result of global PMP optimisation is the optimal equivalence factor used for instantaneous Hamiltonian minimisation, which will be done by the lower-level control loop.

The EF generated from the global optimisation cannot be used solely as a feedforward control, because it was computed using a simplified model and the real speed profile will to some extent always deviate from the predicted values, according to real-time driving events. An inaccurate EF would result either in depleting the battery too early, or not fully using the available electric energy. The high-level calculation is however too demanding to update the EF based on the current SOC and rest of the trip in real-time and therefore the lower-level loop will make feedback corrections to the EF based on the deviations from reference SOC.

Similar SOC-reference tracking using ECMS was implemented in [37], [47] and [48]. [37] assumes a constant charge-sustaining reference, not taking into account any deviations throughout. While no trip information beforehand is necessary, any longer recuperation route segments will lead to reaching upper SOC constraint, resulting in having to dissipate the rest of the energy via brakes, thereby not exploiting the entire recuperation potential of the route. This is taken into account in [47], where approximate velocity profile and route topology is obtained from an onboard navigation system, and reference SOC trajectory is generated with quadratic programming algorithm. Nevertheless, the average-speed segments are still quite large and several heuristic simplifying assumptions for the reference computation, are made.

[48] generates a charge-depletion SOC-reference trajectory for a PHEV based on dividing a trip into segments with similar driving style and calculating the needed energy of each segment. This line then approximately resembles an optimal charge depletion rate to prevent premature battery depletion before the end of the trip. Offline-precalculated maps with values for each driving style are needed for both the feedforward equivalence factors and the energy consumption values for the reference trajectory calculation.

The proposed EMS does not require any offline-precalculated maps, as—compared to the previous implementations—a fairly detailed optimisation problem is solved to obtain a close-to-optimal equivalence factor. Additionally, in the aforementioned work, only few test trips are presented. Several routes with different driving types will be recorded for the purposes of this work and several trips on each of the routes will be used to test the sensitivity to incorrectly predicted speed profile. The model of the vehicle used is P2 parallel configuration. Nevertheless, findings should be applicable to any vehicle topology, assuming a respective model is used. Three degrees of electrification considered are MHEV, HEV and PHEV. The simulation results of each configuration will be compared to an optimal DP solution and a simple rule-based strategy.

Chapter 3

CONTROL STRATEGY DESIGN

The idea of the proposed strategy is to first calculate a theoretically[1] optimal SOC trajectory of a planned route as a function of driven distance using a vehicle model and predicted driving conditions before the start of a trip. Subsequently, this reference would be tracked during the trip, adjusting real-time control accordingly.

The premise for this is to anticipate recuperation opportunities created by braking from high speed or descending a hill, and maximise their potential by using up energy stored in batteries beforehand to avoid having to dissipate the excess through friction brakes if the SOC reaches the upper limit. Similarly, knowing sections of the trip where the engine works with lower efficiency would ensure enough battery charge for the electric motor to be used there. All this should be accomplished while attaining desired SOC level at the end of the trip without depleting the battery too much, or, on the other side of the spectrum, not exploit its full potential.

Even though the theoretically optimal predicted SOC trajectory will never be optimal with respect to real-world driving, the effects of the aforementioned occurrences should still be retained.

3.1 CHALLENGE

To calculate the optimal SOC trajectory on a trip, speed and elevation profiles are needed. From these, required power is calculated at each instant using a vehicle model. Based on the profiles and the vehicle model, the aim is to determine whether this power request should be met by the ICE, EM, or their combination.

Both the route profiles and vehicle model introduce inaccuracies to the prediction, and therefore the generated SOC reference is not optimal with respect to the real world. The route inaccuracies are mainly encompassed in the predicted speed profile due to the inherently random nature of traffic, whereas model inaccuracies can be either simplifications (not taking into account parameter variations with temperature changes, battery aging, transients, etc.), to achieve acceptable computation time, or parameters such as wind speed, rolling resistance and other parameters affected by uncertainty.

All of the above will ultimately lead to different power request or charge depletion than predicted and the algorithm needs to be robust to this behaviour. Hence, the control calculated from the high-level optimisation cannot be used directly as a feedforward function

[1] Optimal with respect to prediction data and simplified vehicle model.

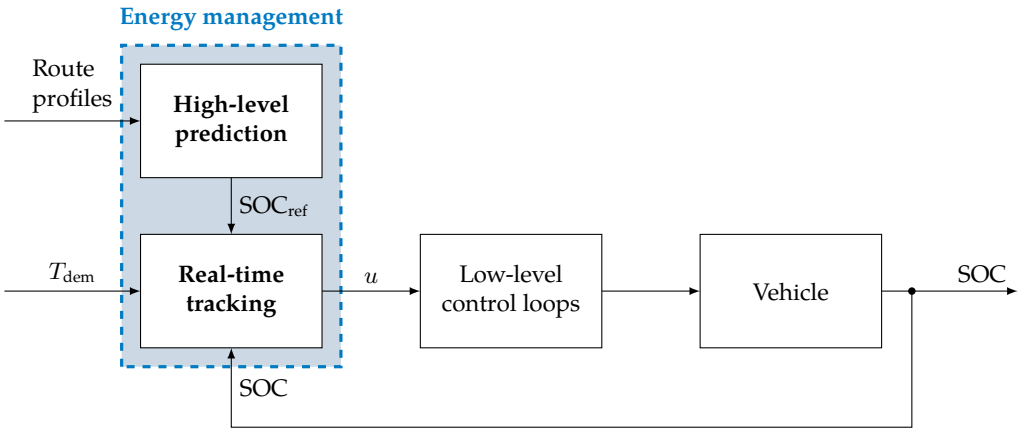

Figure 3.1 Proposed strategy control loop block diagram

of driven distance and a feedback loop at the lower level needs to be implemented to track the reference SOC. Block diagram of this entire control loop is shown in Figure 3.1.

The challenge is, therefore, to develop a computationally efficient optimisation algorithm with a simplified model to calculate reference SOC before the trip in a reasonable[2] time and then create a feedback loop logic for the lower level to track it in real-time. Predicted route profiles are assumed to be already known beforehand and are not part of the algorithm. Depending on the use case, such profiles can be obtained from a navigation system, eco-driving algorithms, or previous trip data.

3.2 VEHICLE MODEL

In this thesis, energy efficiency—which ultimately translates into fuel consumption—based on advantageously splitting power between ICE and EM is observed. Accordingly, a model that captures the important effects, but is not unnecessarily complex, is created. This means mathematically describing needed power for vehicle operation during a trip and consequent fuel and battery capacity dynamics reflecting the use of each unit for propulsion.

Numerous simplifying assumptions were made for the purposes of the thesis as the aim is not to reflect real-life driving in absolute terms and values, but to compare behaviour of different energy management strategies applied to the same vehicle. This is mostly approximating certain parameters as constant (such as gearbox efficiency, rotational-mass coefficient or rolling resistance coefficient), which vary slightly as a function of a different parameter.

Thermal behaviour of components (engine, batteries) and battery load from accessories (such as HVAC) are neglected.[3]

[2] As complete trip optimisation algorithms such as DP with various degrees of model complexity can take several hours to find optimum, a simplified algorithm needs to be developed to obtain a nearly optimal result in order of seconds.

[3] In the real world, not considering accessories may however introduce negative effect on the algorithm when the predicted trip takes a shorter time than the actual trip, leading to additional battery discharge, and thus it is recommended to implement accessories in future work. As this does not alter the dimension of the optimisation, computational time should not be notably worsened.

Table 3.1 Tested vehicle parameters

	MHEV	HEV	PHEV
Mass m	1470 kg	1550 kg	1700 kg
Battery capacity C	8 A h (0.43 kW h)	6.5 A h (1.56 kW h)	37 A h (13.7 kW h)
Battery nominal voltage V	54 V	240 V	370 V
Battery pack configuration	14s1p	62s1p	96s1p
EM nominal power P_{m}	11 kW	65 kW	65 kW
EM coupling gear ratio i_{tc}	2.5	1	1
EM coupling mechanical efficiency η_{tc}	0.98	1	1
Engine	Naturally aspirated SI 1.3L 96 kW		
Rolling resistance coefficient f	0.021		
Drag coefficient c_x	0.31		
Frontal area A_x	2 m^2		
Rotational-mass coeficient δ	1.1		
Inverter efficiency η_{i}	0.95		
Gearbox gear ratios i_{g}	$3.78, 2.05, 1.28, 0.94, 0.78, 0.67$		
Final drive gear ratio i_{fd}	3.56		
Drivetrain mechanical efficiency η_{d}	0.97		
Tire dynamic rolling radius r_{d}	0.3 m		
Gravitational acceleration g	9.81 $\mathrm{m\,s^{-2}}$		
Air density ρ_{a}	1.225 $\mathrm{kg\,m^{-3}}$		
Initial SOC ξ_0	0.7	0.7	0.9
Final SOC ξ_f	0.7	0.7	0.3
Upper SOC limit ξ_{high}	0.8	0.8	0.9
Lower SOC limit ξ_{low}	0.6	0.6	0.2

3.2.1 Vehicle Configuration

The model represents a parallel hybrid electric vehicle in P2 configuration (Fig. 2.4). Three vehicles with different degrees of hybridisation (MHEV, HEV and PHEV) are studied and hence three sets of data listed in Table 3.1 were used to represent each vehicle. The HEV and PHEV have the same 65 kW EM configuration mounted on the input shaft of the gearbox, with the PHEV having a significantly larger battery.

The MHEV has a smaller 11 kW EM coupled to the gearbox input shaft with a gear ratio of 2.5 to increase torque at the wheels. Contrary to the typical BSG configuration, thanks to the P2 topology, the MHEV is also allowed to drive in pure electric mode.

In terms of battery management, both the MHEV and HEV operate in a charge-sustaining mode at 70 % SOC, whereas the PHEV is allowed to discharge its battery from 90 % to 30 %, before switching to charge-sustaining mode.

3.2.2 Required Traction Force

A longitudinal dynamics model is employed to describe the vehicle's motion. The vehicle is considered a point mass, which is being acted upon by forces in the longitudinal direction as shown in Figure 3.2. The placement of forces in the figure is solely supposed to

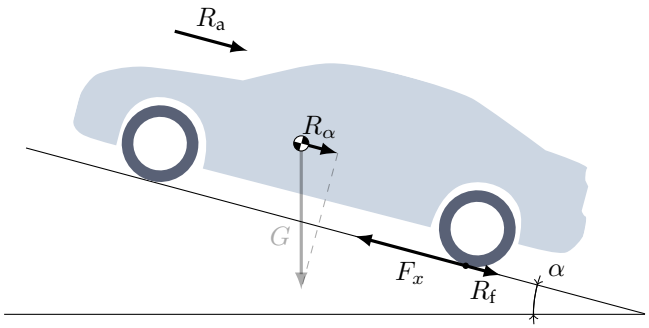

Figure 3.2 Longitudinal-dynamics vehicle model; R_a: aerodynamic resistance, R_α: incline resistance, F_x: traction force, R_f: rolling resistance, G: gravitational force, α: slope angle.

illustrate their nature, as they are considered to act in the center of mass. The vehicle's speed dynamics are then:

$$\dot{v}(t) = \frac{1}{m\delta}\left(F_x(t) - R_\alpha(t) - R_f(t) - R_a\left(v(t)\right)\right) \tag{3.1}$$

where m is the mass of the vehicle, δ the rotational-mass coefficient, taking into account the need to accelerate not only the vehicle but the rotational components of the drivetrain as well. F_x is the traction force, R_α resistance from incline (component of gravitational force G), R_f rolling resistance and R_a aerodynamic resistance. Individual resistance forces are defined as:

$$R_a(t) = \frac{1}{2}\rho_a c_x A_x v^2(t) \tag{3.2a}$$

$$R_\alpha(t) = mgf\sin(\alpha(t)) \tag{3.2b}$$

$$R_f(t) = mgf\cos(\alpha(t)) \tag{3.2c}$$

where c_x is the drag coefficient, A_x the vehicle frontal surface area, g gravitational acceleration, f the rolling coefficient and α the slope angle. Because the input is speed values collected with a certain timestep Δt, (3.1) becomes:

$$\frac{\Delta v(t)}{\Delta t} = \frac{1}{m\delta}(F_x(t) - R_\alpha(t) - R_f(t) - R_a(v(t))) \tag{3.3}$$

from which the required traction force at each instant can be obtained:

$$F_x(t) = m\delta\frac{\Delta v(t)}{\Delta t} + R_\alpha(t) + R_f(t) + R_a(v(t)) \tag{3.4}$$

3.2.3 Drivetrain

Traction force F_x at the wheels is provided by the combination of ICE and EM torque (Fig. 3.3):

$$F_x(t) = \left(T_e(t) + T_m(t) i_{tc}\eta_{tc}\right) i_g(t)\, i_{fd}\, \eta_d\, r_d \tag{3.5}$$

where i_g is the gearbox ratio, i_{fd} the final drive ratio, $\eta_d = \eta_g\,\eta_{fd}$ the combined mechanical efficiency of the gearbox and final drive, and r_d is the dynamic rolling radius of the tire. Constants i_{tc} and η_{tc} are the gear ratio and efficiency of the torque coupling of the EM to the driveline respectively. The torque couple gear ratio also couples angular velocity of the

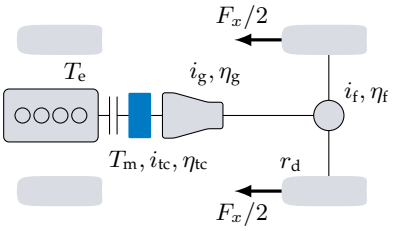

Figure 3.3 Drivetrain model

EM and the ICE by:

$$\omega_e(t) = \frac{\omega_m(t)}{i_{tc}} = \omega(t) \tag{3.6}$$

where ω is the angular velocity of the gearbox input shaft. The effects of tire slip are neglected, therefore ω can be obtained directly from the vehicle speed:

$$\omega(t) = \frac{v(t)\, i_g(t)\, i_{fd}}{r_d} \tag{3.7}$$

Combining (3.4) and (3.5), demanded torque at the gearbox input shaft that needs to be provided by the combination of the EM and the ICE at each instant can be calculated:

$$T_{dem}(t) = T_e(t) + T_m(t) i_{tc} \eta_{tc} = \frac{m\delta \frac{\Delta v(t)}{\Delta t} + R_\alpha(t) + R_f(t) + R_a(v(t))}{i_g(t)\, i_{fd}\, \eta_d\, r_d} \tag{3.8}$$

3.2.4 Battery

The battery charge dynamics are a function of flowing current:

$$\dot{\xi}(t) = -\frac{I(t)}{C} \tag{3.9}$$

where I is the current flowing from or to the battery (positive when battery is being discharged) and C is the battery charge capacity.

Using internal resistance battery model (Fig. 3.4), the current can be obtained from

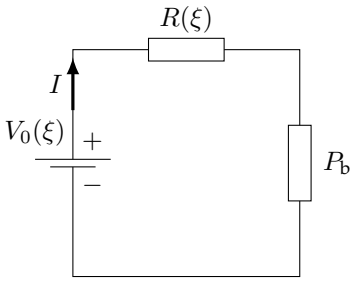

Figure 3.4 Internal resistance battery model; V_0: open-circuit voltage, R: internal resistance, P_b: battery input/output power.

power P_b going to/from the battery by solving the following quadratic equation:

$$R(\xi(t))I(t)^2 - V_0(\xi(t))I(t) + P_\mathrm{b}(t) = 0 \tag{3.10}$$

where R is the battery internal resistance and V_0 the open-circuit voltage, both of which vary with SOC level (Fig. 3.5). Equation (3.10) is essentially power equilibrium with the term RI^2 representing heat losses due to internal resistance, which is higher while charging the battery (Fig. 3.5b), resulting in higher losses.

$$I(t) = \frac{V_0(\xi(t)) \pm \sqrt{V_0^2(\xi(t)) - 4R(\xi(t))P_\mathrm{b}(t)}}{2R(\xi(t))} \tag{3.11}$$

Only the root with minus sign is physically feasible. This equation also defines the battery power limits, because the square root part has to be greater than zero:

$$P_{\mathrm{b,min}}(\xi(t)) \leq P_\mathrm{b}(t) \leq P_{\mathrm{b,max}}(\xi(t)) \tag{3.12}$$

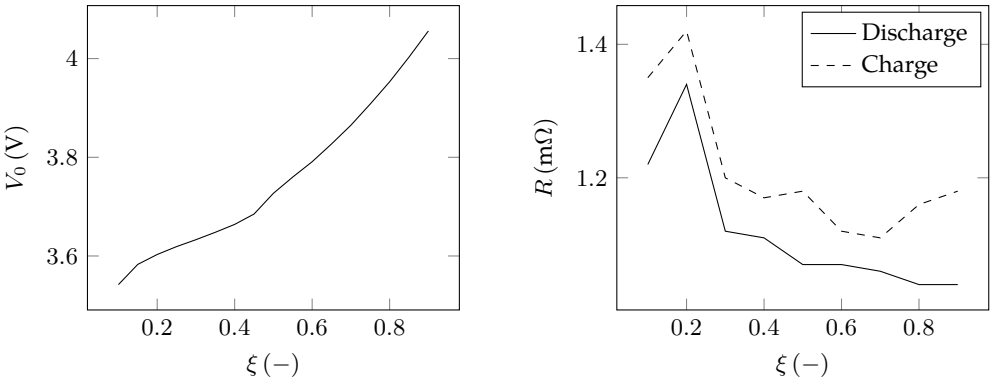

A Open circuit voltage

B Internal resistance

Figure 3.5 Battery cell parameters as a fucntion of SOC (prismatic lithium-ion at 25 °C).

Battery-pack open-circuit voltage and internal resistance were obtained by scaling parameters of a reference prismatic lithium-ion battery cell (Fig. 3.5) according to the battery pack configuration using Ohm's and Kirchoff's laws:

$$V_{0\mathrm{p}} = s\, V_{0\mathrm{c}} \tag{3.13a}$$

$$R_\mathrm{p} = \frac{s}{p} R_\mathrm{c} \tag{3.13b}$$

where s is the number of cells in the battery pack connected in series and p in parallel. Index p denotes parameters of the battery pack and index c the parameters of a cell. To obtain values for different battery capacity, the cell's internal resistance was scaled using formula [51]:

$$R^* = R_\mathrm{c} \frac{C_\mathrm{c}}{C^*} \tag{3.14}$$

where the index c denotes cell's parameters and $*$ the required parameters.

3.2.5 Electric Machine

Battery power can be further quantified by power drawn by the EM P_m:

$$P_\mathrm{b}(t) = \frac{P_\mathrm{m}(t)}{\eta_\mathrm{i}^{\operatorname{sgn} P_\mathrm{m}(t)}} = \frac{T_\mathrm{m}(t)\,\omega_\mathrm{m}(t)}{(\eta_\mathrm{i}\,\eta_\mathrm{m}(T_\mathrm{m}(t),\omega_\mathrm{m}(t)))^{\operatorname{sgn} T_\mathrm{m}(t)}} \tag{3.15}$$

where η_i is the power inverter efficiency and η_m the EM efficiency depending on its operating point (Fig. 3.6). Mechanical power is represented by torque provided by the EM T_m and its angular velocity ω_m which are subject to constraints:

$$T_\mathrm{m,min}(\omega_\mathrm{m}(t)) \leq T_\mathrm{m}(t) \leq T_\mathrm{m,max}(\omega_\mathrm{m}(t)) \tag{3.16}$$

$$0 \leq \omega_\mathrm{m}(t) \leq \omega_\mathrm{m,max} \tag{3.17}$$

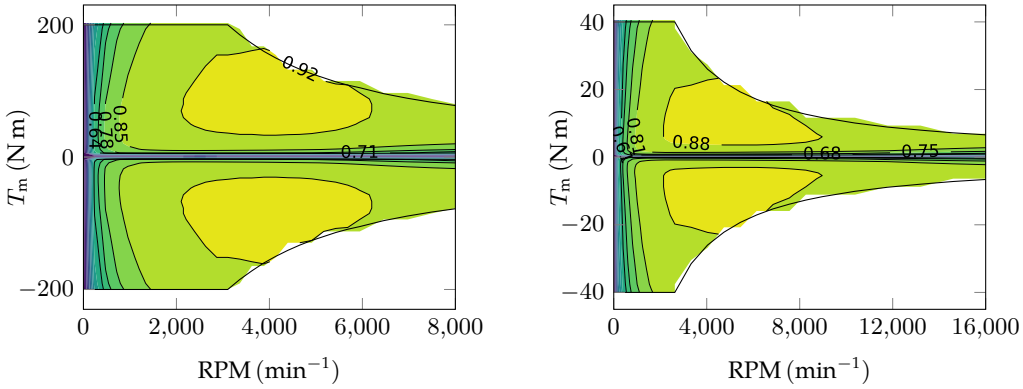

A 65 kW EM for HEV and PHEV

B 11 kW EM for MHEV

Figure 3.6 Efficiency maps and maximum torque curves of the electric machines

3.2.6 Engine

The model of the engine takes into account full load curve and brake-specific fuel consumption based on engine torque T_e and angular velocity ω_e (Fig. 3.7), which are subject to constraints:

$$0 \leq T_\mathrm{e}(t) \leq T_\mathrm{e,max}(\omega_\mathrm{e}(t)) \tag{3.18}$$

$$\omega_\mathrm{e,min} \leq \omega_\mathrm{e}(t) \leq \omega_\mathrm{e,max} \tag{3.19}$$

Fuel consumption is then defined as:

$$\dot{m}_\mathrm{f}(t) = T_\mathrm{e}(t)\,\omega_\mathrm{e}(t)\,\mathrm{BSFC}\,(T_\mathrm{e}(t),\omega_\mathrm{e}(t)) \tag{3.20}$$

The engine is considered warmed-up during operation and no additional temperature behaviour is modeled. As this thesis focuses on energy efficiency only, pollutant emissions have not been included in the model.

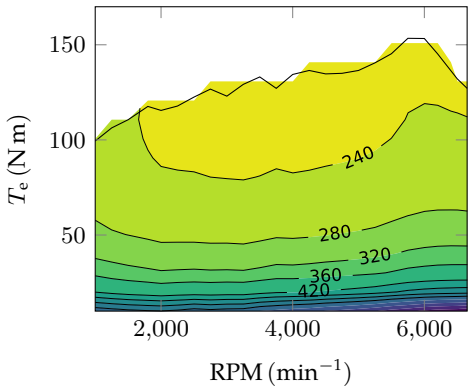

Figure 3.7 BSFC map (in g/kWh) and full load curve of the internal combustion engine

3.2.7 Shifting

While in terms of ideal fuel consumption, gear shifting would be included in the optimisation, because it affects the EM and ICE efficiency, an independent shifting logic is implemented instead. There are several reasons for this. The obvious one is an additional significant computational burden, however, mainly, the objective here is to compare effects of planned-trip information knowledge with a simple rule-based strategy in otherwise identical conditions, therefore different gear shifting would only add irrelevant inconsistencies to the results. The predicted route also has different torque requirements at each instant than in real driving, which would result in the optimised gear being largely suboptimal or even infeasible with respect to engine limits.

The logic implemented here is therefore based on WLTP shifting strategy [52], which essentially imposes the highest gear possible based on instantaneous demanded power and available engine power in each gear, as long as the minimum and maximum engine RPM limits are not violated. This means that in terms of shifting, the vehicle behaves as a conventional ICE vehicle without any EM. While skipping gears during acceleration is not allowed in WLTP and gear can be changed only after 3 seconds, no such rules are implemented here for simplicity and irrelevancy to the results.

When demanded torque is less than or equal to zero, the engine is considered shut off.

3.3 Optimal Control Problem

Since the observed behaviour is fuel consumption, the aim is to find an optimal control $\mathbf{u}^*$ at each instant to minimise the performance measure

$$J(\mathbf{u}) = \int_{t_0}^{t_f} \dot{m}_f(\mathbf{u}(t), t)\,\mathrm{d}t \tag{3.21}$$

representing fuel consumption over the entire trip, subject to constraints specified in Section 3.2:

$$\xi_{\text{low}} \leq \xi(t) \leq \xi_{\text{high}} \tag{3.22a}$$
$$P_{\text{b,min}}(\xi(t)) \leq P_{\text{b}}(t) \leq P_{\text{b,max}}(\xi(t)) \tag{3.22b}$$
$$T_{\text{m,min}}(\omega_{\text{m}}(t)) \leq T_{\text{m}}(t) \leq T_{\text{m,max}}(\omega_{\text{m}}(t)) \tag{3.22c}$$
$$0 \leq \omega_{\text{m}}(t) \leq \omega_{\text{m,max}} \tag{3.22d}$$
$$0 \leq T_{\text{e}}(t) \leq T_{\text{e,max}}(\omega_{\text{e}}(t)) \tag{3.22e}$$
$$\omega_{\text{e,min}} \leq \omega_{\text{e}}(t) \leq \omega_{\text{e,max}} \tag{3.22f}$$

with fixed state and time boundary conditions:

$$t_0 = 0, \quad t_f = T \tag{3.23}$$
$$\xi(t_0) = \xi_0, \quad \xi(t_f) = \xi_f \tag{3.24}$$

where T is the duration of the trip. Vehicle speed is given by the input speed profile and therefore the only controlled state variable as part of the optimisation is ξ:

$$\dot{\mathbf{x}}(t) = [\dot{\xi}(t)] \tag{3.25}$$

which is ultimately affected by the power of the EM, which determines the current flow in and out of the battery. Because independent shifting strategy based on vehicle speed and total demanded torque is implemented, the only control variable is the torque provided by the EM:

$$\mathbf{u}(t) = [T_{\text{m}}(t)] \tag{3.26}$$

which also determines the torque that has to be provided by the ICE:

$$T_{\text{e}}(t) = T_{\text{dem}}(t) - T_{\text{m}}(t)\, i_{\text{tc}}\, \eta_{\text{tc}} \tag{3.27}$$

making the performance measure

$$J(T_{\text{m}}) = \int_0^T T_{\text{e}}(T_{\text{m}}(t), t)\, \omega(t)\, \text{BSFC}\left(T_{\text{e}}(T_{\text{m}}(t), t), \omega(t)\right) \text{d}t \tag{3.28}$$

A term taking into account the energy and time required to turn the engine on could be included in the performance measure to prevent the vehicle from switching modes too often and ensure drivability and comfort. While this factor should be considered in real-life implementation, it is neglected for the purposes of this thesis, as none of the compared methods penalise such behaviour, and therefore it should not affect the results in relative terms.

3.3.1 Constraints

The shifting logic already ensures that the engine speed constraint (3.22f) is satisfied. Because EM speed is linked to engine speed and has wider RPM range, (3.22d) is automatically satisfied as well.

The remaining constraints that need to be taken into account during optimisation are the state inequality constraint (3.22a), control variable inequality constraints (3.22b, 3.22c) and the engine torque constraint (3.22e), which through (3.27) indirectly imposes a limit

on the control variable T_m. The EM torque $T_\mathrm{m}$is therefore bounded at each instant by the EM's maximum torque curve, maximum (minimum) battery power and full load curve of the ICE. The state inequality constraints will be addressed more in-depth in Section 3.4.3.

3.3.2 Solution

Some methods that can be used to solve the set up optimal control problem are briefly introduced in Section 2.2.2. DP will ultimately be used for all tested routes as a benchmark, however, finding solution this way requires a lot of time and cannot be implemented in the control algorithm for real-world driving. Therefore, for the high-level reference SOC trajectory generation, a simplified PMP algorithm will be used, due to its computational efficiency. Additionally, the result of PMP optimisation is not only the reference SOC trajectory but also the reference costate (equivalence factor), which can be subsequently used for the lower-level instantaneous control logic to track the SOC reference.

3.4 HIGH-LEVEL TRAJECTORY GENERATION

The PMP used to solve the optmial control problem from Section 3.3 is formulated based on variational approach for finding extrema of a functional

$$J(\mathbf{u}) = \int_{t_0}^{t_f} g(\mathbf{x}(t), \mathbf{u}(t), t)\,\mathrm{d}t \tag{3.29}$$

subject to state differential equation constraints

$$\dot{\mathbf{x}}(t) = \mathbf{a}(\mathbf{x}(t), \mathbf{u}(t), t) \tag{3.30}$$

using the Lagrange multiplier method. In a control problem where admissible controls are bounded and final state and time are fixed, the PMP states necessary conditions for optimal control $\mathbf{u}^*$ and optimal state trajectory $\mathbf{x}^*$:

$$\left.\begin{aligned} \dot{\mathbf{x}}(t) &= \frac{\partial \mathscr{H}}{\partial \mathbf{p}}(\mathbf{x}^*(t), \mathbf{u}^*(t), \mathbf{p}^*(t), t) && \text{(3.31a)}\\ \dot{\mathbf{p}}(t) &= -\frac{\partial \mathscr{H}}{\partial \mathbf{x}}(\mathbf{x}^*(t), \mathbf{u}^*(t), \mathbf{p}^*(t), t) && \text{(3.31b)}\\ \mathscr{H}(\mathbf{x}^*(t), \mathbf{u}^*(t), \mathbf{p}^*(t), t) &\leq \mathscr{H}(\mathbf{x}^*(t), \mathbf{u}(t), \mathbf{p}^*(t), t) && \text{(3.31c)} \end{aligned}\right\} \forall t \in [t_0, t_f]$$

where $\mathscr{H}$ is the Hamiltonian, which is the penalty function augmented by Lagrange multipliers $\mathbf{p}$ and state constraints $\mathbf{a}$:

$$\mathscr{H}(\mathbf{x}(t), \mathbf{u}(t), \mathbf{p}(t), t) \triangleq g(\mathbf{x}(t), \mathbf{u}(t), t) + \mathbf{p}^T(t)[\mathbf{a}(\mathbf{x}(t), \mathbf{u}(t), t)] \tag{3.32}$$

In other words, the Hamilatonian is minimised (3.31c) at each instant for all $t \in [t_0, t_f]$ and for all admissible controls $\mathbf{u}$ while satisfying the state (3.31a) and costate (3.31b) equations.

Applying the previously set up control problem with one state and one control variable, the vectors become one-dimensional. The system is described by differential equation

$$\dot{\mathbf{x}}(t) = \dot{\xi}(t) = -\frac{I(t)}{C} \tag{3.33}$$

controlled by control variable

$$\mathbf{u}(t) = T_{\mathrm{m}}(t) \tag{3.34}$$

with performance measure

$$J(T_{\mathrm{m}}) = \int_{t_0}^{t_f} \dot{m}_f(T_{\mathrm{m}}(t), t)\,\mathrm{d}t \tag{3.35}$$

making the Hamiltonian

$$\mathscr{H}(\xi(t), T_{\mathrm{m}}(t), p(t), t) = \dot{m}_f(T_{\mathrm{m}}(t), t) + p(t)[\dot{\xi}(\xi(t), T_{\mathrm{m}}(t), t)] \tag{3.36}$$

where p is a Lagrange multiplier known as the costate whose dynamics are described by

$$\dot{p}(t) = -\frac{\partial \mathscr{H}}{\partial \xi}(\xi(t), T_{\mathrm{m}}(t), p(t), t) \tag{3.37}$$

and whose boundary conditions are unknown, because the final state is not included in the penalty function [33]. The initial value of p has to be known to obtain optimal control at each instant using (3.31c), and therefore the goal of the optimisation is to obtain this value.

Because this is a highly nonlinear two-point boundary problem, it cannot be solved analytically and numerical methods have to be employed to some extent.

3.4.1 Problem Simplification

After plugging in the equations from the vehicle model—(3.11) for the battery dynamics and (3.20) for the fuel consumption—the Hamiltonian becomes

$$\begin{aligned}\mathscr{H}(\xi(t), T_{\mathrm{m}}(t), p(t), t) = T_{\mathrm{e}}(T_{\mathrm{m}}(t), t)\,\omega(t)\,\mathrm{BSFC}\,(T_{\mathrm{e}}(T_{\mathrm{m}}(t), t), \omega(t)) - \\ - p(t)\,\frac{V_0(\xi(t)) - \sqrt{V_0^2(\xi(t)) - 4R(\xi(t))P_{\mathrm{b}}(T_{\mathrm{m}}(t))}}{2R(\xi(t))C}\end{aligned} \tag{3.38}$$

Because internal resistance and open-circuit voltage depend on SOC, the battery drop does not only depend on the control variable but the state variable as well. Therefore, the partial derivative (3.37) is non-zero and the differential equation for the costate p needs to be solved at every time step. However, as can be seen in Figure 3.8, the battery parameters' dependency on SOC is not very steep in the operating range (especially for HEVs and MHEVs) and can be considered constant without obtaining a significant error.

This simplifies the Hamiltonian to

$$\begin{aligned}\mathscr{H}(T_{\mathrm{m}}(t), p(t), t) = T_{\mathrm{e}}(T_{\mathrm{m}}(t), t)\,\omega(t)\,\mathrm{BSFC}\,(T_{\mathrm{e}}(T_{\mathrm{m}}(t), t), \omega(t)) - \\ - p(t)\,\frac{V_0 - \sqrt{V_0^2 - 4RP_{\mathrm{b}}(T_{\mathrm{m}}(t))}}{2RC}\end{aligned} \tag{3.39}$$

and because it is now not dependent on the vehicle state, the costate becomes constant:

$$\dot{p}(t) = -\frac{\partial \mathscr{H}}{\partial \xi}(T_{\mathrm{m}}(t), p(t), t) = 0 \tag{3.40}$$

however, its value is still unknown and has to be iterated from an initial guess.

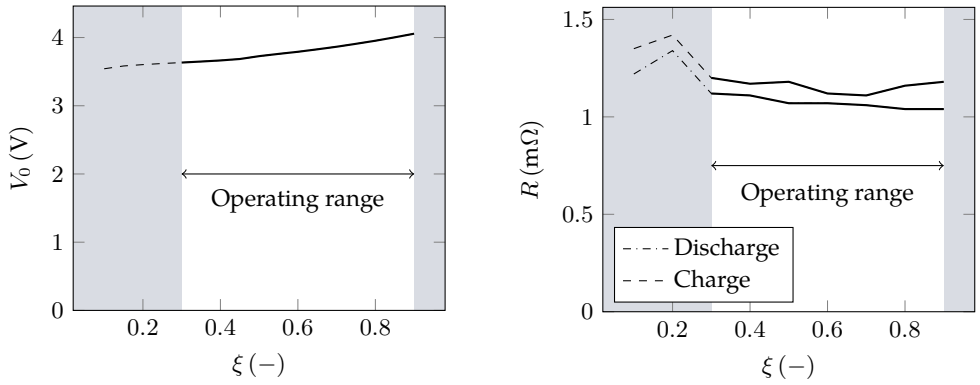

A Open circuit voltage

B Internal resistance

Figure 3.8 Battery parameter variation in the operating SOC range

3.4.2 Problem Solution

From (3.39), it can be seen that the Hamiltonian is essentially a sum of power in fuel and power in electric charge with p being a (negative) constant comparing the cost of fuel to the cost of electricity, known as the *equivalence factor*. For this reason, minimisation of Hamiltonian in this form is referred to as the *Equivalent Consumption Minimisation Strategy* (ECMS). The problem is finding the value of p, which encapsulates the trip characteristics determined by the speed and the elevation profile such as engine operating point efficiency, driving aggressiveness, and energy recuperation potential along a route.

If the absolute value of p is too low, the theoretical cost of electric energy is considered low, leading to overuse of energy from the batteries and not achieving charge-sustaining operation. Similarly, if the absolute value is too high, fuel energy is preferred, not exploiting available electric energy and ending with SOC that is too high. This behaviour is shown in Figure 2.9. Even small changes in p lead to large deviations from the required SOC at the end of the trip, and therefore it is unlikely this value will be correctly guessed without the knowledge of the trip.

However, a reasonable initial guess for the optimisation can be made by exploiting the nature of the Hamiltonian. Using the lower heating value of fuel and the battery parameters along with approximate[4] average efficiencies of each power delivery system, both summed expressions can be equalised to the same unit and theoretical energy cost.

$$H\,\bar{\eta}_\mathrm{e}\,\dot{m}_\mathrm{f} = C\,V\,\bar{\eta}_\mathrm{b}\,\eta_\mathrm{i}\,\bar{\eta}_\mathrm{m}\,\dot{\xi} \tag{3.41}$$

Rearranging then yields:

$$\dot{m}_\mathrm{f} = \frac{C\,V\,\bar{\eta}_\mathrm{b}\,\eta_\mathrm{i}\,\bar{\eta}_\mathrm{m}}{H\,\bar{\eta}_\mathrm{e}}\,\dot{\xi} = p_0\,\dot{\xi} \tag{3.42}$$

Where the value of p_0 can be used as the initial guess. This however does not take into account specific trip characteristics, and therefore is unlikely to yield optimal result by itself.

The trip is then discretised with a predefined time step and the value of control T_m (from of an admissible range) that minimises Hamiltonian at each step is applied. The

[4] True average efficiencies are naturally unknown as they are function of load, therefore approximate values are used.

admissible range of T_m is based on demanded torque, EM's maximum torque curve, maximum (minimum) battery power and full load curve.

Figure 3.9 illustrates the effect of the equivalence factor p on the minimum of Hamiltonian for two different demanded torque values. When the demanded torque is high, and therefore ICE efficiency reasonably high, increasing the cost of electric energy (higher absolute p-value), the location of the minimum makes the vehicle switch from EM-only propulsion to ICE-only propulsion. Whereas when the demanded torque is low, which would result in low ICE efficiency, increasing the cost of electric energy results in the vehicle shifting from EM-only propulsion to ICE propulsion while simultaneously charging the battery, obtaining an ICE operation point with higher efficiency.

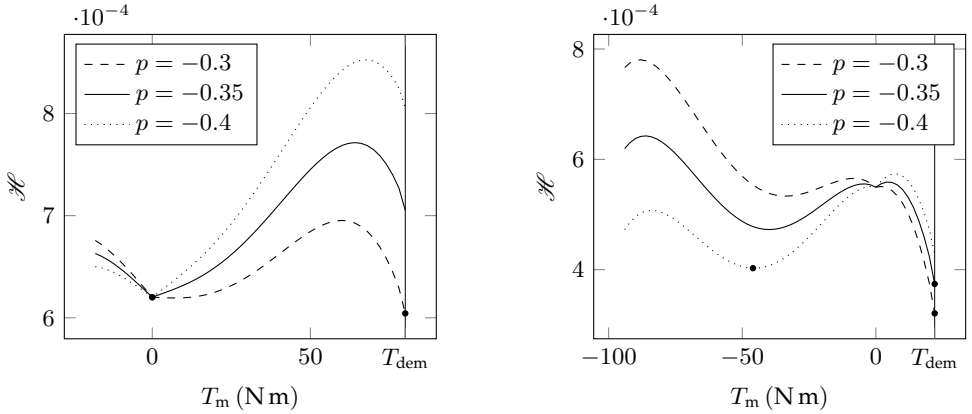

A $T_\mathrm{dem} = 80\,\mathrm{N\,m}$ B $T_\mathrm{dem} = 20\,\mathrm{N\,m}$

Figure 3.9 Hamiltonian for two demanded torque values as a function of p. Discontinuities at zero are due to the effect of losses and battery internal resistance based on the direction of power from/to the battery. Dots denote minimum of Hamiltonian. Example from a trip with optimal (charge-sustaining) $p^* = -0.35$.

Minimising the Hamiltonian at each time step results in a SOC trajectory along the entire trip. Based on the difference between the resulting SOC value at the end of the trip $\xi(t_f)$ and the required final SOC value ξ_f, p is updated for the next iteration until the trajectory reaches required $\xi(t_f)$ [5]. The iteration process to achieve charge-sustaining ($\xi_0 = \xi_f$) operation is illustrated in Figure 3.10.

3.4.3 State Inequality Constraints

From Figure 3.10, it is clear that in the optimal control problem described by (3.39) and (3.40), there is nothing preventing the violation of inequality constraints (3.22a) of the vehicle state – battery SOC bounds ξ_low and ξ_high which the vehicle should stay in (typically $\pm 10\,\%$ from required value for charge-sustaining HEVs). The final ξ trajectory in Figure 3.10 did not violate these constraints, however, the issue becomes more prominent on routes with long descends or with vehicles with small battery capacity (such as MHEVs), whose boundaries are easily exceeded. This is illustrated in Figure 3.11, where the same route from Figure 3.10 is optimised for HEV and MHEV without active state constraints.

Numerous approaches for solving PMP problems with inequality constraints are given in [53]. The *indirect adjoining method* was used here for the HEV optimal control problem.

[5] Small deviation $\Delta\xi_f = 0.003$ is allowed to ensure mathematical feasibility.

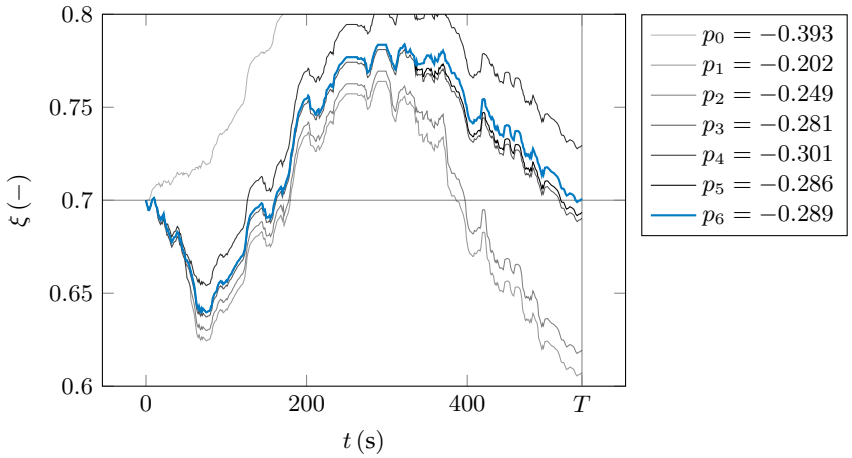

Figure 3.10 Iteration process of equivalence factor p for charge-sustaining operation

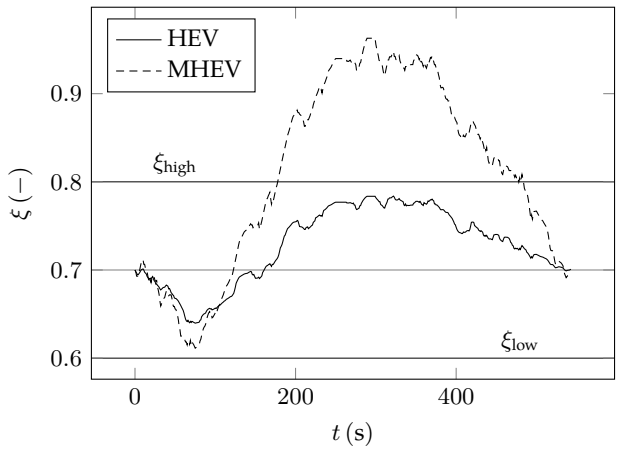

Figure 3.11 SOC trajectory for HEV and MHEV

The inequality (3.22a) can be represented in the form $\mathbf{h}(t) \geq \mathbf{0}$:

$$h_1(t) = \xi_{\text{high}} - \xi(t) \geq 0 \tag{3.43a}$$
$$h_2(t) = \xi(t) - \xi_{\text{low}} \geq 0 \tag{3.43b}$$

In the indirect adjoining method, pure state constraints (that don't explicitly depend on the control variable) are differentiated as many times before the control variable T_{m} appears explicitly and then are adjoined with multiplier ν to the original Hamiltonian $\mathscr{H}$ forming Lagrangian $\mathscr{L}$.
In the case of (3.44), only one differentiation is necessary, resulting in:

$$h_1^1(t) = -\dot{\xi}(T_{\text{m}}(t)) \tag{3.44a}$$
$$h_2^1(t) = \dot{\xi}(T_{\text{m}}(t)) \tag{3.44b}$$

where the superscript 1 denotes first derivative. Augmenting the Hamiltonian results in

Lagrangian

$$\begin{aligned}\mathscr{L}(T_{\mathrm{m}}(t), p(t), \boldsymbol{\nu}(t), t) &= \mathscr{H}(T_{\mathrm{m}}(t), p(t), t) + \boldsymbol{\nu}(t)\mathbf{h}^1(T_{\mathrm{m}}(t)) = \\ &= \dot{m}_{\mathrm{f}}(T_{\mathrm{m}}(t), t) + (p(t) - \nu_1(t) + \nu_2(t))\,\dot{\xi}(T_{\mathrm{m}}(t))\end{aligned} \tag{3.45}$$

The constraints $\mathbf{h}$ reduce the admissible control variable region on the boundary as $\mathbf{h}^1 \geq \mathbf{0}$ has to hold true for (3.44) to hold true. Applied to the HEV model, this translates to that the battery can only be discharged ($\dot{\xi} \leq 0$) while on the upper boundary and vice versa. The optimal control is control from the new admissible region that minimises the Hamiltonian.

The costate

$$\dot{p}(t) = -\frac{\partial \mathscr{L}}{\partial \xi}(T_{\mathrm{m}}(t), p(t), \boldsymbol{\nu}(t), t) = 0 \tag{3.46}$$

remains constant as $\mathscr{L}$ is still not dependent on the state variable ξ, and therefore obtaining the trajectory of $\boldsymbol{\nu}$ is not needed. However, the jump condition states that the costate may have a discontinuity at each time τ the state reaches or exits the boundary:

$$p(\tau^+) = p(\tau^-) - \boldsymbol{\eta}(\tau)\frac{\partial \mathbf{h}}{\partial \xi}(\tau) \tag{3.47}$$

where the τ^+ and τ^- denote the left-hand side and the right-hand side limits, respectively, and $\boldsymbol{\eta}$ is the jump parameter – a vector for each point τ_i of discontinuity of the costate p.

After plugging the differentiation of $\mathbf{h}$ into (3.47), the discontinuity condition becomes

$$p(\tau^+) = p(\tau^-) \pm \boldsymbol{\eta}(\tau) \tag{3.48}$$

where the sign depends on whether the upper or the lower boundary of ξ is reached.

All this means that every time the SOC reaches either ξ_{low} or ξ_{high}, the constant costate is increased/decreased by an unknown value $\eta(\tau_i)$ (different for each contact time τ_i). At the contact time, $\mathbf{h}^1 \geq \mathbf{0}$ has to hold true not to violate constraints.

Based on these conditions, the original problem of finding p over time interval $[0, T]$ is broken down into finding optimal p_i at each interval between time points τ_i, where the constraints are violated, which results in a p trajectory with discontinuous jumps.

The procedure is as follows. Firstly, the unconstrained problem is solved. If it does not violate SOC constraints, the solution is considered optimal. If the state constraints are violated, time τ_i, where the constraint is violated 'the most' (furthest from the boundary) is considered a contact time and therefore a point of p-discontinuity. Because it is a maximum (minimum), it is clear that the condition $\mathbf{h}^1 \geq \mathbf{0}$ will hold true. At this time τ_i, the value of SOC $\xi(\tau_i)$ is set to a value of the boundary it violates as a boundary condition for two subproblems, breaking down the time interval into two ($[0, \tau_i]$ and $[\tau_i, T]$). The optimal problem is then solved for each of the two subintervals with boundary conditions:

$$\begin{aligned} t_{10} = 0,\ t_{1f} = \tau_i, \quad \xi(t_{10}) = \xi_0,\ \xi(t_{1f}) = \xi_{\text{high/low}} \\ t_{20} = \tau_i,\ t_{2f} = T, \quad \xi(t_{20}) = \xi_{\text{high/low}},\ \xi(t_{1f}) = \xi_f \end{aligned} \tag{3.49}$$

obtaining unique p_i for each one. If after this the constraints are still violated at a certain point, the procedure is repeated, subdividing the intervals further with previously set SOC boundary conditions (3.49) as fixed.

Iterated ξ trajectories in this fashion are shown in Figure 3.12, where 3 iterations were required before the constraints were not violated at any point. Naturally, multiple iter-

ations increase the computation time of the algorithm, however, in a lot of cases, the state constraints are not violated (hence no additional iterations are needed). Additionally, computation time decreases roughly linearly when decreasing the time steps inside an interval, making optimisation on subdivided intervals faster.

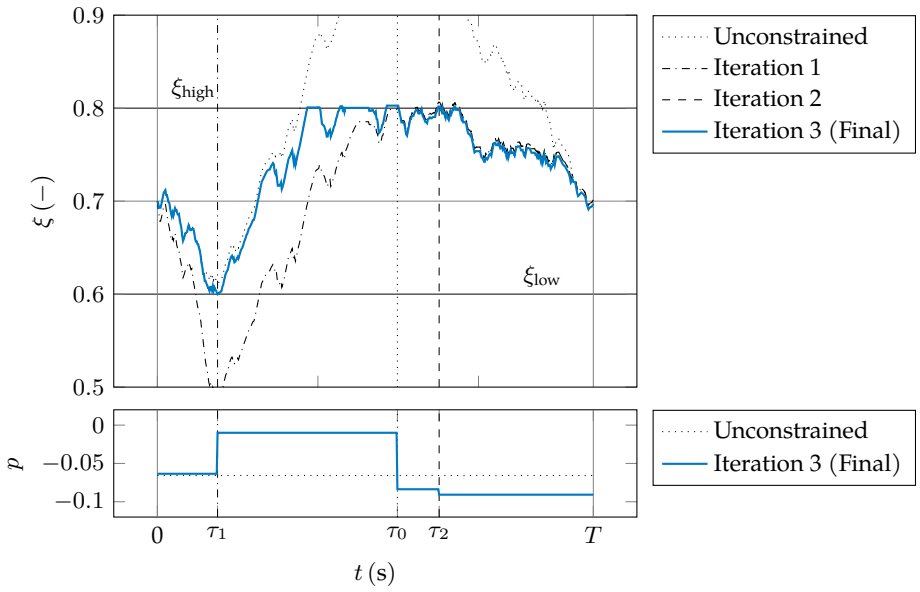

Figure 3.12 Costate (equivalence factor) p iteration to satisfy state ξ inequality constraints; vertical lines repesent divison into subintervals after each iteration.

The resulting trajectory from Figure 3.12 is compared in Figure 3.13 with trajectory optimised with dynamic programming, where inequality constraints can be handled simply by not including values exceeding the boundaries in the state vector, or by setting the cost to reach final state from forbidden states to a high value. It can be seen that apart from small allowed deviations, the PMP approach yields optimal results in accordance with DP, and therefore can be used for reference trajectory generation.

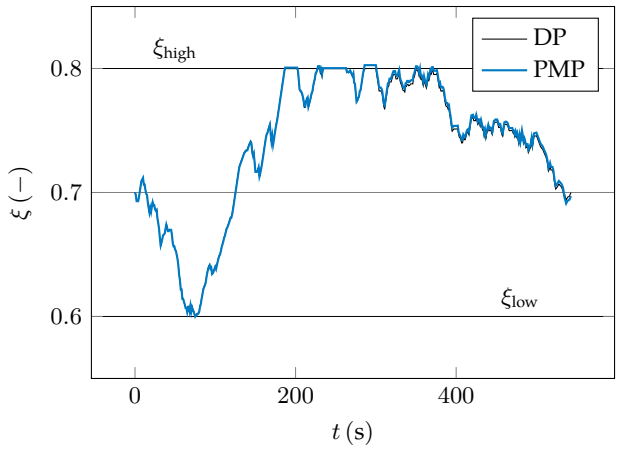

Figure 3.13 Comparison of DP and PMP generated state trajectory with active inequality constraints

3.4.4 Efficiency Maps Approximation

One of the main execution-speed bottlenecks is the lookup table form of efficiency maps of the the ICE and the EM (Figs. 3.6 and 3.7), as both values need to be calculated for every value of the control variable T_m at each time step. Performing bilinear interpolation every time these efficiency values are needed is not very computationally effective, and therefore the lookup tables were approximated by polynomial surfaces as a function of T_e or T_m and ω. Three degrees for each dimension was deemed sufficient for the EMs, resulting in a function in the form:

$$\begin{aligned} f(x,y) = a_{00} + a_{10}x + a_{01}y + a_{20}x^2 + a_{11}xy + a_{02}y^2 + \\ + a_{30}x^3 + a_{21}x^2y + a_{12}xy^2 + a_{03}y^3 \end{aligned} \tag{3.50}$$

where x represents RPM, y represents torque and a_{ij} are coefficients unique for each map.

Because the accuracy of the BSFC map plays an important role in the Hamiltonian, especially the variation of torque with constant RPM, second degree polynomial in x-direction and fifth degree polynomial in the y-direction was selected instead. This improves the accuracy for different torque values, although simultaneously increases the computation time. The resulting form of the surface formula is:

$$\begin{aligned} f(x,y) = a_{00} + a_{10}x + a_{01}y + a_{20}x^2 + a_{11}xy + a_{02}y^2 + a_{21}x^2y + a_{12}xy^2 + a_{03}y^3 + \\ + a_{22}x^2y^2 + a_{13}xy^3 + a_{04}y^4 + a_{23}x^2y^3 + a_{14}xy^4 + a_{05}y^5 \end{aligned} \tag{3.51}$$

Original and approximated maps are shown in Figures 3.14, 3.15 and 3.16, along with respective coefficients of determination describing the quality of the approximation.

Tested on a loop of one million value calculations, plugging into (3.50) is roughly 17 times faster than using a lookup table. While the increased degree of polynomials in (3.51) makes it roughly 1.7 times slower than (3.50), it still constitutes a significant improvement over a lookup table. Maximum torque curve values are calculated only once every time step and therefore have been kept in a lookup-table form.

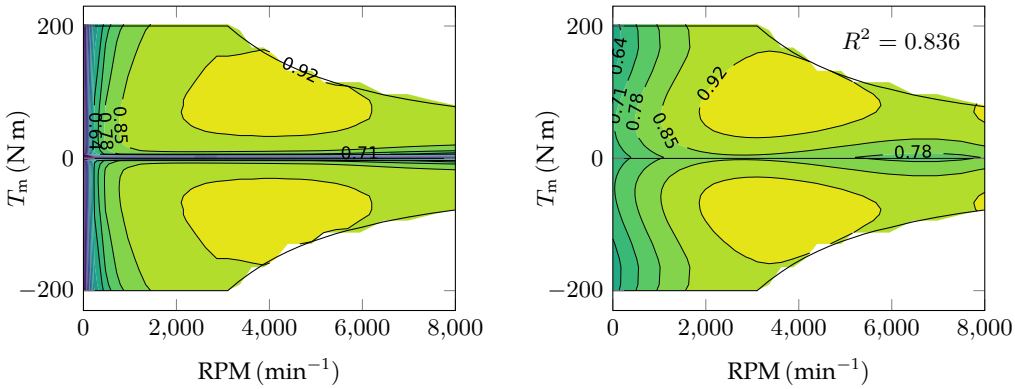

A Original B Approximation

Figure 3.14 Approximation of 65 kW EM efficiency map

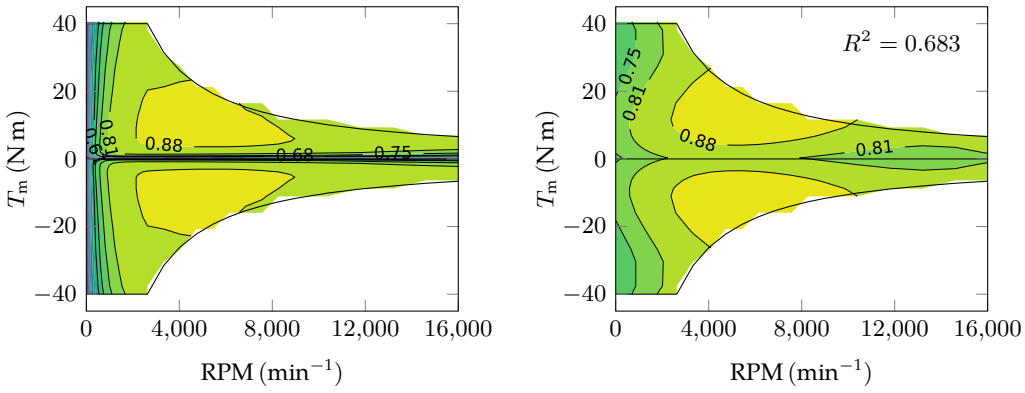

A Original B Approximation

Figure 3.15 Approximation of 11 kW EM efficiency map

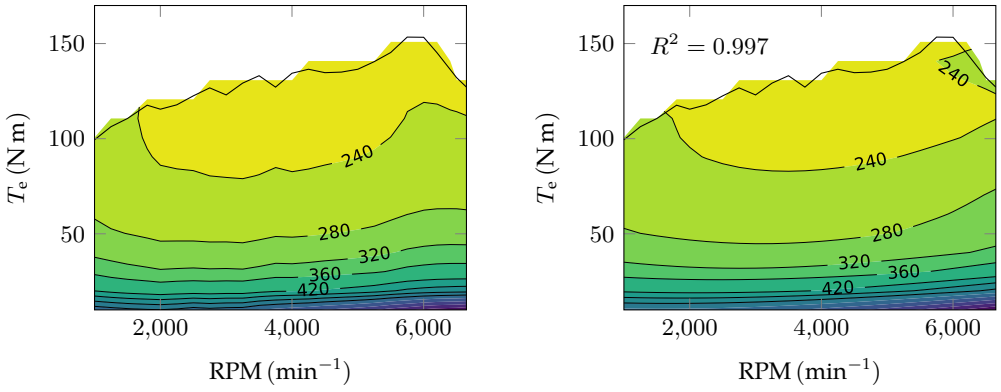

A Original B Approximation

Figure 3.16 Approximation of ICE BSFC map

3.4.5 Computational Speed

In the current state, the reference trajectory generation takes around $2 - 4$ ms for every second of the trip in real-time, depending on the number of required iterations. In the cases where the state constraints are violated, the algorithm takes at least twice as much up to depending on the number of violations. This was measured using *Python 3.7* on an *Intel 8th Generation* CPU running approximately at 3.5 GHz. Because Python is an interpreted language, its execution speed is quite low, and therefore the algorithm can be made significantly faster by implementing it in *C* language. Even at lower clock speed, the algorithm should be reasonably fast for reference trajectory generation before a trip.

Different processing units and languages make it difficult to assess the execution speed of the algorithm in absolute terms, however, in relative comparison to DP, the PMP algorithm is significantly faster[6]. DP using the simplified model and approximate maps takes around 250 ms per second of trip real-time, making PMP 60 times faster. DP us-

[6]The execution speed of DP naturally depends on the step size of state (SOC) discretisation. Based on the comparison with PMP results, $\Delta\xi = 0.001$ was deemed sufficient for the purposes of the thesis

ing non-simplified model and look-up table maps takes around 700 ms, making the PMP algorithm around 200 times faster than the original optimal control problem solved by DP. These numbers are even higher when a SOC trajectory for PHEV is optimised, as the state vector is several times larger. In that case, DP computation for PHEV takes 6 times longer than DP for charge sustaining HEV and MHEV, whereas PMP is unaffected by the SOC range. Figure 3.17 illustrates the computation speed differences between these methods.

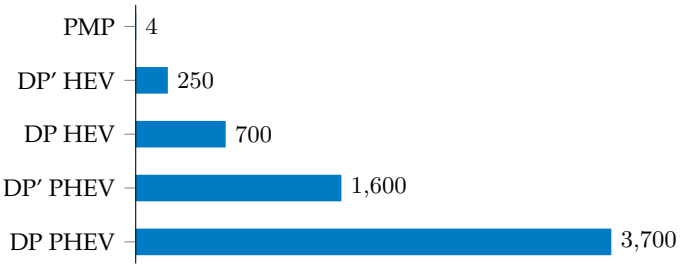

Figure 3.17 Computation speed comparison of different algorithms (in ms/s). DP' represents DP with the same simplified model used for PMP. DP state step size: $\Delta\xi = 0.001$.

Because the simplified model uses functions for efficiency maps, which makes the Hamiltonian a continuous function with an only discontinuity at $T_{\mathrm{m}} = 0$ where the efficiency sign changes, further potential speed improvements can be made by minimising it analytically instead of finding minimum by plugging in values of discretised control variable T_{m}.

3.5 LOW-LEVEL TRACKING LOGIC

In an ideal world, the equivalence factor p that results in the generated reference SOC trajectory would simply be used to minimise the Hamiltonian in real-time driving to obtain optimal control at each instant and the reference SOC would be automatically tracked. However, because the vehicle model is simplified and some parameters are uncertain, the change in SOC due to the work done by the EM (and therefore the whole SOC trajectory) will deviate from the reference (Fig. 3.18) and would not be charge-sustaining even if the speed profile was predicted with perfect accuracy. In other words, the reference value of p is optimal only with respect to the simplified model, but true optimal value is different to an extent dependent on the accuracy of the model.

In addition, the trip speed profile can never be perfectly predicted due to the randomness of driver behaviour, traffic or road obstacles.

The idea is, therefore, to assume that the equivalence factor that generates the reference SOC trajectory is close to the optimal value, and to use it for minimisation of the Hamiltonian in real-time, however, as the SOC trajectory deviates from the reference one, its value will be corrected in feedback to track the reference trajectory. This should result in both obtaining close-to-optimal control with respect to fuel consumption and achieving charge-sustaining operation. A block diagram of the control loop in its final form is shown in Figure 3.19.

3.5.1 Equivalence Factor Feedback

SOC deviations can be corrected by increasing the absolute value of the equivalence factor whenever SOC is being depleted more than reference, and decreasing the value whenever

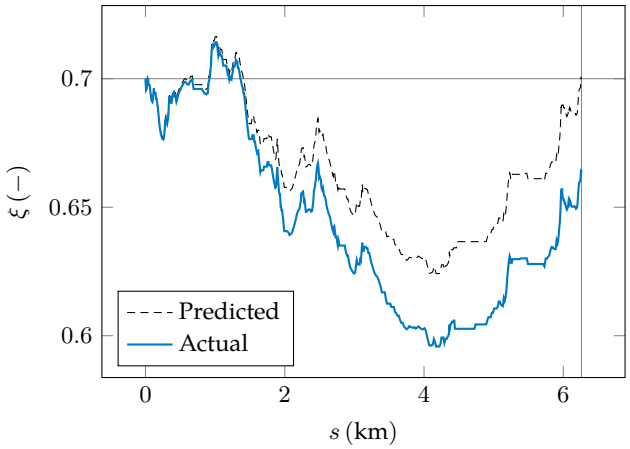

Figure 3.18 Deviation of SOC using reference p due to an inaccurate model

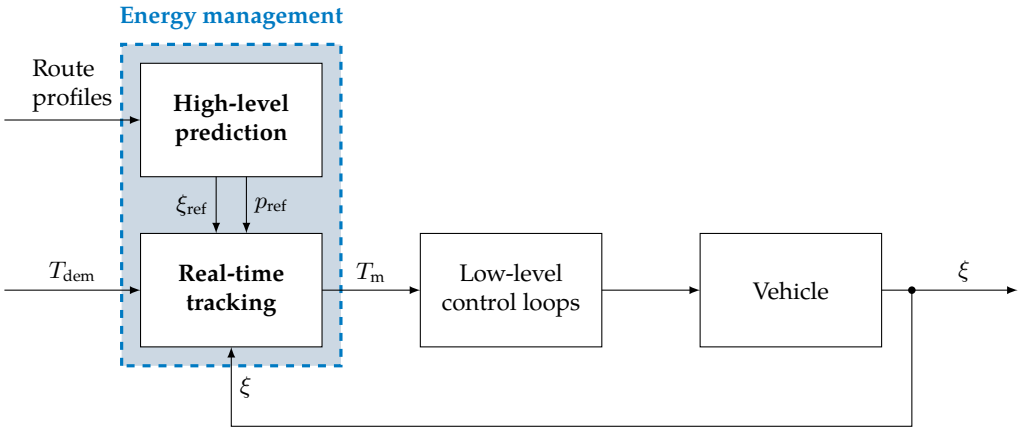

Figure 3.19 Energy management control loop

electric energy is not used enough, resulting in higher SOC than reference. Therefore, a logic similar to PID controller is implemented to correct p at each instant:

$$p(t) = p_{\text{ref}}(t) + K_{\text{p}}(\xi_{\text{ref}}(t) - \xi(t)) + K_{\text{i}} \int (\xi_{\text{ref}}(t) - \xi(t))\, \mathrm{d}t \tag{3.52}$$

Only the proportional and integral terms are used, as the ξ values in a real-life scenario will be affected by an error, making their derivative very inaccurate. For this reason, the proportional term is also calculated from a mean of several past ξ values. A block diagram of the resulting SOC-tracking control loop is shown in Figure 3.20.

Because the assumption is that the reference equivalence factor is nearly optimal, relatively small values for the control coefficients can be chosen. While higher values would track the reference SOC trajectory better, it would result in big jumps in p, leading to the vehicle overcompensating by constantly charging and draining the battery, and hence poor performance over the entire trip. Perfectly tracking the reference is also undesirable, as it is optimal only with respect to the simplified prediction and true optimal trajectory will be different.

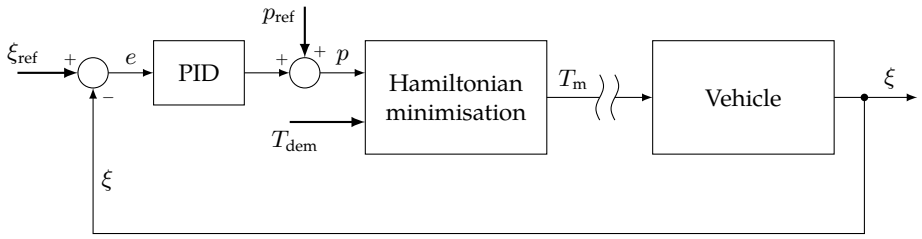

Figure 3.20 Real-time-tracking control loop; thick lines denote inputs.

The values of K_{p} and K_{i} will naturally differ for each of the vehicle configurations, because different capacities (and other parameters) of their battery packs result in different relative SOC depletion based on work done by the EM. By trial and error, values for HEV were obtained. Subsequently, by loosely scaling based on battery capacities, values listed in Table 3.2 were chosen for all configurations. To prevent integral windup, the integral value is zeroed every time the error crosses zero.

Table 3.2 Control term coefficients for each vehicle configuration.

	K_{p}	K_{i}
MHEV	-0.1	-0.0012
HEV	-0.3	-0.003
PHEV	-2	-0.03

Figure 3.21 shows the same route from Figure 3.18 but now with p corrections. While there is still a small deviation from the final SOC value, it is much smaller than in the previous case, where the deviation would additionally grow with the length of the trip. In this example, both the predicted and actual speed profiles were the same, however, when this is not the case, the deviation at the end may become larger even with the implemented corrections. To prevent such effect, the PI control coefficients are set to a several times larger value shortly before the end of the trip, forcing the vehicle to recharge or charge the battery to finish with the required SOC level ξ_f.[7]

The violation of SOC constraints in the prediction is prevented by the optimal-control algorithm, however, since the optimised equivalence factor is only approximate with respect to real driving and the reference-SOC is not tracked precisely, the constraints could end up being violated. Therefore, a rule preventing the use of electric energy when the lower battery limit is reached, and a rule preventing battery charging when the upper battery limit is reached, is implemented.

In the current state of the algorithm, reference SOC is calculated as a function of distance, which assumes the real trip to be the same length as the prediction. This can however be easily violated due to unexpected obstacles, detours or simply by driving in a different lane. In the future, it would be therefore beneficial to track the reference based on the nearest GPS location to accommodate these deviations.

[7] This forced charge-sustaining behaviour is implemented only for fair comparison purposes. In a real scenario, it could be more beneficial starting the next trip with higher/lower SOC and discharge/recharge the battery more efficiently.

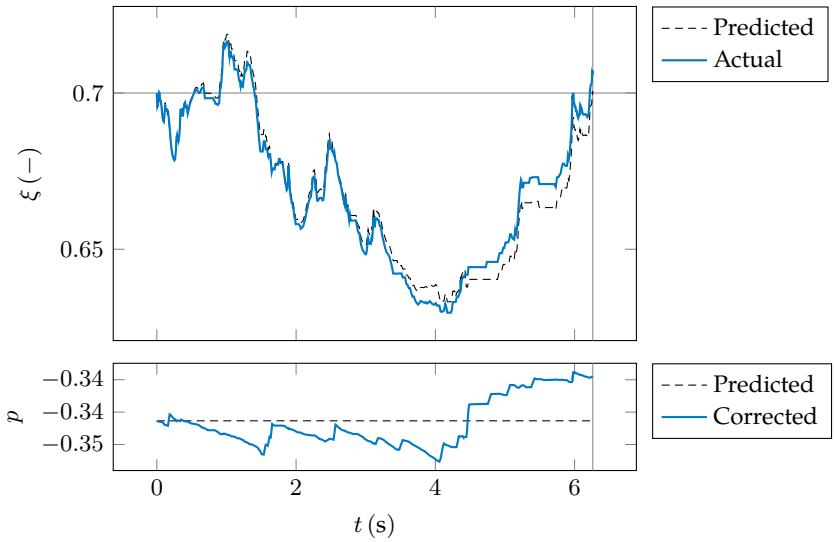

Figure 3.21 Reference and corrected equivalence factor trajectory with resulting SOC trajectory

3.5.2 Errors in Prediction

Ultimately, the prediction inflicts three types of errors:

1. the Hamiltonian is minimised using inaccurate model/maps, therefore the vehicle 'does not know' true optimal operating points, resulting in applying suboptimal control T_{m}, leading to higher fuel consumption;
2. SOC change as a function of applied optimal control is different than the predicted, leading to over-charging or depleting the battery;
3. demanded torque at each instant is different than the prediction, because of different speed or different vehicle parameters, resulting in incorrect p-value, leading again to over-charging or depleting the battery.

Each of these affects the performance of the proposed EMS in some way. While the model can be to some extent tuned to minimise the first two effects and uncertain vehicle parameters, the options to make an accurate speed profile prediction are limited, and therefore robustness to this error is crucial and will be studied in Chapter 4, where the strategy is tested on several routes.

The effect of uncertain parameters was already shown in previous Figures 3.18 and 3.21. To take this into account in the simulations, the trip prediction will assume—apart from simplified efficiency and battery maps—slightly different values than in Table 3.1. More about this and the entire simulation setup will be discussed in the following Section 3.6.

The value of Hamiltonian has a significant effect on performance, as it is used both in the prediction and the real-time control. This means that the engine efficiency and electric path efficiency[8] (battery, inverter, motor) for different operating points should be finely tuned to obtain the best results. This is especially true for the engine BSFC map, as fuel consumption is the target of the optimisation and if the vehicle tries to keep the engine in

[8]The equivalence factor does not play a role in this, as it only linearly scales the relative efficiency of the EM with respect to the ICE without changing the optimal operating point of the EM.

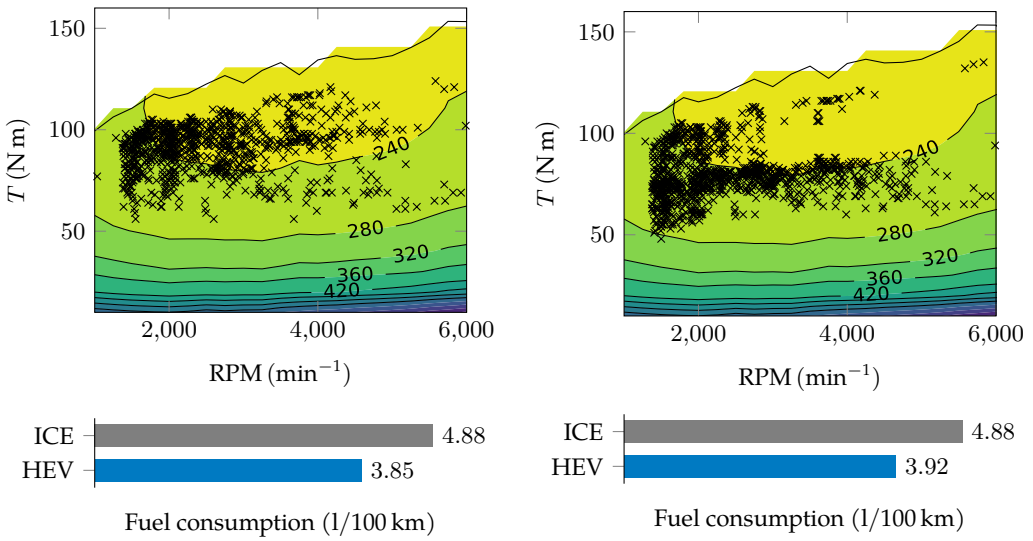

A Fifth-degree polynomial in y direction

B Third-degree polynomial in y direction

Figure 3.22 Resulting engine operating points and fuel consumption using different BSFC map surface approximations, overlaid on a true BSFC map; ICE: vehicle with conventional powertrain for absolute comparison, HEV: optimised hybrid vehicle.

the most efficient operating points of an approximation, which are not the most efficient in reality, the performance quickly decreases.

Using approximations in the Hamiltonian for the trip prediction does not result in a significant difference in performance, because the change in SOC trajectory and equivalence factor is quite small to affect the tracking of the PID. However, the real-time Hamiltonian minimisation at the low level then tries to keep the engine operating at points that are not optimal in reality, and therefore, even though the result will be charge-sustaining behaviour, it will not be reached in the most efficient manner. An example of this is shown in Figure 3.22, where a trip was optimised using different levels of approximation for a BSFC map. The inaccuracy of the only third-degree approximation causes the algorithm to keep the engine operating at points which are less efficient in reality, resulting in increased fuel consumption.

Because the surface interpolation approximation was introduced for computational efficiency of the prediction, more accurate lookup tables can be used in real-time, where the Hamiltonian is only minimised once instead of several thousand times, and therefore the computational burden is not as high. Nevertheless, some error will always be present. This will be simulated by using surface interpolations and constant battery parameters instead of real lookup table maps for both the prediction and the low level, because the 'real' vehicle here is already simplified by lookup tables, which do not take into account thermal behaviour or transients.

3.6 SIMULATION SETUP

The EMS is tested on several routes to test its overall performance and robustness to errors and uncertainties from the previous section. Each configuration (HEV, MHEV and PHEV) is tested separately and every result is compared to:

1. optimal solution using dynamic programming
2. rule-based strategy without knowledge of the trip
3. conventional (non-hybrid) vehicle

With respect to the relatively slow vehicle speed dynamics and frequency of collected route data, the simulation is discretised with a step size of 1 s. The control variable T_{m} is discretised in both DP and PMP with step size of 2 N m for HEV and PHEV, and 1 N m for MHEV.

For DP, the state variable ξ was discretised with a step size of 0.00025 for the HEV and 0.0005 for the MHEV, as smaller battery capacity leads to higher battery percentage depletion per work done by the EM, which means that the step does not need to be as small. Contrary to this logic, step size of 0.001 was selected for the PHEV. This is due to the fact that the PHEV has a wider SOC range of operation, which would lead to a very long solution computation. A larger step size, combined with the numerical nature of DP, means that the DP results presented in the following section may not be perfectly accurate due to numerical errors and is solely indicative of the fuel consumption improvement limits for the proposed strategy, which may in some cases outperform the DP 'optimum'.

3.6.1 Vehicle Parameters

To test the robustness of the strategy to the disturbance caused by simplified and uncertain model, two sets of parameters are used for each of the hybrid vehicle configurations – one for the simplified predicted model and one for the real vehicle.

Simply put, the prediction makes several simplifying assumptions to increase computation speed, and some of the vehicle parameters might be slightly different in real life than the algorithm assumes. This means that the prediction is made using one set of parameters, but the behaviour of the real vehicle is then governed by the actual parameters. The reference SOC and equivalence factor trajectory are therefore generated assuming the simplified model. The reference SOC is then tracked on the actual trip by the vehicle with real parameters, however, using the simplified model and uncertain parameters for the real-time Hamiltonian minimisation. Both dynamic programming and the rule-based strategy naturally use the parameters of the real vehicle for comparison.

The parameters of the real vehicle are the ones listed in Table 3.1, whereas the simplified, uncertain vehicle uses slightly modified values of some of these. The differences are summed up in Table 3.3. The parameters that are not common for all HEV configurations are naturally approximated by different values/functions.

Table 3.3 Real vehicle and simplified vehicle parameters

	Real	**Simplified**
Engine BSFC	lookup table (RPM, T)	$f(\mathrm{RPM}, T)$
EM efficiency	lookup table (RPM, T)	$f(\mathrm{RPM}, T)$
Battery internal resistance R	lookup table (ξ)	const.
Battery open-circuit voltage V_0	lookup table (ξ)	const.
Rolling resistance coefficient f	0.021	0.019
Tire dynamic rolling radius r_d	0.3	0.31
Drag coefficient c_x	0.31	0.29

3.6.2 Routes

Data from several routes was collected to represent multiple trip types (city, highway, extra-urban) as well as different elevation characteristics. This was done by recording speed and elevation data with a frequency of 1 Hz using *GPS Tracks* mobile application while driving along predefined routes, and afterwards manually filtering the collected data in *Microsoft Excel* to eliminate unrealistic acceleration and road slope peaks.

While the accuracy of mobile phone GPS placed inside a car is not ideal to perfectly reflect the real motion of the vehicle, as long as the collected data is physically feasible and realistic in terms of road infrastructure, it should be sufficient for EMS comparison.

To test the robustness of the proposed EMS with respect to variation of the real speed profile to a predicted one, each route was recorded multiple times, where the first of the speed profiles takes the role of the prediction and the rest as actual speed. Shorter routes were recorded four times, resulting in one prediction profile and three test runs, while the longer routes only three times, resulting in one prediction profile and two test runs. In other words, the predicted speed profile for every tested trip on the same route stays the same while the other speed profiles are used as the actual speed. A test trip where the actual speed profile is the same as the predicted profile is done for each of the routes as well, showing the robustness of the EMS only with respect to the simplified vehicle model and parameter uncertainty. Because the reference SOC trajectory is tracked based on driven distance, it was necessary that each trip on the same route was the same length.

Table 3.4 Route parameters with average speed of each trip; ↩ denotes a return route. Average speed does not take into account the time the vehicle is stationary to better represent the driving style differences.

	Length (km)	Ascent (m)	Descent (m)	Δ (m)	Trip avg speed (km/h) 0	1	2	3
1 | City 1	3.85	14	−116	−102	26.8	33.2	30.6	29.9
2 | City 1 ↩	3.62	117	−15	102	30.3	32.0	29.6	29.9
3 | City 2	6.26	121	−67	54	35.4	33.5	33.8	34.4
4 | City 2 ↩	6.24	63	−117	54	40.4	36.0	36.7	42.4
5 | Extra-urban	44.4	600	−777	−177	63.9	60.4	66.9	-
6 | Highway/City	47.1	609	−464	145	69.2	73.7	63.8	-
7 | Highway/City ↩	55.5	537	−614	−77	74.2	78.1	74.3	-
8 | Highway/Extra-urban	122.4	1486	−1163	323	79.6	80.9	80.5	-
9 | Highway/Extra-urban ↩	123.9	1384	−1718	−334	81.1	77.9	82.7	-

The recorded routes with their parameters and individual trip average speeds are listed in Table 3.4, where the name represents major driving types. The following figures (Figs. 3.23–3.31) show speed and elevation profiles of each route with GPS data overlaid on a map. The predicted speed profile is always denoted with a solid line and subsequent speed profiles are then considered real driving and are denoted with dashed, dotted and dash-dotted lines, respectively. HEV and MHEV are tested on all the listed routes, whereas PHEV—which can complete most of them in electric mode only—is tested only on routes 8 and 9 and on a combination of 6 and 7.

The driving style or 'aggressiveness' remained the same across all trips, so the differences on the same routes are due to the inherent randomness of driving behaviour and traffic. The maximum acceleration values rarely exceed 2 m s^{-2} for accelerating and 3 m s^{-2} for braking.

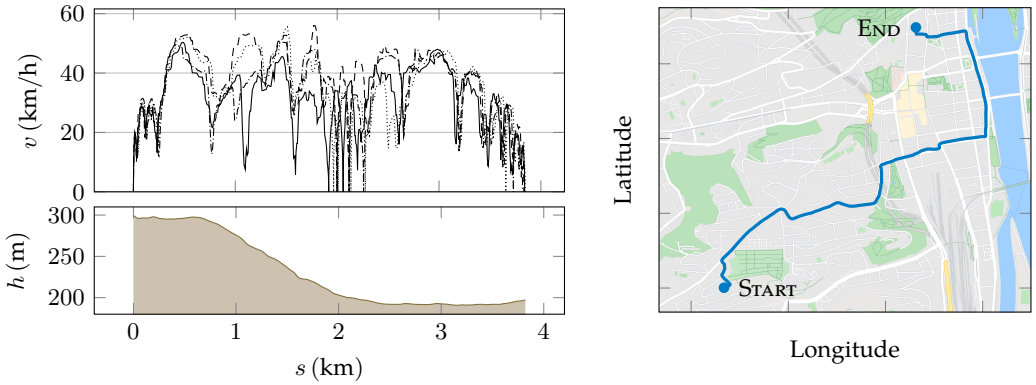

Figure 3.23 Route 1 (City 1)

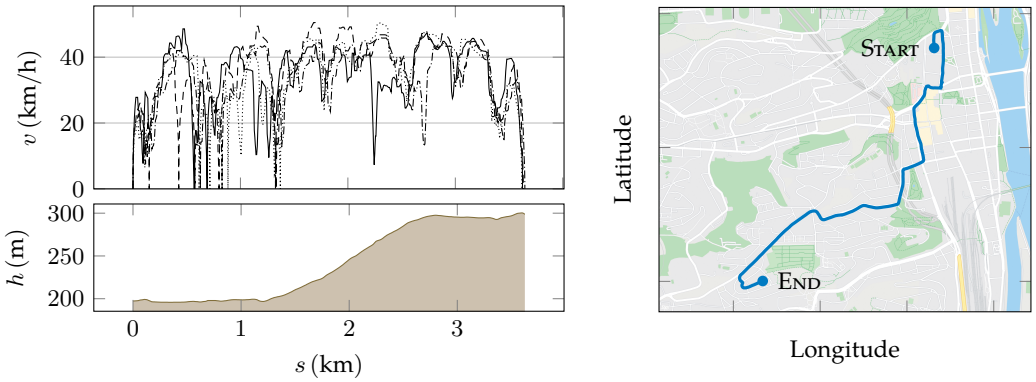

Figure 3.24 Route 2 (City 1 Return)

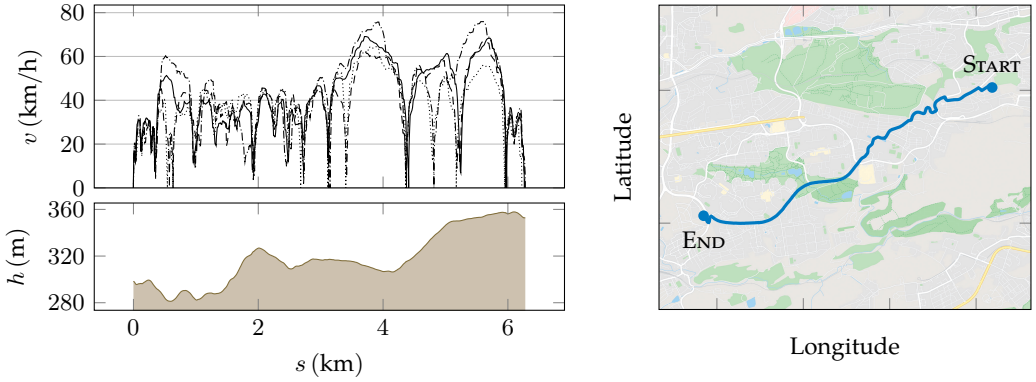

Figure 3.25 Route 3 (City 2)

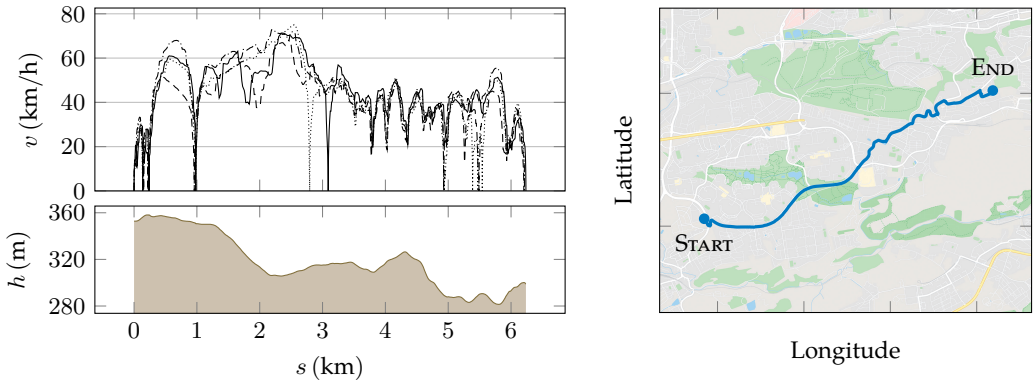

Figure 3.26 Route 4 (City 2 Return)

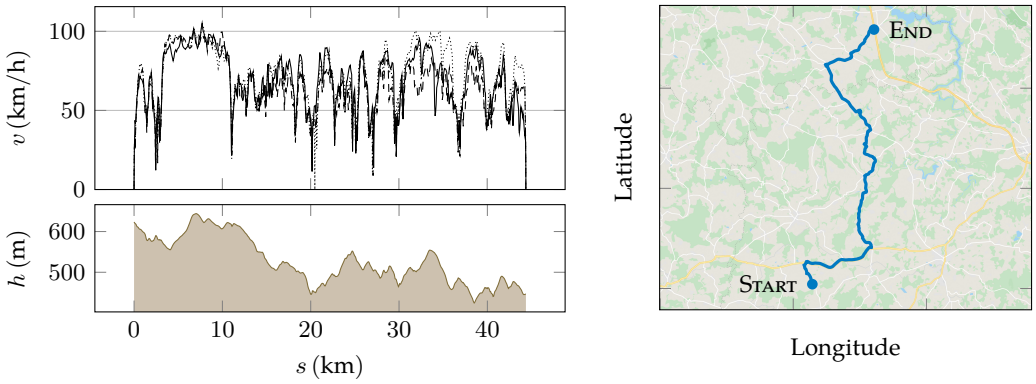

Figure 3.27 Route 5 (Extra-urban)

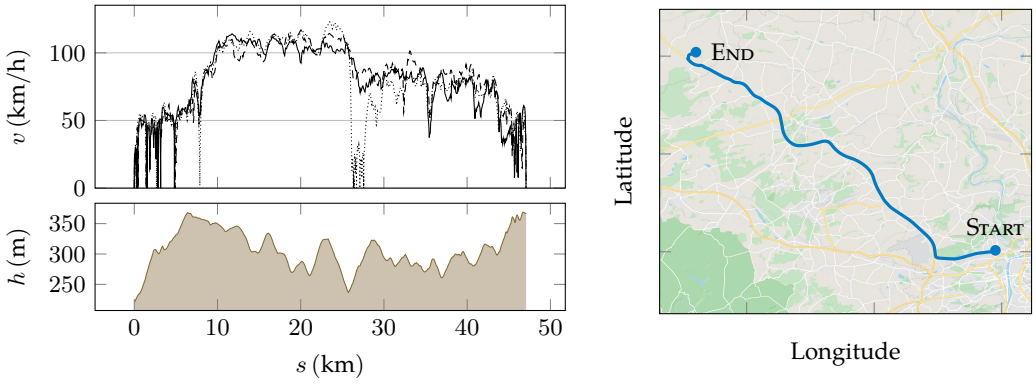

Figure 3.28 Route 6 (Highway/City)

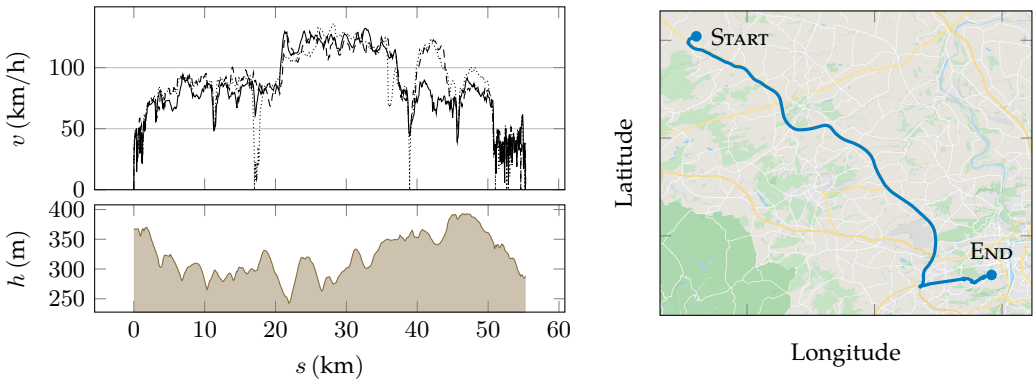

Figure 3.29 Route 7 (Highway/City Return)

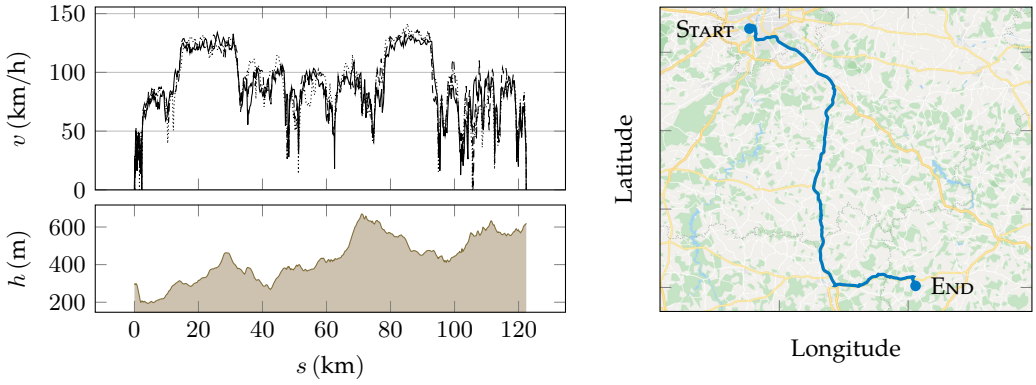

Figure 3.30 Route 8 (Highway/Extra-urban)

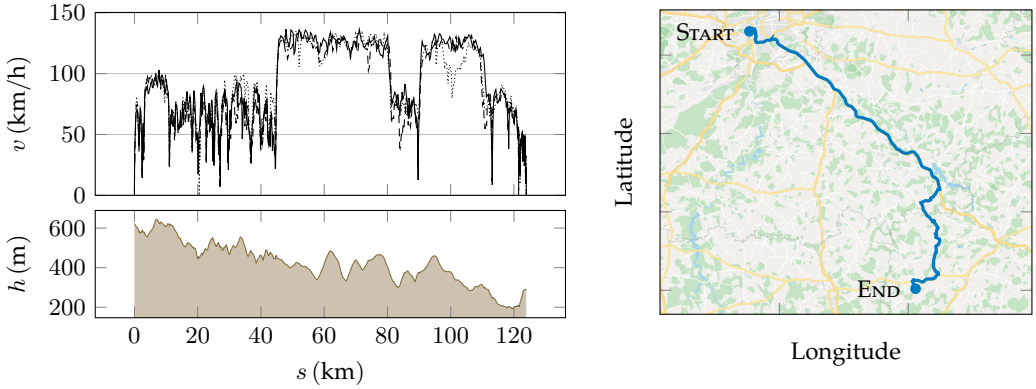

Figure 3.31 Route 9 (Highway/Extra-urban Return)

3.6.3 Performance Comparison

To assess the performance of the proposed strategy, each trip is compared to results from a rule-based strategy (RB), which is usually in some form used in passenger vehicles and which does not take into account trip characteristics, and to an optimal result using dynamic programming (DP), which assumes full knowledge of the trip and the vehicle parameters. Ideally, the resulting fuel consumption from the proposed strategy would lie in between these two, closer to the optimal result. For reference and absolute savings comparison, fuel consumption of a vehicle with conventional ICE-only powertrain (weighing 20 kg less than the MHEV) is included as well.

The same shifting strategy from Section 3.2.7 is used for all of the compared strategies, hence the only control variable is T_{m}.

Rule-Based Strategy

For this comparison, a simple rule-based strategy was designed, slightly different for each of the vehicle configurations (HEV, MHEV and PHEV). The rules are based on intuition and adjusted using the tested trips to achieve approximately charge-sustaining operation. Since the RB does not know when the current trip is going to end, the SOC at the end of the trip will generally not be exactly the required value, but higher than that on some trips and lower than that on other.

Because in the real world, operation of the vehicle does not end with one trip and any excess of battery charge can be used in the next one, the fuel consumption calculation converts this amount of energy to approximate amount of fuel saved in the future based on powertrain efficiencies:

$$m_{\mathrm{f}} = -(\xi(t_f) - \xi_f)\, C\, V \frac{\eta_{\mathrm{i}}\, \bar{\eta}_{\mathrm{b}}\, \bar{\eta}_{\mathrm{m}}\, \eta_{\mathrm{tc}}}{H\, \bar{\eta}_{\mathrm{e}}} \tag{3.53}$$

This value is then subtracted from the value of the total fuel consumed. Similarly, reaching SOC value below the charge-sustaining value ξ_f means that the battery will have to be charged in the future with a certain efficiency, resulting in additional fuel consumption

$$m_{\mathrm{f}} = -(\xi(t_f) - \xi_f)\, C\, V \frac{1}{\eta_{\mathrm{i}}\, \bar{\eta}_{\mathrm{b}}\, \bar{\eta}_{\mathrm{m}}\, \eta_{\mathrm{tc}}\, H\, \bar{\eta}_{\mathrm{e}}} \tag{3.54}$$

While this calculation is approximate and may benefit not achieving charge-sustaining SOC value in some cases, the longer the trip, the smaller effect it will have on the calculated average fuel consumption.

An algorithm flowchart of the charge-sustaining rule-based strategy is shown in Figure 3.32. Simply put, the vehicle uses regenerative braking whenever possible (if the SOC is not too high) and uses the EM to cover low-torque requests, where the efficiency of the ICE is very low. Furthermore, depending on whether the SOC is above or under the charge-sustaining value ξ_f, ICE or EM is used accordingly. Soft SOC constraints $\xi_{\text{low, soft}}$ and $\xi_{\text{high,soft}}$ were additionally introduced to determine how much electric energy can be used, or whether the battery should be recharged by the engine.

Strategies for HEV and MHEV differ only in constants used in the EM torque T_{m} calculations (how small torque request has to be to be covered by the EM only and to which extent the vehicle uses torque assist). Strategy for PHEV consists of a charge-depleting mode, where only the EM is used before reaching the charge-sustaining value ξ_f, after

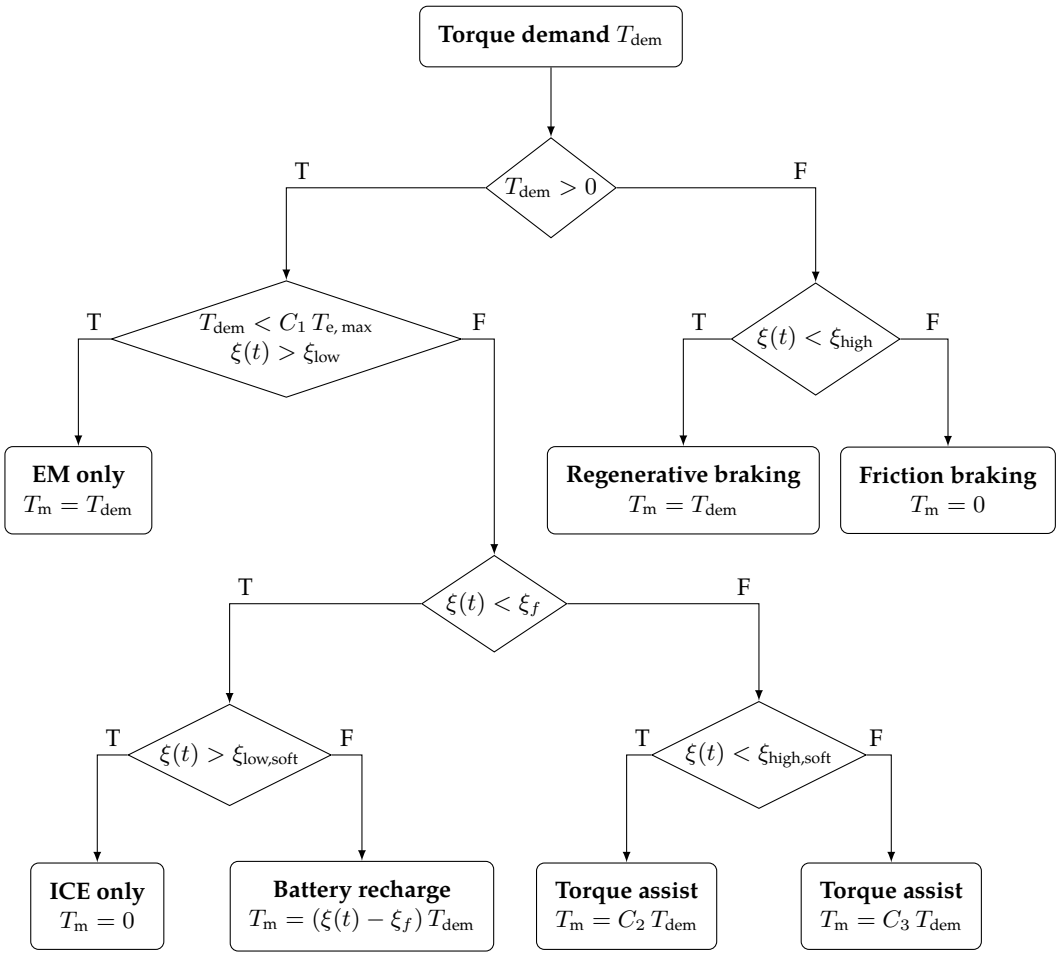

Figure 3.32 Rule-based strategy flowchart; T: True, F: False, constants C_1, C_2 and C_2 are different for HEV (PHEV) and MHEV; if calculated T_{m} values are too high for the EM, maximum possible torque is applied.

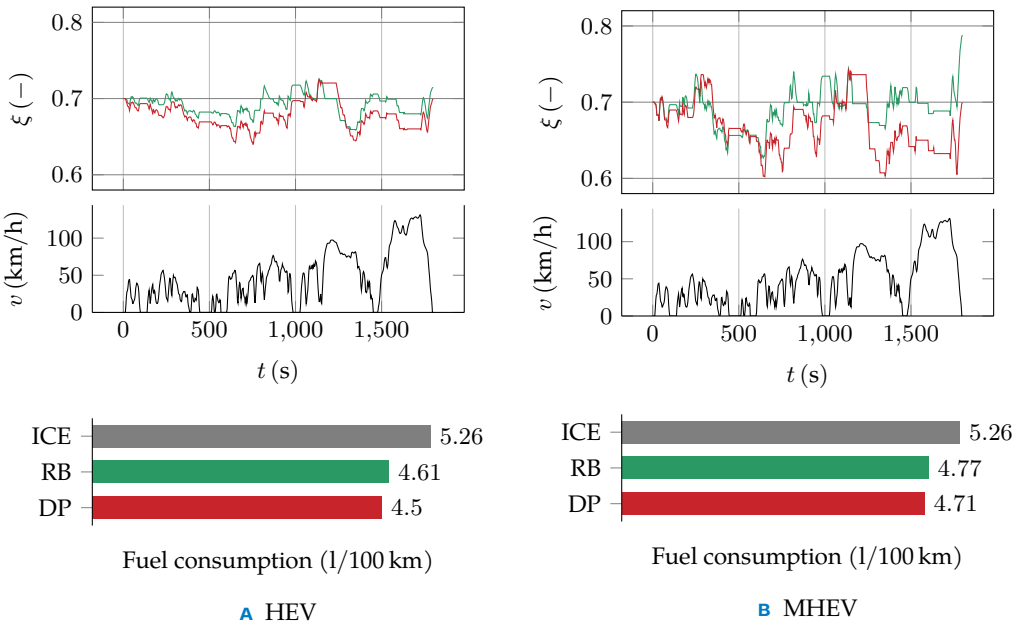

Figure 3.33 Rule-based strategy test cycle (WLTP), showing SOC trajectory, speed profile and fuel consumption; ICE: vehicle with ICE-only propulsion, RB: rule-based, DP: dynamic programming.

which the same strategy as for the HEV is employed.

To compare EMSs in the same conditions, no control logic or penalty is implemented to take into account frequent engine starts.

Figure 3.33 shows performance of the rule-based strategy on a HEV and MHEV driving WLTP cycle. The result is compared with the same trip optimised with DP and fuel consumption of a vehicle with a conventional ICE powertrain. It is worth noting that the difference between a rule-based algorithm and optimal solution on trips like these, where large part of the total energy is used for highway driving (with high ICE efficiency and no recuperation possibilities), is in absolute terms already quite small, especially for a MHEV, and therefore there is only a small room for improvement, as the proposed EMS should lie somewhere in between. PHEV was not tested separately, because it can complete this cycle in charge-depleting mode using battery energy only and its charge-sustaining control logic is the same as the HEV.

Chapter 4

RESULTS

Testing each vehicle on all of the routes specified in Section 3.6.2 results in 31 trips for both the HEV and MHEV, and 9 trips for the PHEV. An exhaustive list of all the results without commentary is included in Appendix A. This chapter highlights only some of the results showing the characteristic behaviour of the EMS and its shortcomings, including a comparison to the other tested strategies. To save space and avoid repetition, Table 4.1 explains the color codes used in the graphs throughout this chapter.

Table 4.1 Legend for the following graphs

Predicted	2LVL	DP	RB	Predicted speed	Real Speed	Elevation
.....	———	———	———	.....	———	———

Overall, the proposed EMS (further referred to as 2LVL) outperformed the rule-based strategy in most cases and the results were close to the optimal solution from DP. The improvement percentages for every trip are listed in Tables 4.2, 4.3 and 4.4 for HEV, MHEV and PHEV, respectively. The percentages show the relative improvement over the rule-based strategy with respect to ICE-only consumption using formula:

$$\Delta FC_{rel} = \frac{FC_{ICE} - FC_{2LVL}}{FC_{ICE}} - \frac{FC_{ICE} - FC_{RB}}{FC_{ICE}} = \frac{FC_{RB} - FC_{2LVL}}{FC_{ICE}} \tag{4.1}$$

where FC is the fuel consumption and ΔFC_{rel} the relative improvement. The numbers in parentheses denote the upper limit[1] for improvement using DP. Because trip 0 is a trip where the real speed was the same as the predicted speed, it in most cases leads to a result closer to DP than the rest, as there is one fewer source of disturbance. It therefore only acts as an indication to what extent different speed profiles affect the results and does not count towards the average improvement.

There are two possible ways of interpreting the results. In absolute terms – how big the fuel consumption improvement is with respect to the RB strategy (numbers in tables above), or in relative terms – how close the 2LVL result is to the optimal solution on the DP-RB scale. To assess the performance of the strategy itself, the relative comparison is more appropriate. However, in a real application, absolute values are ultimately of bigger importance, whether the savings outweigh the efforts of implementation.

[1] As discussed in Section 3.6, the 2LVL strategy in some cases outperforms DP, which is more prone to numerical errors, especially in the case of PHEV where bigger state step size was selected. The upper limit for improvement is therefore only indicative.

Table 4.2 Relative improvement over the rule-based strategy with respect to ICE-only consumption for HEV (in percent); numbers in parentheses denote DP result.

	Trip 0	Trip 1	Trip 2	Trip 3	Avg
1 | City 1	19.6 (21.3)	17 (17.6)	18.6 (21)	19.9 (19.8)	**18.5**
2 | City 1 ↩	2.1 (1.7)	1.3 (1.7)	0.3 (2.1)	3.5 (5.7)	**1.7**
3 | City 2	4.4 (4.2)	3.6 (4.7)	2.3 (4.9)	1.2 (3.6)	**2.4**
4 | City 2 ↩	7.3 (6.9)	6.1 (6.1)	7 (7.2)	5.3 (5.9)	**6.1**
5 | Extra-urban	4.4 (4.2)	4 (4.4)	3.9 (3.8)	-	**4**
6 | Highway/City	1.6 (1)	1 (0.9)	1 (1.5)	-	**1**
7 | Highway/City ↩	1.4 (1)	1.3 (1)	1.6 (1.4)	-	**1.5**
8 | Highway/Extra-urban	1.7 (1.7)	1.1 (1.3)	1.1 (1.2)	-	**1.1**
9 | Highway/Extra-urban ↩	1.5 (1.9)	2.1 (1.9)	2.1 (2)	-	**2.1**

Table 4.3 Relative improvement over the rule-based strategy with respect to ICE-only consumption for MHEV (in percent); numbers in parentheses denote DP result.

	Trip 0	Trip 1	Trip 2	Trip 3	Avg
1 | City 1	12.6 (13.7)	11.2 (12.9)	9.9 (11.3)	12.1 (14.6)	**11.1**
2 | City 1 ↩	0.2 (0.4)	−0.5 (0.2)	0.3 (1.3)	0.9 (2)	**1.7**
3 | City 2	1.8 (2.3)	1.2 (2.4)	1 (2.1)	0.7 (1.8)	**1**
4 | City 2 ↩	3.1 (3.7)	1.1 (3.1)	3.5 (4.8)	2.6 (3.4)	**3.1**
5 | Extra-urban	1.7 (2.1)	1.3 (2.1)	1.3 (1.9)	-	**1.3**
6 | Highway/City	0.4 (0.6)	0.3 (0.6)	0.2 (0.9)	-	**0.3**
7 | Highway/City ↩	0.1 (0.4)	0.1 (0.5)	0.1 (0.7)	-	**0.1**
8 | Highway/Extra-urban	0.6 (0.8)	0.3 (0.7)	0.1 (0.6)	-	**0.2**
9 | Highway/Extra-urban ↩	0.7 (1)	0.6 (1)	0.6 (1)	-	**0.6**

Table 4.4 Relative improvement over the rule-based strategy with respect to ICE-only consumption for PHEV (in percent); numbers in parentheses denote DP result..

	Trip 0	Trip 1	Trip 2	Avg
6+7 | Highway/City & ↩	4.1 (4)	3.7 (3.7)	3.8 (3.8)	**3.8**
8 | Highway/Extra-urban	4.6 (4.6)	4.2 (3.9)	4.3 (4)	**4.3**
9 | Highway/Extra-urban ↩	3 (3.4)	3.3 (3.1)	3.3 (3.2)	**3.3**

4.1 HEV & MHEV

The goal of an EMS in a charge-sustaining HEV is, in general, to use the electric energy obtained from recuperated[2] potential and kinetic energy in the most efficient manner. Hence, the more energy recuperated on a trip, the bigger the potential improvement in fuel consumption there is for a 'smarter' strategy such as the proposed 2LVL. Similarly, the less electric energy available, the smaller the potential for improvement and the smaller the margin of error there is for when conditions are predicted incorrectly or certain vehicle aspect is neglected in the model.

Overall, the results support this theory as the amount of possible improvement (DP-RB scale) with respect to ICE-only vehicle is roughly linearly consistent with the ratio of negative to positive energy required on each trip. Meaning, that the more energy available for recuperation (and consequent EM propulsion) there is, the bigger the possible improvement. As it follows, the biggest fuel savings of the 2LVL compared to RB were attained on such trips.

City driving with stop-and-go traffic or extra-urban driving with braking into curves, combined with elevation variations are consequently applications, where the results are more significant. Figure 4.1 shows an example of these types of trips – 4.1a shows downhill city driving and 4.1b extra-urban driving, attaining 17 % and 4 % improvement, respectively. Obviously, 4.1a is an extreme example of a specific (and short) trip, because a vehicle cannot keep driving only downhill in its lifetime and every elevation loss needs to be compensated in the future by an elevation gain, where the recuperation potential is smaller, averaging out the results over the long-term.

Correspondingly, on trips with mostly uphill driving, or where most of the energy spent is at a constant speed and the elevation does not change much—such as highway driving—the margin of improvement is small. Examples are shown in Figure 4.2. While the 2LVL result is close to the one of DP on the relative scale between DP and RB, the absolute improvement in fuel consumption is very small – 1 % and 1.1 %, respectively.

Similarly, while the behaviour of the EMS applied to HEV and MHEV is similar between these two configurations, due to less electric energy available (lower EM power and smaller battery), the band for improvement between RB and DP is already quite narrow, making the absolute fuel consumption savings very small – around 1 % in most cases (Tab. 4.3).

However, while important to assess the absolute savings on different types of trips, these findings are not really inherent to the performance of the proposed strategy itself. The characteristics of the 2LVL will now be expanded on.

4.1.1 General Observations

Overall, the 2LVL performs quite well, reasonably close to optimal results, even with speed profile variations to the predicted ones (to some extent) and uncertain vehicle parameters.

However, as it turns out, the idea behind SOC trajectory tracking is only partly responsible for good results, as the true optimal DP trajectory may in some cases significantly deviate from the prediction due to the inflicted errors. Hence, only small values for the PID coefficients were selected – to follow the SOC trajectory on a larger scale (low frequencies of the SOC trajectory), while not overcompensating for disturbances on a smaller scale (high frequencies of the SOC trajectory).

[2] ICE charging is not very frequent in an optimal solution, because of the efficiency of double energy conversion.

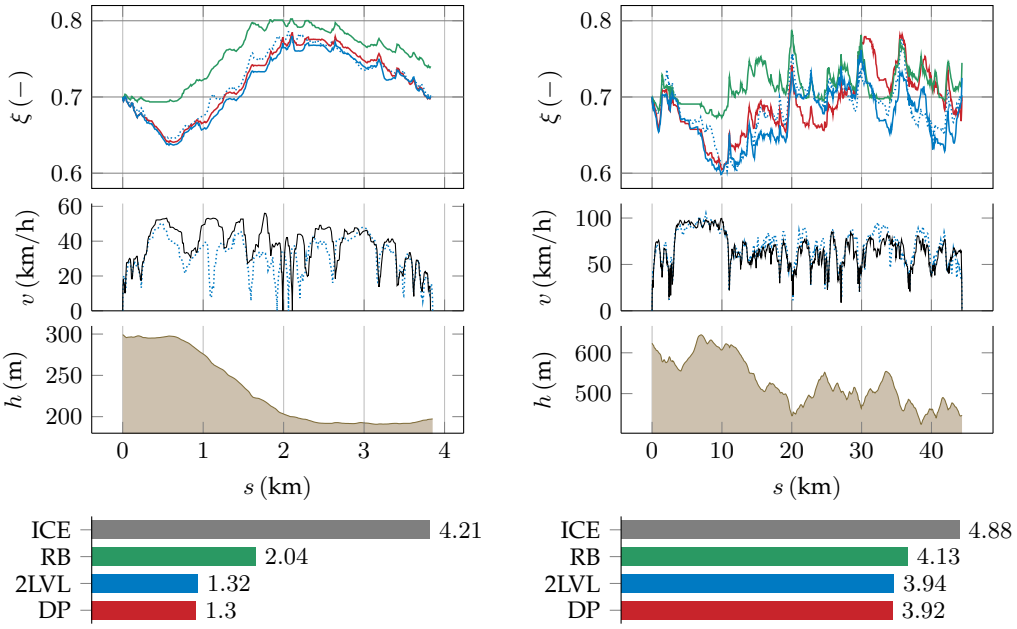

A Route 1 (City 1), trip 1;
negative/positive energy ratio: 1.15

B Route 5 (Extra-urban), trip 1;
negative/positive energy ratio: 0.35

Figure 4.1 Trips with large recuperation potential (HEV results)

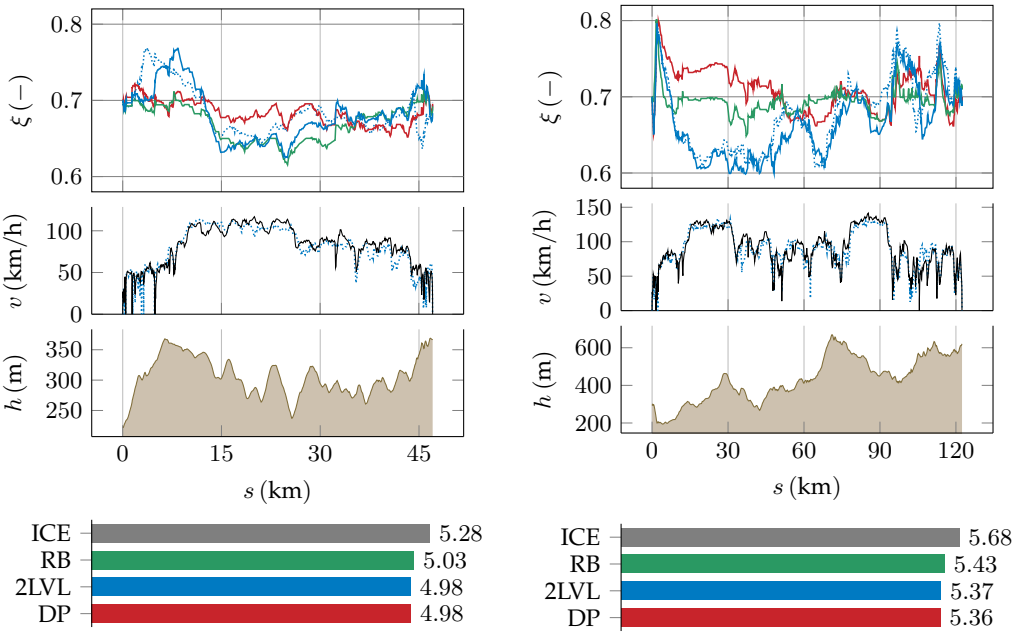

A Route 6 (Highway/City), trip 1;
negative/positive energy ratio: 0.11

B Route 8 (Highway/Extra-urban), trip 2;
negative/positive energy ratio: 0.13

Figure 4.2 Trips with small recuperation potential (HEV results)

The more important role is played by the equivalence factor p, which is generated before the trip and which is used for the minimisation of the Hamiltonian in real-time. Because the generated reference equivalence factor is usually close to the real optimal value, when the speed profile is predicted somewhat correctly, the SOC is automatically tracked. However, when the speed is predicted incorrectly in a section of the trip, the SOC will start to deviate from the prediction in this section (leading to some error and p-correction), but the original reference equivalence factor (and resulting SOC trajectory) might still be close to optimal with respect to the real trip and too large corrections would only lead to bad performance.

Naturally, there needs to be a compromise in order for the strategy to attain charge-sustaining behaviour if the speed profile keeps changing from the prediction, but not over-compensate too much by constantly charging and recharging the battery. Figure 4.3 shows two different results with the same PID coefficients. In 4.3a, the 2LVL deviates from the prediction, because of a different speed, but follows the shape of the optimal SOC trajectory by DP. The PID coefficients are small enough that the vehicle is not forced to follow the predicted non-optimal SOC trajectory. On the other hand, in 4.3b, the vehicle follows the optimal DP trajectory in the beginning by minimising the Hamiltonian with the generated equivalence factor value, however, as the accumulated error grows, correcting p too much, the vehicle is forced to adhere to the non-optimal prediction, only having to over-compensate in the other direction later again. While the result still outperforms the RB strategy, it is further from the optimal DP result than in 4.3a.

The key to obtain close-to-optimal control is therefore to use accurate maps and parameters for the Hamiltonian and the approximate equivalence factor generated by the prediction for its minimisation, which results in keeping the engine operating with good ef-

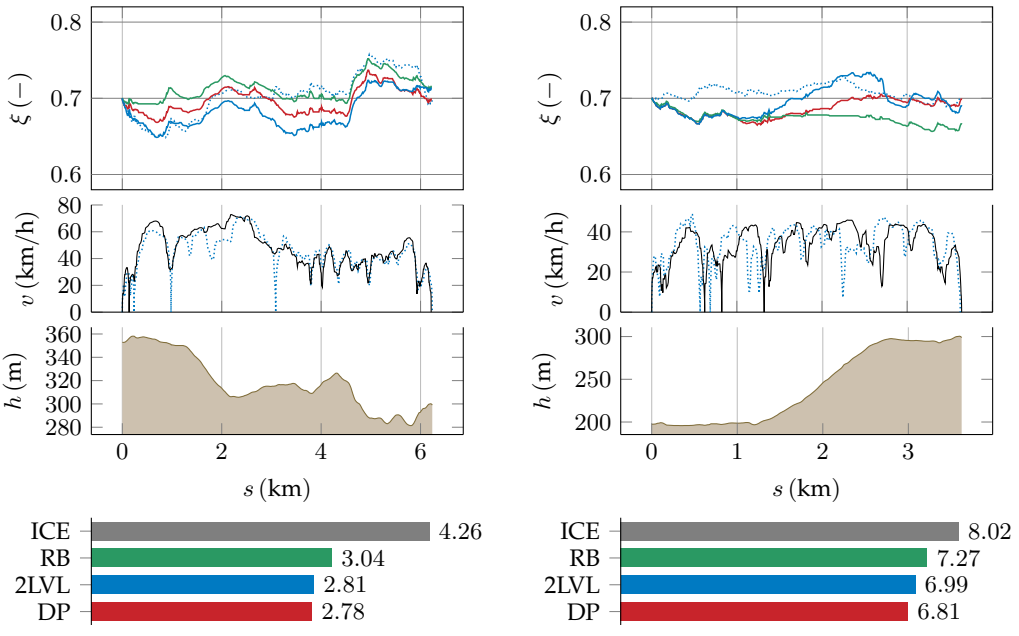

A Desired behaviour; Route 4 (City 2 Return), trip 3.

B Undesired behaviour; Route 2 (City 1 Return), trip 3.

FIGURE 4.3 Desired and undesired p-correction behaviour (HEV results)

ficiency. Charge-sustaining operation is then achieved through small equivalence factor corrections based on the error from reference SOC.

4.1.2 Performance

As already discussed in the previous sections, overall, the 2LVL strategy achieves results close to the optimal solution, in spite of speed profile and parameter disturbances of the tested magnitude. It is able to select nearly optimal control based on generated reference equivalence factor, resulting in following the 'high-frequency' optimal SOC trajectory shape, which turns out to be the key to good performance. On routes that have a specific characteristic such as differences between driving types or significant elevation profile, it results in using the whole admissible range of the battery accordingly to maximise recuperation possibilities, or to recharge the battery for EM propulsion.

Two examples are presented in Figure 4.4. In 4.4a, it can be seen that 2LVL anticipates the downhill secion and uses electric energy beforehand, as the battery will be recharged later, whereas the RB does not take advantage of this and has to dissipate the excess potential energy by friction brakes, because the SOC constraint was reached. Similarly, in 4.4b, the 2LVL uses the whole admissible range of the battery and charges it at the end before exiting the highway to use EM propulsion in city driving where it is more efficient.

However, the strategy starts to 'slip up' when the error in the predicted speed profile is of significant magnitude in terms of battery usage over the entire trip. This means that on trips where there is already not much space for battery use and the predicted speed profile makes the predicted SOC trajectory deviate from the real optimal one, the EMS forces the

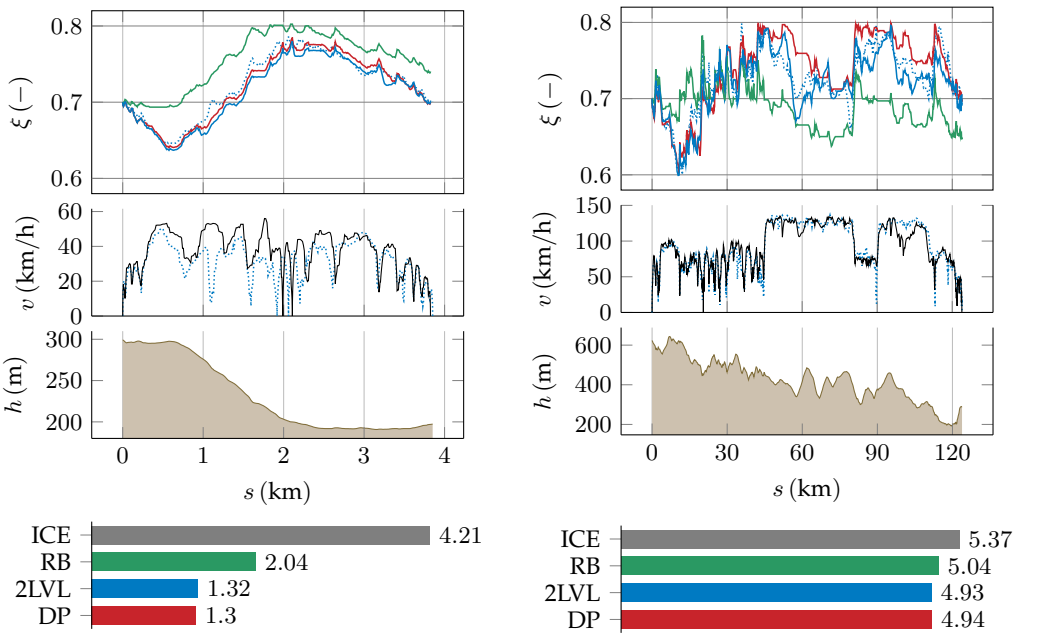

A Route 1 (City 1), trip 1

B Route 9 (Highway/Extra-urban Return), trip 2

Figure 4.4 EMS effectively using admissible range of the battery (HEV results)

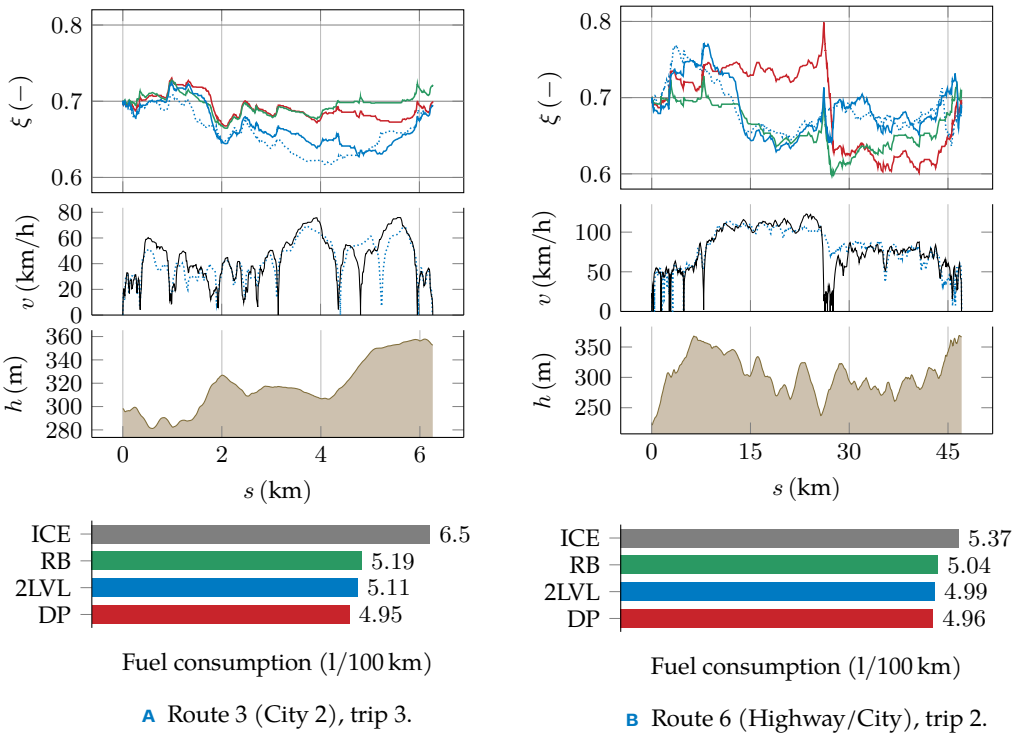

A Route 3 (City 2), trip 3.

B Route 6 (Highway/City), trip 2.

FIGURE 4.5 Effect of inaccurate prediction on 2LVL performance (HEV results)

battery to discharge and subsequently charge (or vice versa) instead of not using the battery as much, leading to sub-optimal fuel consumption due to double energy conversion. This overcompensation effect was already partly discussed in the previous section.

Figure 4.5 shows examples of this. In 4.5a, the trip is quite short, hence even though the 'high-frequency' shape is the same as DP, the forced 'low-frequency' charging and discharging of the battery over the length of the trip (because of inaccurate prediction) noticeably worsens the performance. A similar behaviour can be seen in already discussed Figure 4.3b. In 4.5b, an unpredicted congestion occurred during highway driving, before which the battery would have been ideally fully charged (as per DP solution) to use the EM for the low-speed and low-torque driving. However, only half of the battery capacity was available in reality and the subsequent SOC drop also caused the algorithm to overcompensate and charge the battery with the ICE to follow the predicted SOC instead of continuing to use the EM and charge the battery with higher efficiency later.

While the 2LVL strategy in these cases still performs better than the RB, the improvements are negligible.

4.2 PHEV

Because the PHEV is able to complete shorter city and extra-urban routes using electric energy only, the only tested routes were the longer 8 and 9, and a combination of 6 and 7. Technically, the shorter routes could be tested on a loop to simulate the operation of PHEV on multiple short trips around the city without charging in-between, however, it is unlikely that driving information of such trip could be predicted in real scenario with reasonable accuracy.

While in the case of the HEV, the application of the 2LVL strategy on longer trips resulted in negligible savings, the PHEV achieved consistent 3-4 % improvements (Tab. 4.4). This consistency is attributed to the fact that all of the trips are similar in length and type, and the deviations in speed profile are not as significant in terms of the length of the trip, leading to small differences in the equivalence factor between the prediction and reality.

As discussed in Chapter 2, the normal operation of PHEV consists of charge-depleting mode, where the vehicle runs on electricity only, and subsequent charge-sustaining mode, where the vehicle acts as a regular HEV vehicle after the battery has been discharged to a certain point. This naturally works for shorter trips, because EM-only propulsion is preferred over ICE propulsion for various reasons. However, for longer trips, where the battery capacity is not sufficient, it is beneficial to use the battery charge gradually over the length of the trip, depending on where it is the most efficient.

This is essentially an equivalent to the discussion in the previous section about using obtained electric energy efficiently. However, whereas charge-sustaining HEVs and MHEVs have to obtain electric energy for EM propulsion by recuperation, PHEVs have additional energy introduced from the grid, and therefore more potential for a smart strategy to use it more efficiently. Obviously, unlike the recuperated energy, this energy has to obtained somewhere at a certain cost, nevertheless, that is out of the scope of this thesis.

An example of a result from each of the routes is shown in Figure 4.6, where the discharge trajectory roughly resembles a straight line spanning the length of the trip. However, based on the types of driving along a trip, the trajectory may deviate significantly more. The actual behaviour of the EMS is similar to the application on HEV and MHEV, hence the conditions for good results pertain to the PHEV as well.

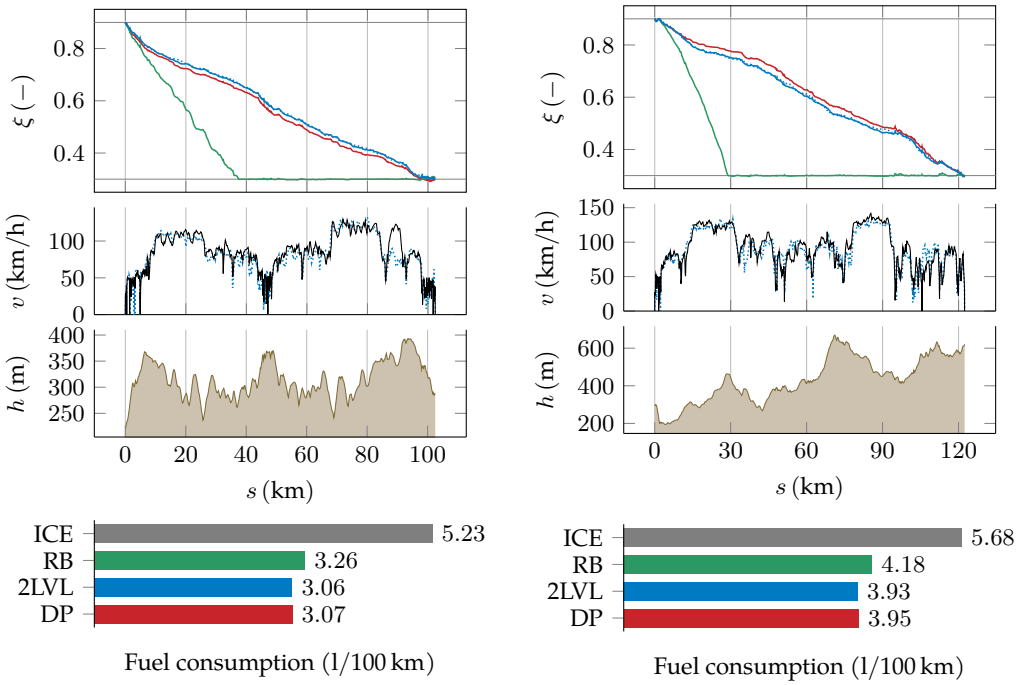

A Route 6+7 (Highway/City & Return), trip 1

B Route 8 (Highway/Extra-urban), trip 2

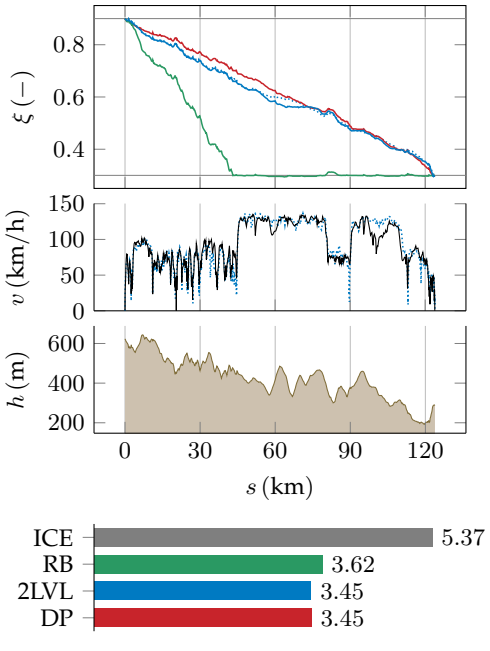

C Route 9 (Highway/Extra-urban Return), trip 2

FIGURE 4.6 PHEV results

Chapter 5

CONCLUSIONS

A research was conducted to examine the current state of hybrid vehicle control. Strategies with an optimal-control character using some sort of trip information have the potential to achieve better results than heuristic strategies used in passenger vehicles today, which are mostly based on intuitive rules.

According to this, an EMS using information of a planned route was designed. The strategy generates reference SOC and equivalence factor trajectories before a trip and subsequently uses these to obtain close-to-optimal control. The input is a predicted speed profile and elevation profile of a planned route, from which the reference trajectories are generated using an optimisation algorithm based on Pontryagin's minimum principle and a simplified vehicle model. The equivalence factor is then used for instantaneous Hamiltonian minimisation in real-time to obtain close-to-optimal torque-split between the ICE and the EM. The reference SOC trajectory is tracked by correcting the value of the equivalence factor in feedback with a PI regulator to compensate for errors made in the prediction to achieve charge-sustaining operation.

The strategy was tested on vehicles with three levels of electrification – HEV, MHEV and PHEV. Several routes to include the majority driving types were selected for the testing to gain insight into where the implementation makes sense and where it performs the best (or at all). The results were compared to optimal solutions from dynamic programming and results from a heuristic rule-based strategy that selects the propulsion mode based on SOC level and demanded torque only.

The proposed strategy seems to be robust enough to the speed profile disturbances on the tested trips and the equivalence factor correction compensates well for the uncertain parameters and simplified vehicle model to the tested extent. The RB strategy was therefore outperformed in most cases and the results were fairly close to the optimal solution. The determining factor for good results turned out to be the usage of accurate engine maps for the Hamiltonian in the real-time control and using relatively small PI coefficients not to overcompensate for prediction errors, but large enough to achieve charge-sustaining operation.

Despite the good results relative to DP, in MHEV application in general and HEV application on routes with low recuperation possibilities such as constant-speed driving on a highway, the potential improvement between RB and DP is already quite small and only small fuel savings (around 1 %) were accomplished. Higher fuel savings (1-5 %) were accomplished in city and extra-urban driving where the vehicle brakes more often and the elevation profile is more significant.

The PHEV was tested only on the longer routes which exceeded its electric-only range. The result was a consistent 3-4 % improvement over the traditional charge-depleting/charge-sustaining RB strategy, as it is more efficient to gradually deplete the battery over the entire trip, which the proposed strategy accomplishes.

These improvements stem from the fact, that a 'smart' strategy such as the proposed one is able to exploit the available electric energy obtained by recuperation or from the grid in a more efficient manner than a heuristic RB strategy would, leading to an improvement approximately linearly dependent on the amount of electric energy available compared to the expended energy needed for propulsion.

Ultimately, the proposed strategy amplifies the benefits of the nature of a hybrid electric vehicle, hence in applications where a HEV does not generally bring significant savings, the absolute benefit of a 'smart' EMS decreases with respect to a simpler, less-complex-to-implement one.

5.1 FUTURE WORK

Because the results presented are based on a simulation taking into account only energy required for vehicle propulsion and neglecting some potentially important effects, the improvement in real scenario will likely be to some extent smaller. Further testing on a higher-fidelity model is therefore the logical next step.

For example, incorporating energy required to power electric auxiliaries such as HVAC, pumps or lighting, which would result in electric load even when the vehicle is stationary, introducing another source of disturbance dependent on the difference in duration of the predicted and actual trip. Thermal behaviour of mainly the engine and the batteries should be also modelled in the simulation, as the parameters of these components vary with temperature, which may affect the performance as well.

So far, no penalty or energy consideration for frequent engine starts was implemented, which would have to be taken into account for real application. While this may not affect the performance of the proposed strategy relative to the RB, the improvement with respect to ICE only propulsion will be smaller.

The proposed strategy achieved good results with the speed disturbances tested in this thesis, however, it would be interesting to examine how much the real speed profile can deviate from the predicted one in terms of driving styles (higher accelerations, not exploiting vehicle inertia by coasting as much) to still obtain worthwhile savings, or how averaging some of the speed sections to facilitate faster calculation affects the predicted equivalence factor and subsequent results.

Lastly, at this point, the SOC tracking was realised by feedback based on driven distance, which requires the predicted and actual trip to be the same length. Implementing tracking based on GPS location would make the strategy more robust towards small distance deviations originating from detours, driving in different lanes or avoiding obstacles.

SYMBOLS AND ACRONYMS

A_x	Vehicle frontal area
BSFC	Brake-specific fuel consumption
C	Battery capacity
c_x	Vehicle drag coefficient
f	Rolling resistance coefficient
F_x	Traction force
FC	Fuel consumption
g	Gravitational acceleration
h	State constraints, elevation
H	Lower heating value
$\mathscr{H}$	Hamiltonian
i	Gear ratio
I	Current
J	Performance measure
K_i	Integral PID coefficient
K_p	Proportional PID coefficient
$\mathscr{L}$	Lagrangian
m	Vehicle mass
m_f	Fuel mass
p	Lagrange multiplier (EF)
P	Power
r_d	Tire dynamic rolling radius
R	Battery internal resistance
R_a	Aerodynamic resistance
R_f	Rolling resistance
R_α	Incline resistance
RPM	Revolutions per minute
s	Distance
t	Time
T	Torque
u	Control variable
v	Vehicle speed
V	Nominal voltage
V_0	Open-circuit voltage
x	State variable
α	Slope angle
δ	Rotational-mass coefficient
η	Efficiency
ν	State constraint lagrange multiplier
ξ	Battery state of charge
ρ_a	Air density
τ	State boundary time
ω	Angular velocity

INDICES

0	Initial
b	Battery
d	Drivetrain
dem	Demanded
e	Engine
f	Final
fd	Final drive
g	Gearbox
i	Inverter
m	Electric machine
ref	Reference
tc	Torque coupling
*	Optimal

ACRONYMS

2LVL	Proposed two-level strategy
BEV	Battery electric vehicle
DP	Dynamic programming
ECMS	Equivalent consumption minimisation strategy
EF	Equivalence factor
EM	Electric machine
EMS	Energy management strategy
FL	Fuzzy logic
GPS	Global positioning system
HEV	Hybrid electric vehicle
HVAC	Heating, ventilation, and air conditioning
ICE	Internal combustion engine
MHEV	Mild hybrid electric vehicle
MPC	Model predictive control
PHEV	Plug-in hybrid electric vehicle
PID	Proportional-integral-derivative controller
PMP	Pontryagin's minimum principle
RB	Rule-based
SOC	State of charge
V2X	Vehicle-to-everything communication
WLTP	Worldwide harmonised light-duty vehicles test procedure

BIBLIOGRAPHY

[1] Toyota Global. *The Story Behind the Birth of the Prius* [online]. 13 December 2017. [Accessed 4 February 2021]. Available from: https://global.toyota/en/prius20th/challenge/birth/01/

[2] KIMURA, A. Drive force control of a parallel-series hybrid system. *JSAE Review* [online]. 1999, **20**(3), 337-341. [Accessed 4 February 2021]. ISSN 03894304. Available from: doi:10.1016/S0389-4304(99)00017-X

[3] GUZZELLA, L. and A. SCIARRETTA. *Vehicle Propulsion Systems* [online]. Berlin, Heidelberg: Springer Berlin Heidelberg, 2013 [Accessed 4 February 2021]. ISBN 978-3-642-35912-5. Available from: doi:10.1007/978-3-642-35913-2

[4] ABAS, M.A., W.S. WAN SALIM, M.I. ISMAIL, S. RAJOO and R. MARTINEZ-BOTAS. Fuel consumption evaluation of SI engine using start-stop technology. *Journal of Mechanical Engineering and Sciences* [online]. 2017, **11**(4), 2967-2978 [Accessed 10 February 2021]. ISSN 22894659. Available from: doi:10.15282/jmes.11.4.2017.1.0267

[5] WISHART, J. and M. SHIRK. *Quantifying the Effects of Idle-Stop Systems on Fuel Economy in Light-Duty Passanger Vehicles* [online]. Idaho National Laboratory. December 2012. [Accessed 10 February 2021]. Available from: https://www.energy.gov/sites/prod/files/2014/02/f8/idle-stop_light_duty_passenger_vehicles.pdf

[6] BALDIZZONE, S. *Performance and Fuel Economy Analysis of a Mild Hybrid Vehicle Equipped with Belt Starter Generator*. Windsor, Canada, 2012. Master's thesis. University of Windsor. December 2012.

[7] AL-SAMARI, A. Study of emissions and fuel economy for parallel hybrid versus conventional vehicles on real world and standard driving cycles. *Alexandria Engineering Journal* [online]. 2017, **56**(4), 721-726 [Accessed 11 February 2021]. ISSN 11100168. Available from: doi:10.1016/j.aej.2017.04.010

[8] CHUNG, I., H. KANG, J. PARK and J. LEE. Fuel Economy Improvement Analysis of Hybrid Electric Vehicle. *International Journal of Automotive Technology* [online]. 2019, **20**(3), 531-537 [Accessed 11 February 2021]. ISSN 1229-9138. Available from: doi:10.1007/s12239-019-0050-7

[9] PITANUWAT, S. and A. SRIPAKAGORN. An Investigation of Fuel Economy Potential of Hybrid Vehicles under Real-World Driving Conditions in Bangkok. *Energy Procedia* [online]. 2015, **79**, 1046-1053 [Accessed 11 February 2021]. ISSN 18766102. Available from: doi:10.1016/j.egypro.2015.11.607

[10] JUNG, H. Fuel Economy of Plug-In Hybrid Electric and Hybrid Electric Vehicles: Effects of Vehicle Weight, Hybridization Ratio and Ambient Temperature.*World Electric Vehicle Journal* [online]. 2020, **11**(2) [Accessed 23 February 2021]. ISSN 2032-6653. Available from: doi:10.3390/wevj11020031

[11] GONDER, J. and T. MARKEL. Energy Management Strategies for Plug-In Hybrid Electric Vehicles. *SAE Technical Paper 2007-01-0290* [online]. 2007. [Accessed 23 February 2021]. Available from: doi:10.4271/2007-01-0290

[12] TRIBIOLI, L., M. BARBIERI, R. CAPATA, E. SCIUBBA, E. JANNELLI and G. BELLA. A Real Time Energy Management Strategy for Plug-in Hybrid Electric Vehicles based on Optimal Control Theory. *Energy Procedia* [online]. 2014, **45**, 949-958 [Accessed 23 February 2021]. ISSN 18766102. Available from: doi:10.1016/j.egypro.2014.01.100

[13] WONG, J. Y. Vehicle Ride Characteristics. *Theory of Ground Vehicles*. Third Edition. New York: John Wiley & Sons, 2001, 431-484. ISBN 0-471-35461-9.

[14] ZULKIFLI, S. A., S. MOHD, N. SAAD and A. R. A. AZIZ, Split-parallel through-the-road hybrid electric vehicle: Operation, power flow and control modes. *2015 IEEE Transportation Electrification Conference and Expo* (*ITEC*) [online]. IEEE, 2015, 2015, s. 1-7 [Accessed 15 February 2021]. ISBN 978-1-4673-6741-7. Available from: doi:10.1109/ITEC.2015.7165774

[15] ZHANG, X., C. LI, D. KUM and H. PENG. Prius$^+$ and Volt$^-$: Configuration Analysis of Power-Split Hybrid Vehicles With a Single Planetary Gear. *IEEE Transactions on Vehicular Technology* [online]. 2012, **61**(8), 3544-3552 [Accessed 16 February 2021]. ISSN 0018-9545. Available from: doi:10.1109/TVT.2012.2208210

[16] MAMDANI, E. H. Application of fuzzy algorithms for control of simple dynamic plant. *Proceedings of the Institution of Electrical Engineers* [online]. 1974, **121**(12) [Accessed 26 February 2021]. ISSN 00203270. Available from: doi:10.1049/piee.1974.0328

[17] TAKAGI, T. and M. SUGENO. Fuzzy identification of systems and its applications to modeling and control. *IEEE Transactions on Systems, Man, and Cybernetics* [online]. 1985, SMC-**15**(1), 116-132 [Accessed 26 February 2021]. ISSN 0018-9472. Available from: doi:10.1109/TSMC.1985.6313399

[18] ZHANG, Q. and X. FU. A Neural Network Fuzzy Energy Management Strategy for Hybrid Electric Vehicles Based on Driving Cycle Recognition. *Applied Sciences* [online]. 2020, **10**(2) [Accessed 26 February 2021]. ISSN 2076-3417. Available from: doi:10.3390/app10020696

[19] SCHOUTEN, N. J., M. A. SALMAN and N. A. KHEIR. Fuzzy logic control for parallel hybrid vehicles. *IEEE Transactions on Control Systems Technology* [online]. 2002, **10**(3), 460-468 [Accessed 26 February 2021]. ISSN 10636536. Available from: doi:10.1109/87.998036

[20] NÜESCH, T., A. CEROFOLINI, G. MANCINI, N. CAVINA, C. ONDER and L. GUZZELLA. Equivalent Consumption Minimization Strategy for the Control of Real Driving NOx Emissions of a Diesel Hybrid Electric Vehicle. *Energies* [online]. 2014, **7**(5), 3148-3178 [Accessed 1 March 2021]. ISSN 1996-1073. Available from: doi:10.3390/en7053148

[21] OPILA, D. F., D. ASWANI, R. MCGEE, J. A. COOK and J. W. GRIZZLE. Incorporating drivability metrics into optimal energy management strategies for Hybrid Vehicles. *2008 47th IEEE Conference on Decision and Control* [online]. IEEE, 2008, 2008, s. 4382-4389 [Accessed 1 March 2021]. ISBN 978-1-4244-3123-6. Available from: doi:10.1109/CDC.2008.4738731

[22] SERRAO, L., S. ONORI, A. SCIARRETTA, Y. GUEZENNEC and G. RIZZONI. Optimal energy management of hybrid electric vehicles including battery aging. *Proceedings of the 2011 American Control Conference* [online]. IEEE, 2011, 2011, s. 2125-2130 [Accessed 1 March 2021]. ISBN 978-1-4577-0080-4. Available from: doi:10.1109/ACC.2011.5991576

[23] SUNDSTRÖM, O., L. GUZZELLA and P. SOLTIC. Optimal Hybridization in Two Parallel Hybrid Electric Vehicles using Dynamic Programming. *IFAC Proceedings Volumes* [online]. 2008, **41**(2), 4642-4647 [Accessed 2 March 2021]. ISSN 14746670. Available from: doi:10.3182/20080706-5-KR-1001.00781

[24] YUAN, Z., L. TENG, S. FENGCHUN and H. PENG. Comparative Study of Dynamic Programming and Pontryagin's Minimum Principle on Energy Management for a Parallel Hybrid Electric Vehicle. *Energies* [online]. 2013, **6**(4), 2305-2318 [Accessed 2 March 2021]. ISSN 1996-1073. Available from: doi:10.3390/en6042305

[25] KIM, N., S. CHA and H. PENG. Optimal Control of Hybrid Electric Vehicles Based on Pontryagin's Minimum Principle. *IEEE Transactions on Control Systems Technology* [online]. 2011, **19**(5), 1279-1287 [Accessed 2 March 2021]. ISSN 1063-6536. Available from: doi:10.1109/TCST.2010.2061232

[26] NÜESCH, T., P. ELBERT, M. FLANKL, C. ONDER and L. GUZZELLA. Convex Optimization for the Energy Management of Hybrid Electric Vehicles Considering Engine Start and Gearshift Costs. *Energies* [online]. 2014, **7**(2), 834-856 [Accessed 1 March 2021]. ISSN 1996-1073. Available from: doi:10.3390/en7020834

[27] HADJ-SAID, S., G. COLIN, A. KETFI-CHERIF and Y. CHAMAILLARD. Convex Optimization for Energy Management of Parallel Hybrid Electric Vehicles. *IFAC-PapersOnLine* [online]. 2016, **49**(11), 271-276 [Accessed 1 March 2021]. ISSN 24058963. Available from: doi:10.1016/j.ifacol.2016.08.041

[28] SAMANTA, C. K., S. K. PADHY, S. P. PANIGRAHI and B. K. PANIGRAHI. Hybrid swarm intelligence methods for energy management in hybrid electric vehicles. *IET Electrical Systems in Transportation* [online]. 2013, **3**(1), 22-29 [Accessed 1 March 2021]. ISSN 2042-9738. Available from: doi:10.1049/iet-est.2012.0009

[29] MONTAZERI-GH, M., A. POURSAMAD and B. GHALICHI. Application of genetic algorithm for optimization of control strategy in parallel hybrid electric vehicles.*Journal of the Franklin Institute* [online]. 2006, **343**(4-5), 420-435 [Accessed 1 March 2021]. ISSN 00160032. Available from: doi:10.1016/j.jfranklin.2006.02.015

[30] BELLMAN, R. E. The *Theory of Dynamic Programming.* Santa Monica, California: The Rand Corporation, 1954.

[31] LEROY, T., F. VIDAL-NAQUET and P. TONA. Stochastic Dynamic Programming based Energy Management of HEV's: an Experimental Validation. *IFAC Proceedings Volumes* [online]. 2014, **47**(3), 4813-4818 [Accessed 3 March 2021]. ISSN 14746670. Available from: doi:10.3182/20140824-6-ZA-1003.01868

[32] C. LIN, H. PENG and J.W. GRIZZLE. A stochastic control strategy for hybrid electric vehicles. *Proceedings of the 2004 American Control Conference* [online]. IEEE, 2004, 2004, 4710-4715 vol.5 [Accessed 3 March 2021]. ISBN 0-7803-8335-4. Available from: doi:10.23919/ACC.2004.1384056

[33] KIRK, D. E. *Optimal control theory: an introduction*. Dover edition. Mineola: Dover Publications, 2004. ISBN 978-0486434841.

[34] PAGANELLI, G. General supervisory control policy for the energy optimization of charge-sustaining hybrid electric vehicles. *JSAE Review* [online]. **22**(4), 511-518 [Accessed 5 March 2021]. ISSN 03894304. Available from: doi:10.1016/S0389-4304(01)00138-2

[35] MUSARDO, C., G. RIZZONI, Y. GUEZENNEC and B. STACCIA. A-ECMS: An Adaptive Algorithm for Hybrid Electric Vehicle Energy Management. *European Journal of Control* [online]. 2005, **11**(4-5), 509-524 [Accessed 5 March 2021]. ISSN 09473580. Available from: doi:10.3166/ejc.11.509-524

[36] SCIARRETTA, A., L. GUZZELLA and M. BACK. A Real-Time Optimal Control Strategy for Parallel Hybrid Vehicles with On-Board Estimation of the Control Parameters. *IFAC Proceedings Volumes* [online]. 2004, **37**(22), 489-494 [Accessed 5 March 2021]. ISSN 14746670. Available from: doi:10.1016/S1474-6670(17)30391-9

[37] ENANG, W. and C. BANNISTER. Robust proportional ECMS control of a parallel hybrid electric vehicle. *Proceedings of the Institution of Mechanical Engineers, Part D: Journal of Automobile Engineering* [online]. 2017, **231**(1), 99-119 [Accessed 5 March 2021]. ISSN 0954-4070. Available from: doi:10.1177/0954407016659198

[38] JEOUNG, H., K. LEE and N. KIM. Methodology for Finding Maximum Performance and Improvement Possibility of Rule-Based Control for Parallel Type-2 Hybrid Electric Vehicles. *Energies* [online]. 2019, **12**(10) [Accessed 8 March 2021]. ISSN 1996-1073. Available from: doi:10.3390/en12101924

[39] XU, Q., X. LUO, X. JIANG and M. ZHAO. Research on double fuzzy control strategy for parallel hybrid electric vehicle based on GA and DP optimisation. *IET Electrical Systems in Transportation* [online]. 2018, **8**(2), 144-151 [Accessed 5 March 2021]. ISSN 2042-9738. Available from: doi:10.1049/iet-est.2017.0067

[40] HU, Y., W. LI, H. XU and G. XU. An Online Learning Control Strategy for Hybrid Electric Vehicle Based on Fuzzy Q-Learning. *Energies* [online]. 2015, **8**(10), 11167-11186 [Accessed 5 March 2021]. ISSN 1996-1073. Available from: doi:10.3390/en81011167

[41] HU, Y., W. LI, K. XU, T. ZAHID, F. QIN and C. LI. Energy Management Strategy for a Hybrid Electric Vehicle Based on Deep Reinforcement Learning. *Applied Sciences* [online]. 2018, **8**(2) [Accessed 5 March 2021]. ISSN 2076-3417. Available from: doi:10.3390/app8020187

[42] HE, H., J. ZHANG and G. LI. Model Predictive Control for Energy Management of a Plug-in Hybrid Electric Bus. *Energy Procedia* [online]. 2016, **88**, 901-907 [Accessed 9 March 2021]. ISSN 18766102. Available from: doi:10.1016/j.egypro.2016.06.109

[43] WU, G., K. BORIBOONSOMSIN and M. J. BARTH. Development and Evaluation of an Intelligent Energy-Management Strategy for Plug-in Hybrid Electric Vehicles. *IEEE Transactions on Intelligent Transportation Systems* [online]. 2014, **15**(3), 1091-1100 [Accessed 9 March 2021]. ISSN 1524-9050. Available from: doi:10.1109/TITS.2013.2294342

[44] YUAN, J. and L. YANG. Predictive energy management strategy for connected 48V hybrid electric vehicles. *Energy* [online]. 2019, **187** [Accessed 9 March 2021]. ISSN 03605442. Available from: doi:10.1016/j.energy.2019.115952

[45] GUO, L., B. GAO, Y. GAO and H. CHEN. Optimal Energy Management for HEVs in Eco-Driving Applications Using Bi-Level MPC. *IEEE Transactions on Intelligent Transportation Systems* [online]. 2017, **18**(8), 2153-2162 [Accessed 9 March 2021]. ISSN 1524-9050. Available from: doi:10.1109/TITS.2016.2634019

[46] ZHENG, Q., H. YUAN, J. WU and B. GAO. Equivalent Consumption Minimization Strategy Based on Dynamic Programming for Plug-in Hybrid Electric Vehicle. IFAC-PapersOnLine [online]. 2018, **51**(31), 612-617 [Accessed 9 March 2021]. ISSN 24058963. Available from: doi:10.1016/j.ifacol.2018.10.146

[47] AMBUHL, D. and L. GUZZELLA. Predictive Reference Signal Generator for Hybrid Electric Vehicles. *IEEE Transactions on Vehicular Technology* [online]. 2009, **58**(9), 4730-4740 [Accessed 8 March 2021]. ISSN 0018-9545. Available from: doi:10.1109/TVT.2009.2027709

[48] YU, H., M. KUANG and R. MCGEE. Trip-oriented Energy Management Control strategy for plug-in hybrid electric vehicles. *IEEE Conference on Decision and Control and European Control Conference* [online]. IEEE, 2011, 2011, s. 5805-5812 [Accessed 8 March 2021]. ISBN 978-1-61284-801-3. Available from: doi:10.1109/CDC.2011.6160609

[49] TORREGLOSA, J. P., P. GARCIA-TRIVIÑO, D. VERA and D. A. LÓPEZ-GARCÍA. Analyzing the Improvements of Energy Management Systems for Hybrid Electric Vehicles Using a Systematic Literature Review: How Far Are These Controls from Rule-Based Controls Used in Commercial Vehicles? *Applied Sciences* [online]. 2020, **10**(23) [Accessed 8 March 2021]. ISSN 2076-3417. Available from: doi:10.3390/app10238744

[50] WATZENIG, D. and B. BRANDSTÄTTER, ed. *Comprehensive Energy Management – Eco Routing & Velocity Profiles* [online]. Cham: Springer International Publishing, 2017 [Accessed 10 March 2021]. SpringerBriefs in Applied Sciences and Technology. ISBN 978-3-319-53164-9. Available from: doi:10.1007/978-3-319-53165-6

[51] TOMAN, R., J. KANERA and J. SOUKUP. Evaluation of a CO_2 Potentials for Different HEV Options Using ECMS Algorithm. Technical Report. *50th International Scientific Conference of Czech and Slovak Universities and Institutions Dealing With Motor Vehicles and Internal Combution Engines Research*. 2019.

[52] TUTUIANU, M. et al. *Development of a World-wide Harmonized Light Duty Driving Test Cycle (WLTC)* [online]. Technical Report. UN/ECE/WP.29/GRPE/WLTP-IG. December 2013. [Accessed 18 May 2021]. Available from: https://unece.org/DAM/trans/doc/2014/wp29grpe/GRPE-68-03e.pdf

[53] HARTL, R. F., S. P. SETHI and R. G. VICKSON. A Survey of the Maximum Principles for Optimal Control Problems with State Constraints. *SIAM Review, Society for Industrial and Applied Mathematics*. 1995, **37**(2), 181-218.

Appendix A

FULL ROUTE RESULTS

The results from every trip of each route and all vehicle configurations are included on the following pages. Each result is comprised of a comparison of the SOC trajectory and corresponding fuel consumption of the proposed strategy (2LVL) to the RB strategy and optimal result obtained from dynamic programming. Fuel consumption of a conventional ICE-only powertrain is included as well.

First trip (trip 0) of each route is always a trip that assumes that the real speed matches the predicted speed, and therefore generally achieves the best result with respect to the optimal DP solution. In some cases, especially for the PHEV, the 2LVL strategy outperforms the DP solution due to reasons discussed in Section 3.6.

The colors and lines used in the following graphs are listed in Table A.1 to act as a legend.

Table A.1 Legend for the following graphs

Predicted	2LVL	DP	RB	Predicted speed	Real Speed	Elevation
.....	———	———	———	.....	———	———

A.1 HEV

Route 1 (City 1)

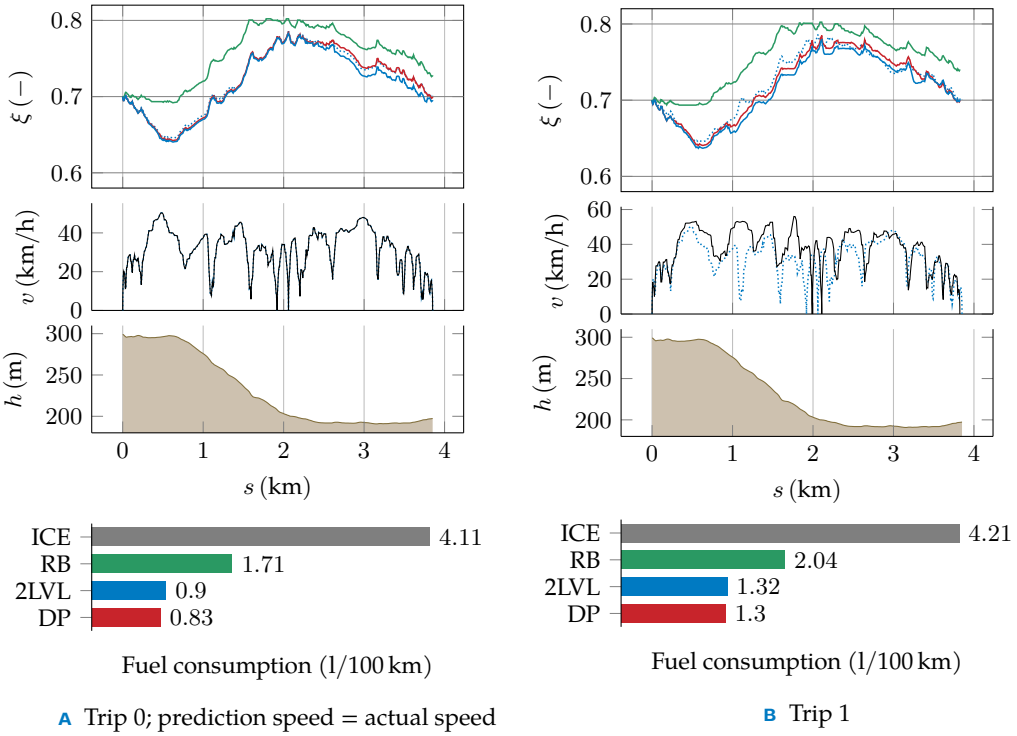

A Trip 0; prediction speed = actual speed

B Trip 1

C Trip 2

D Trip 3

Figure A.1 HEV Route 1 (City 1) results

Route 2 (City 1 Return)

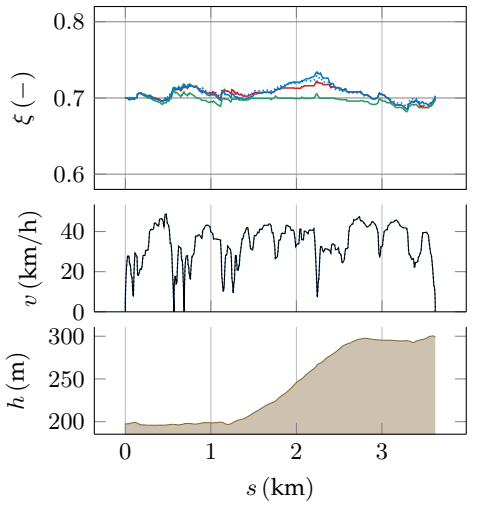

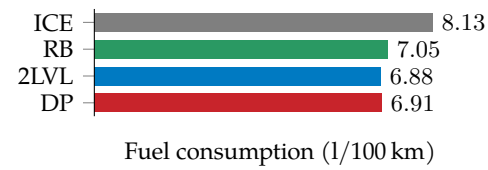

A Trip 0; prediction speed = actual speed

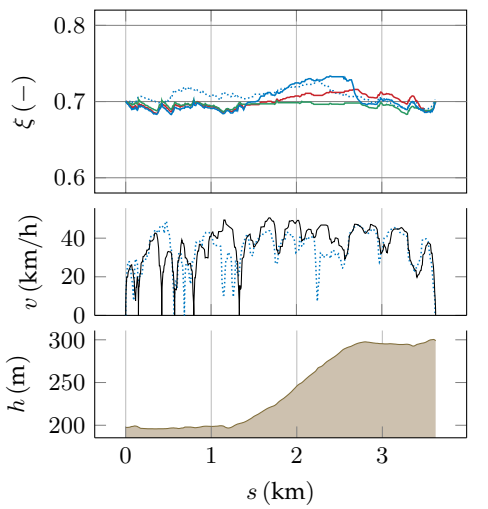

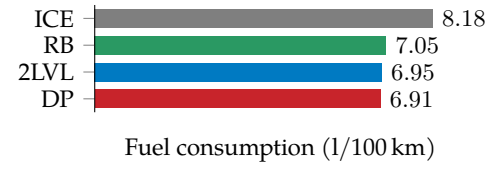

B Trip 1

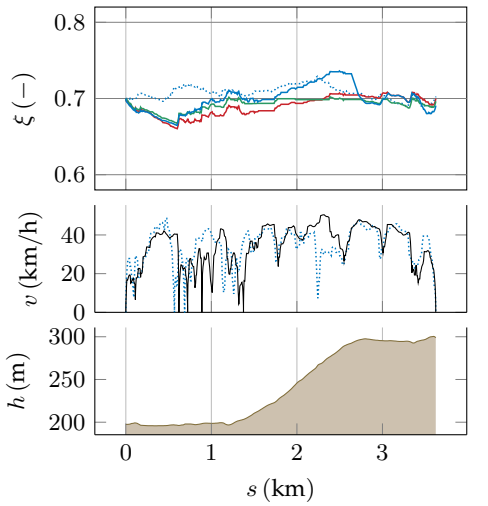

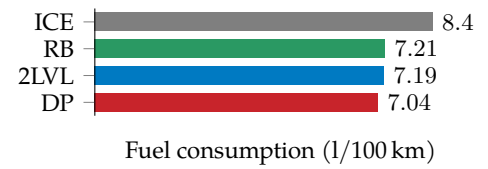

C Trip 2

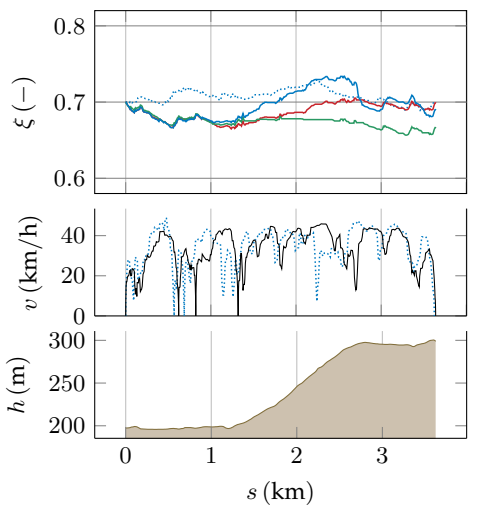

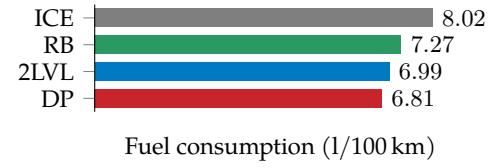

D Trip 3

Figure A.2 HEV Route 2 (City 1 Return) results

Route 3 (City 2)

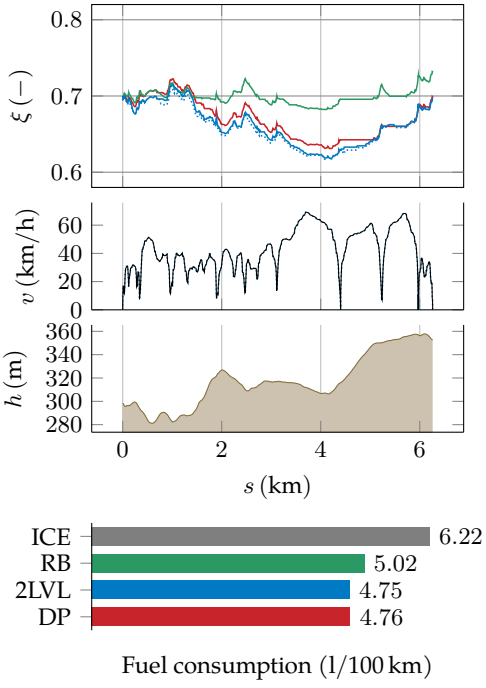

A Trip 0; prediction speed = actual speed

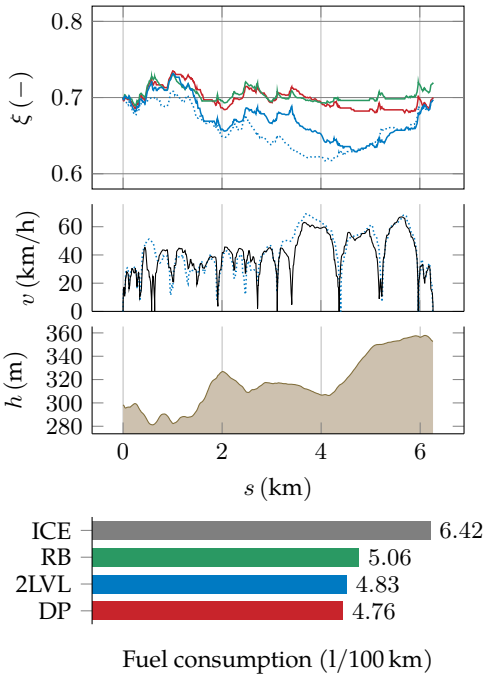

B Trip 1

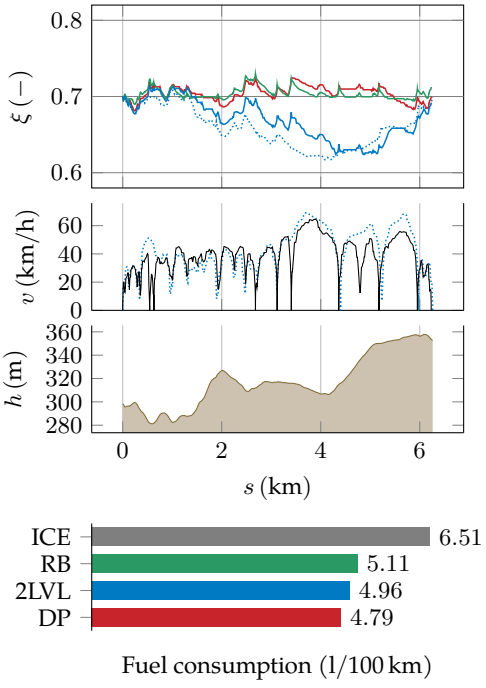

C Trip 2

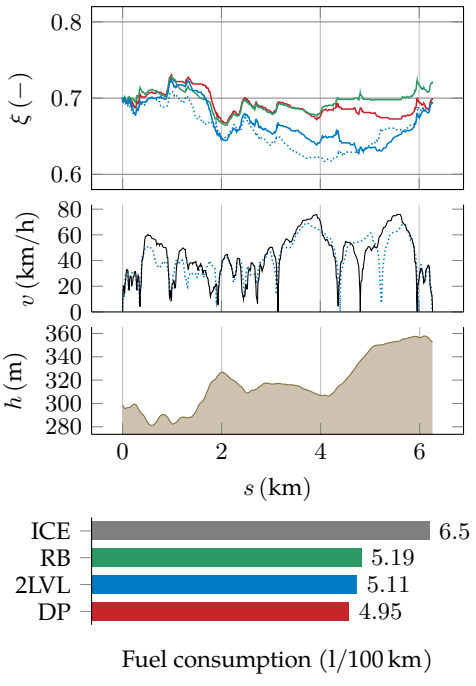

D Trip 3

Figure A.3 HEV Route 3 (City 2) results

Route 4 (City 2 Return)

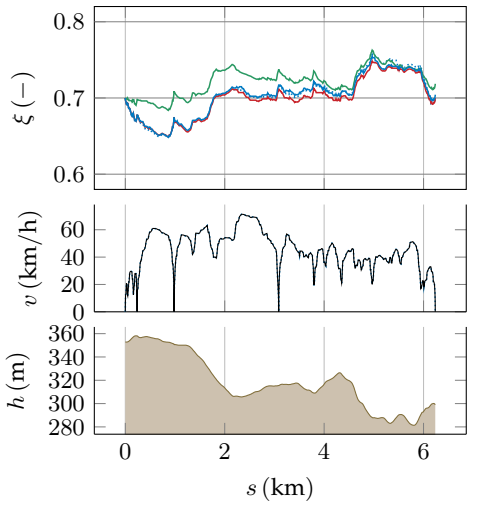

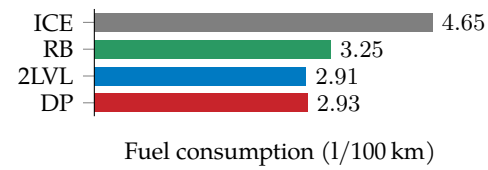

A Trip 0; prediction speed = actual speed

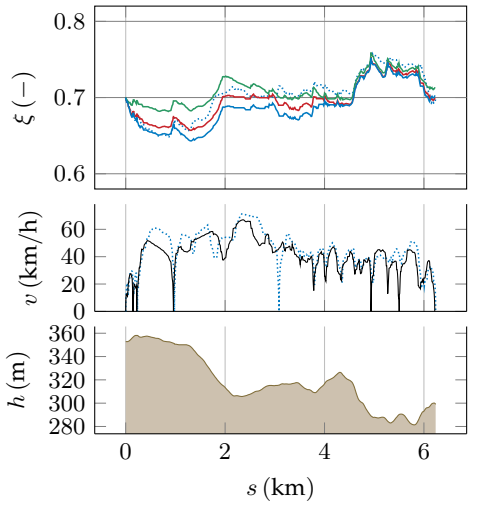

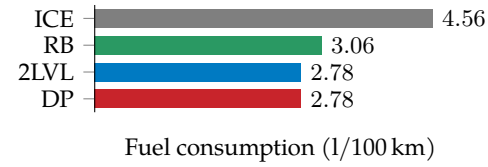

B Trip 1

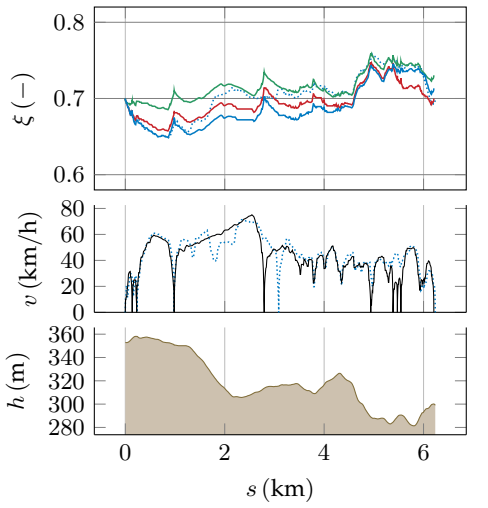

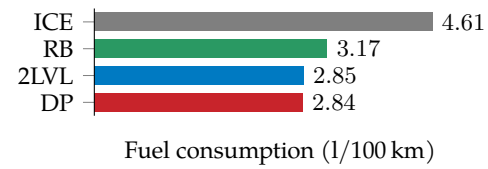

C Trip 2

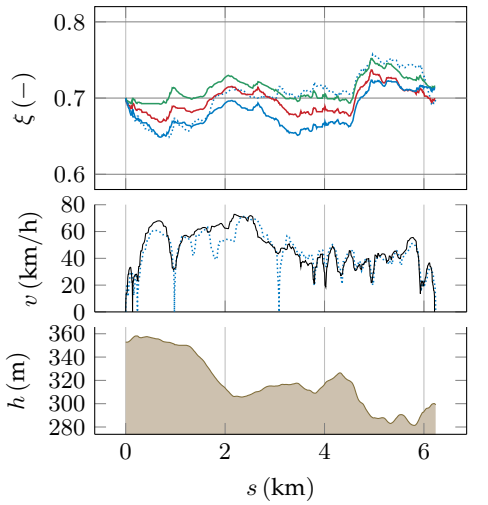

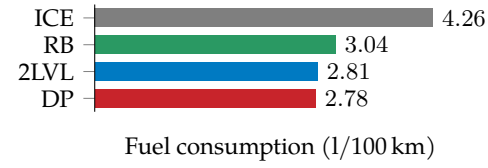

D Trip 3

Figure A.4 HEV Route 4 (City 2 Return) results

Route 5 (Extra-urban)

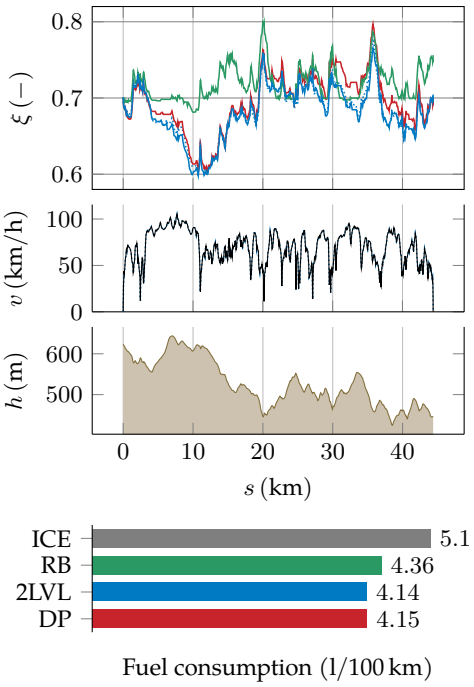

A Trip 0; prediction speed = actual speed

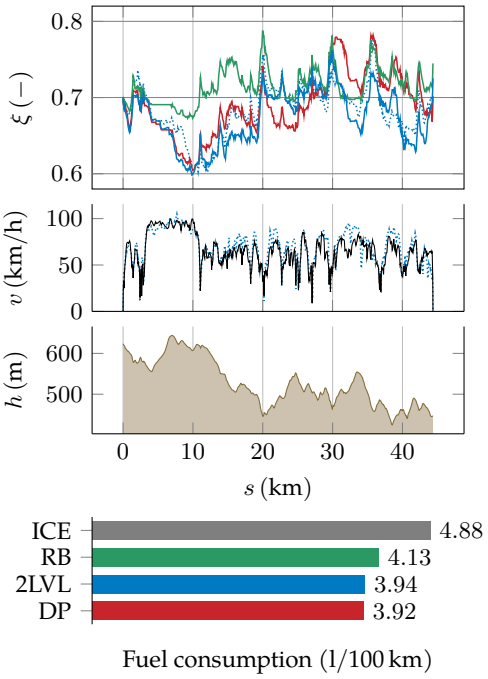

B Trip 1

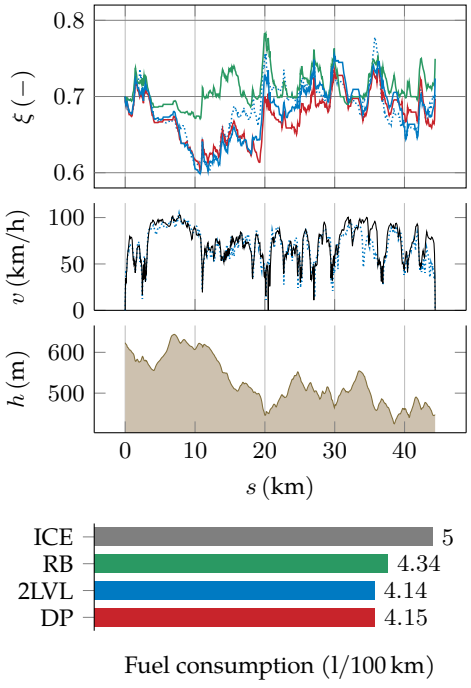

C Trip 2

Figure A.5 HEV Route 5 (Extra-urban) results

Route 6 (Highway/City)

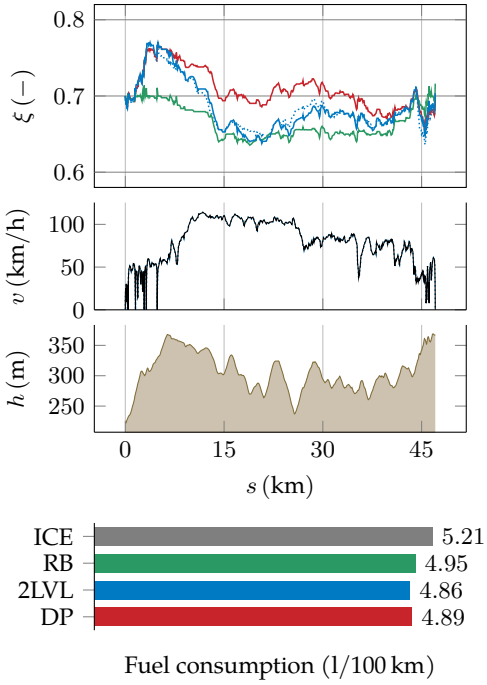

A Trip 0; prediction speed = actual speed

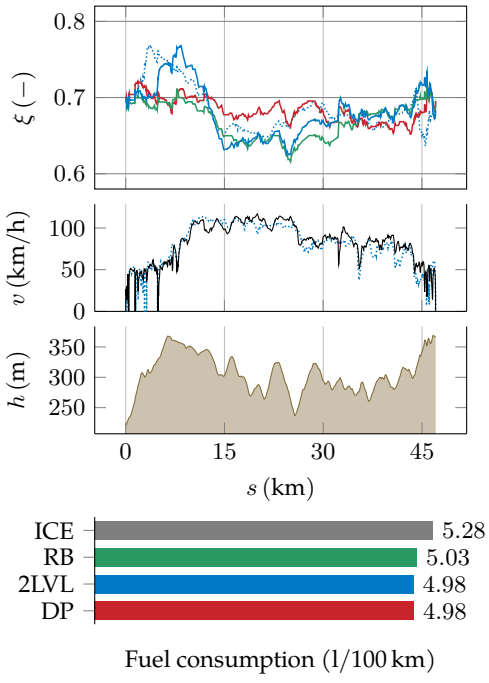

B Trip 1

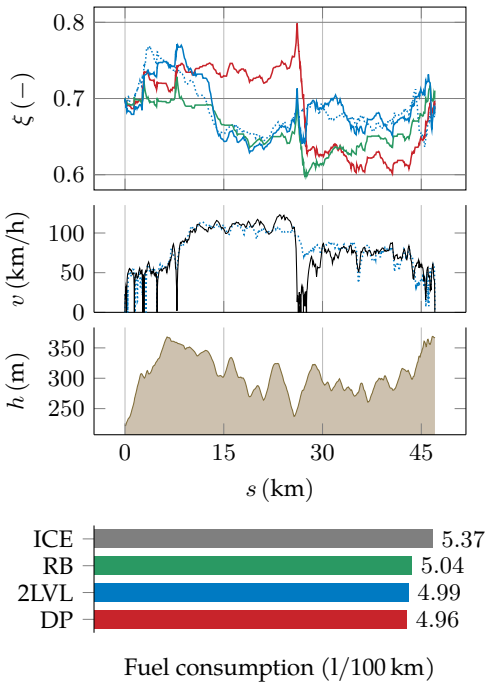

C Trip 2

Figure A.6 HEV Route 6 (Highway/City) results

Route 7 (Highway/City Return)

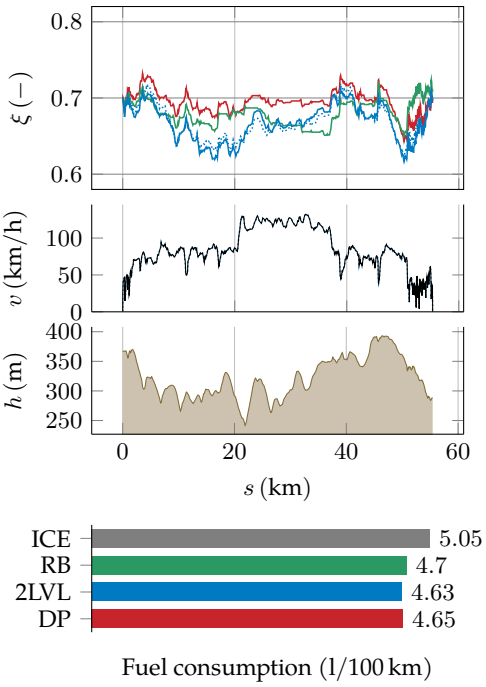

A Trip 0; prediction speed = actual speed

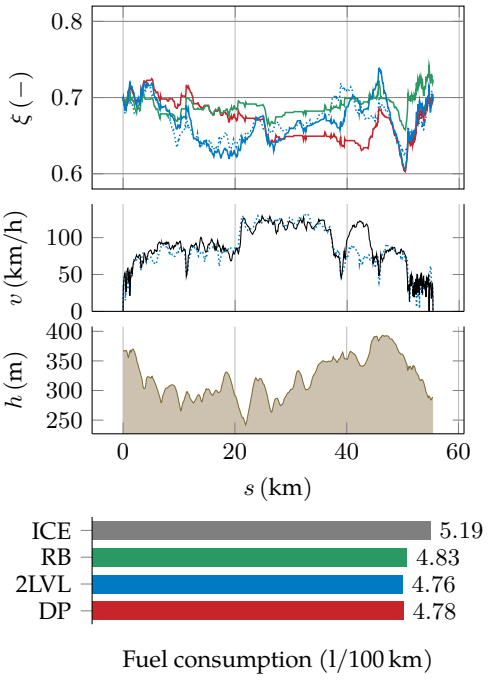

B Trip 1

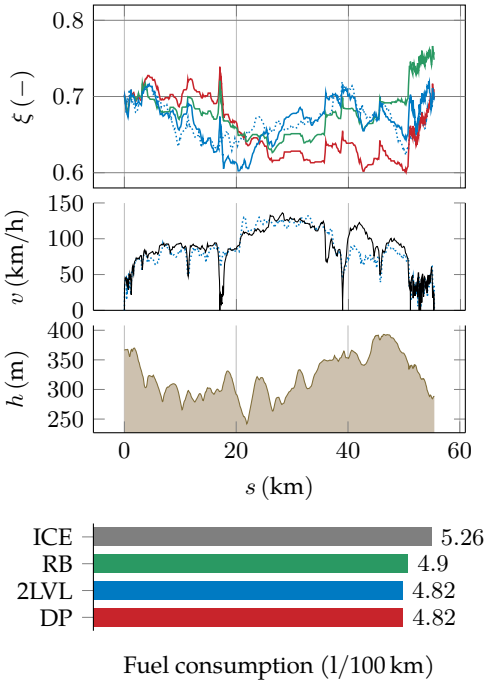

C Trip 2

Figure A.7 HEV Route 7 (Highway/City Return) results

Route 8 (Highway/Extra-urban)

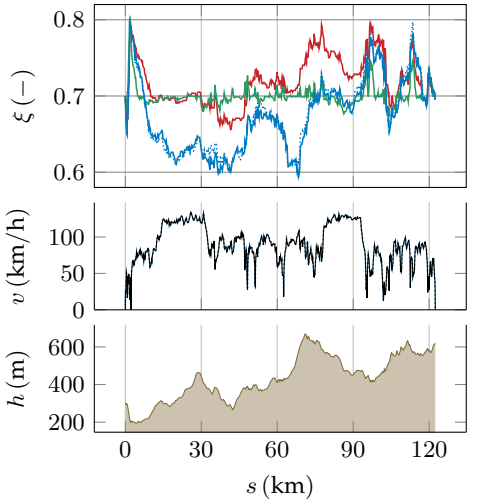

Fuel consumption (l/100 km)

A Trip 0; prediction speed = actual speed

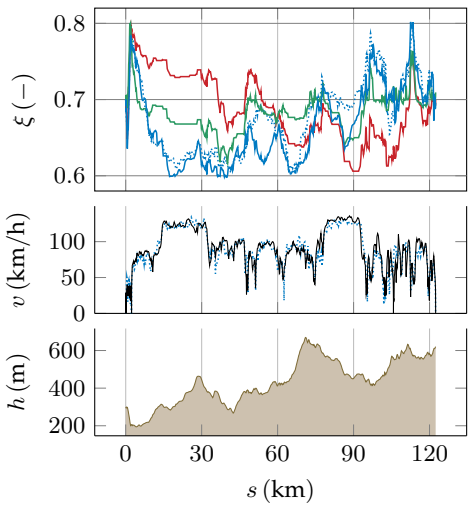

Fuel consumption (l/100 km)

B Trip 1

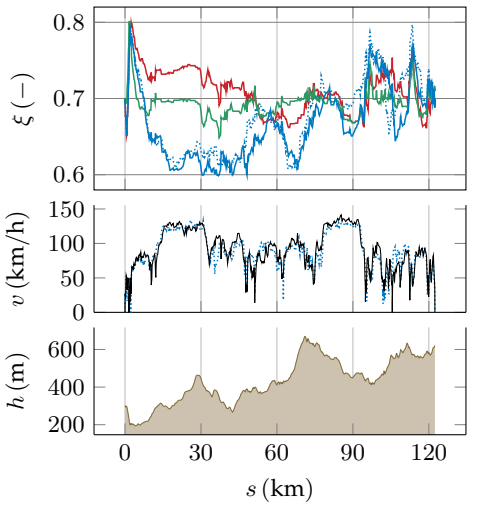

Fuel consumption (l/100 km)

C Trip 2

Figure A.8 HEV Route 8 (Highway/Extra-urban) results

Route 9 (Highway/Extra-urban Return)

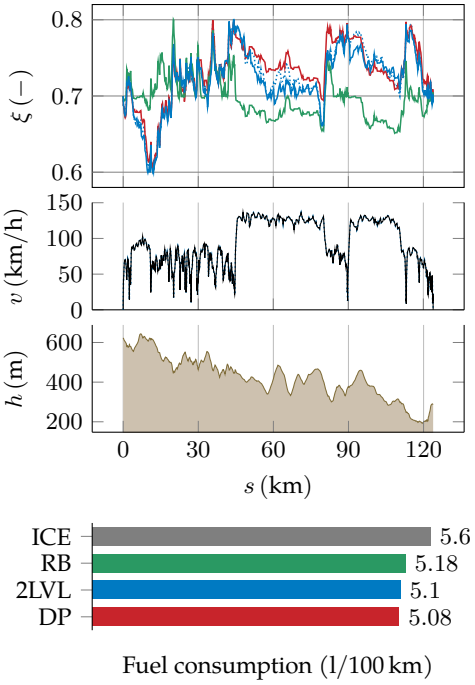

A Trip 0; prediction speed = actual speed

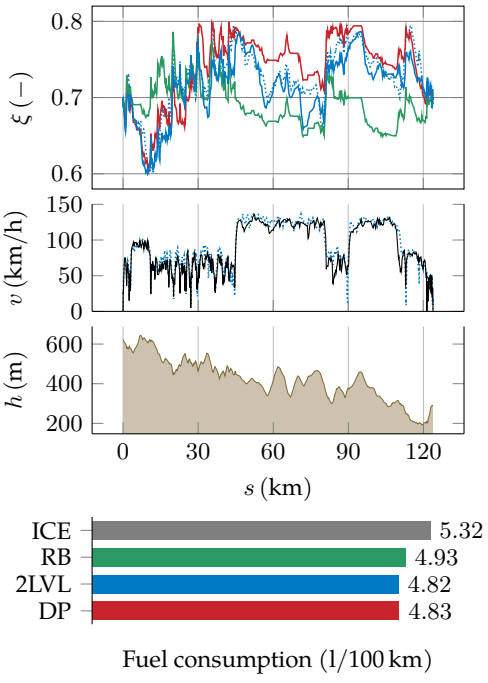

B Trip 1

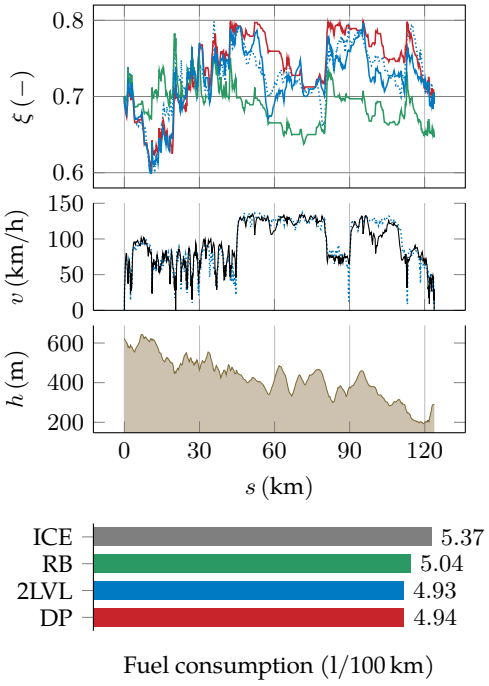

C Trip 2

Figure A.9 HEV Route 9 (Highway/Extra-urban Return) results

A.2 MHEV

Route 1 (City 1)

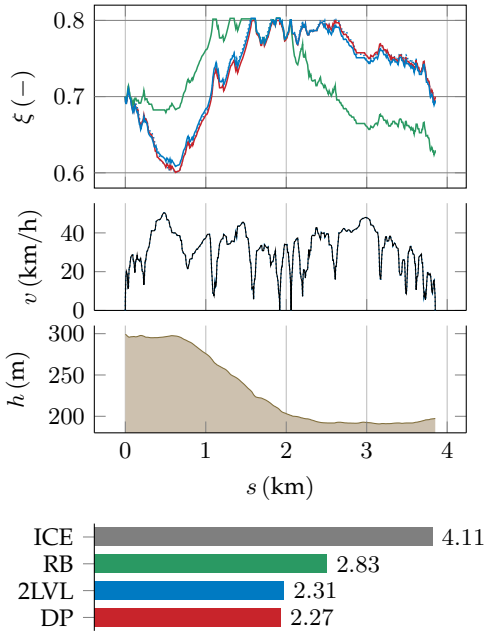

A Trip 0; prediction speed = actual speed

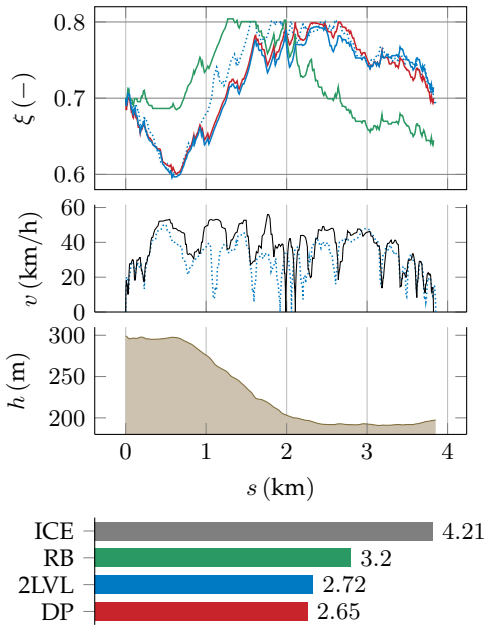

B Trip 1

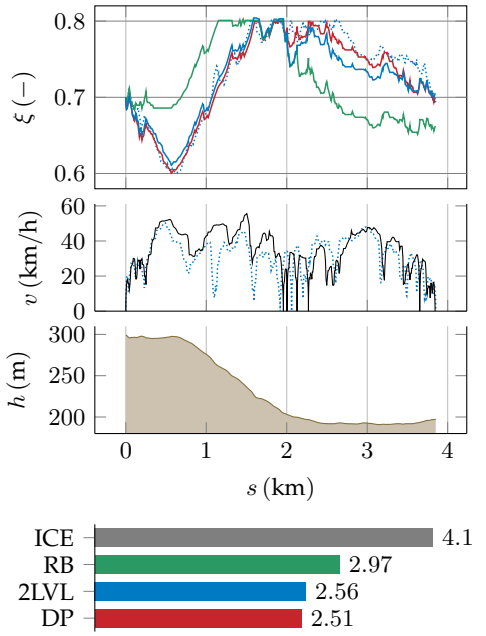

C Trip 2

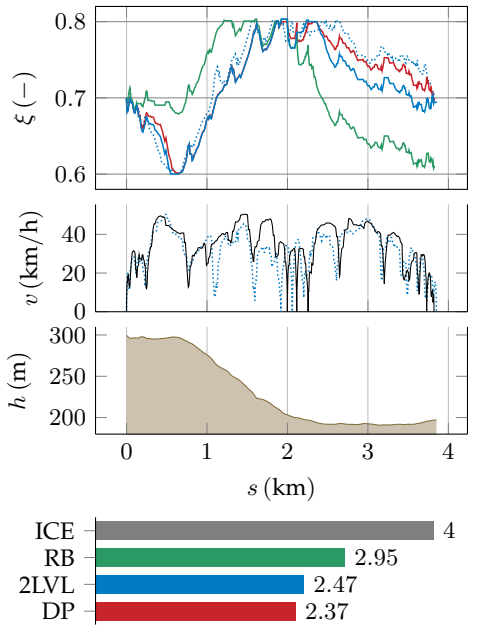

D Trip 3

Figure A.10 MHEV Route 1 (City 1) results

Route 2 (City 1 Return)

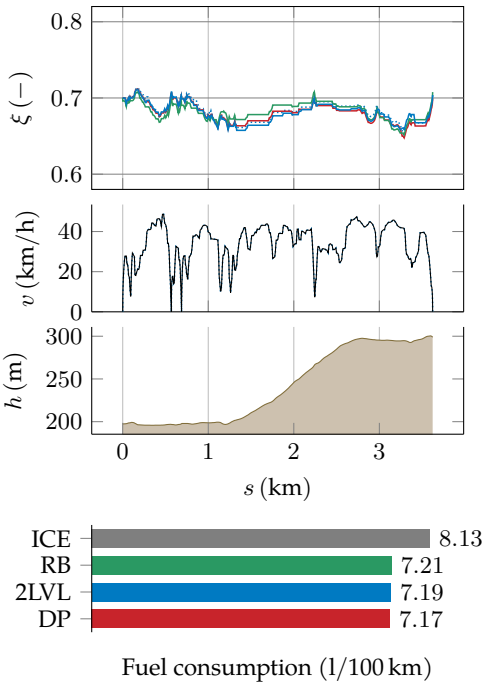

A Trip 0; prediction speed = actual speed

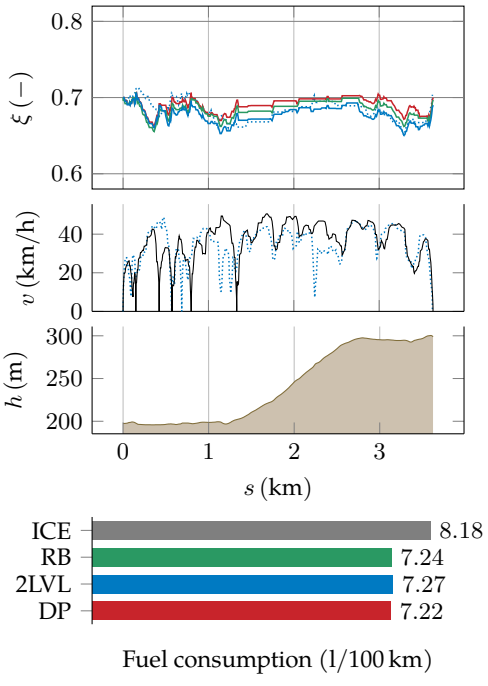

B Trip 1

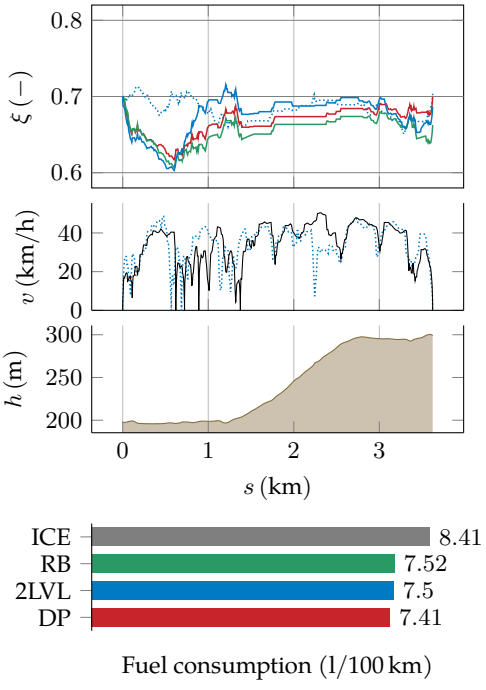

C Trip 2

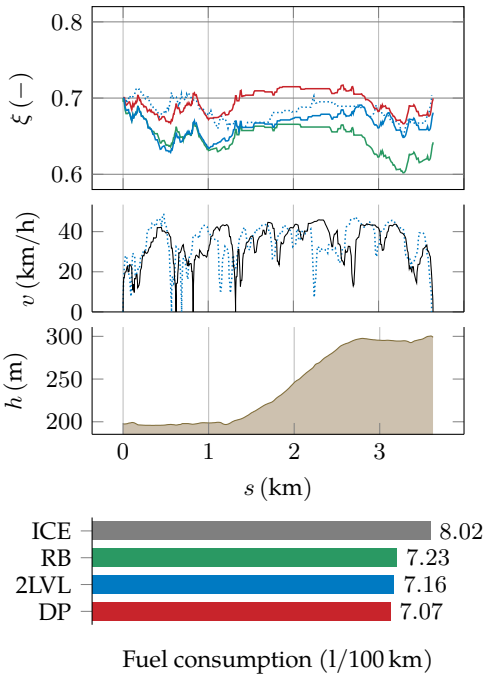

D Trip 3

Figure A.11 MHEV Route 2 (City 1 Return) results

Route 3 (City 2)

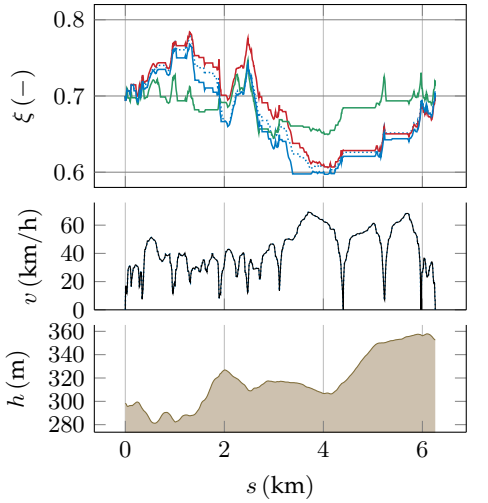

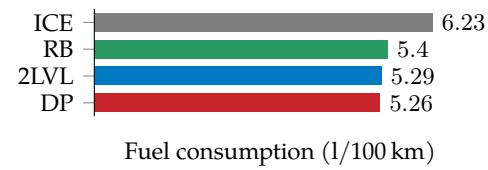

Fuel consumption (l/100 km)

A Trip 0; prediction speed = actual speed

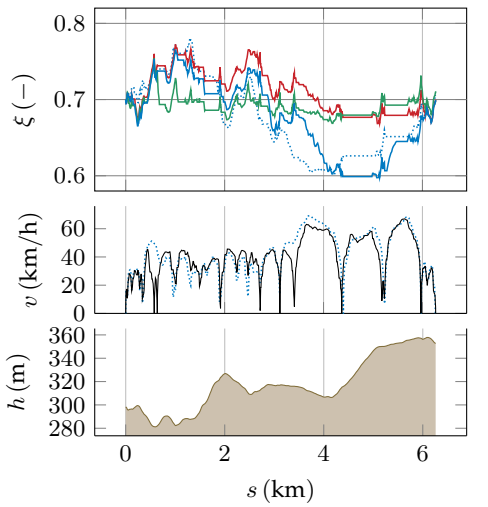

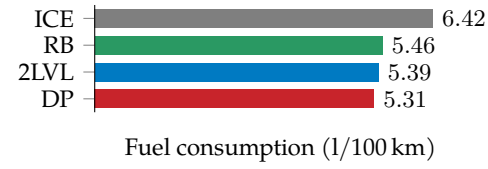

Fuel consumption (l/100 km)

B Trip 1

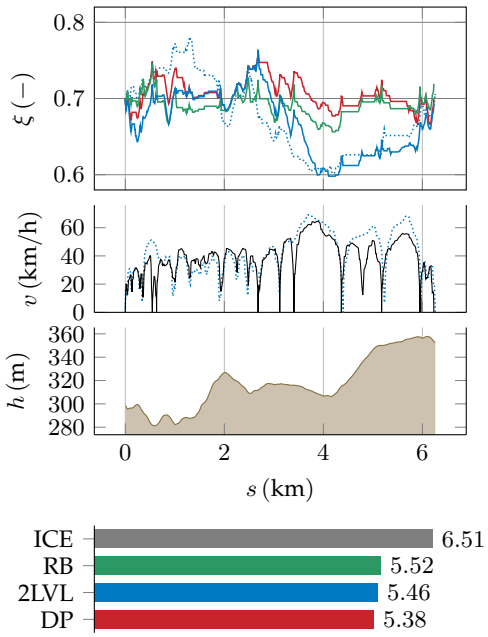

Fuel consumption (l/100 km)

C Trip 2

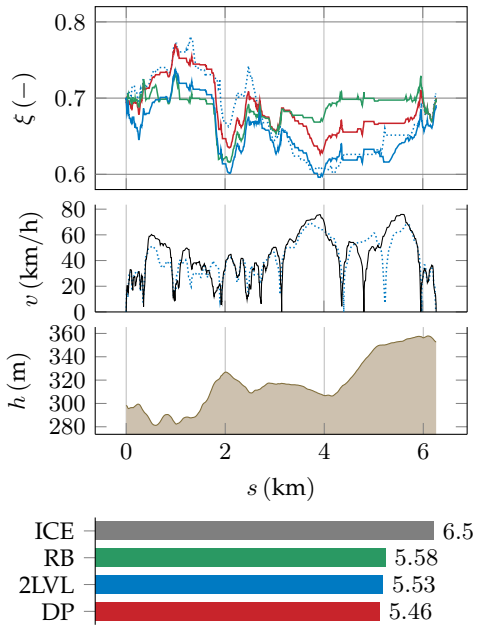

Fuel consumption (l/100 km)

D Trip 3

Figure A.12 MHEV Route 3 (City 2) results

Route 4 (City 2 Return)

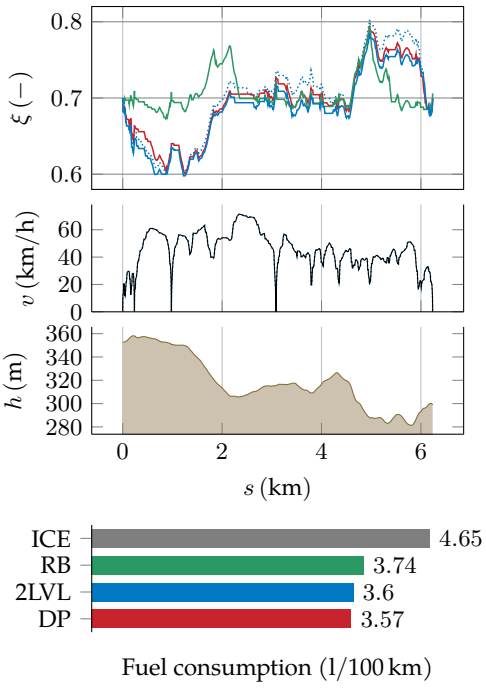

A Trip 0; prediction speed = actual speed

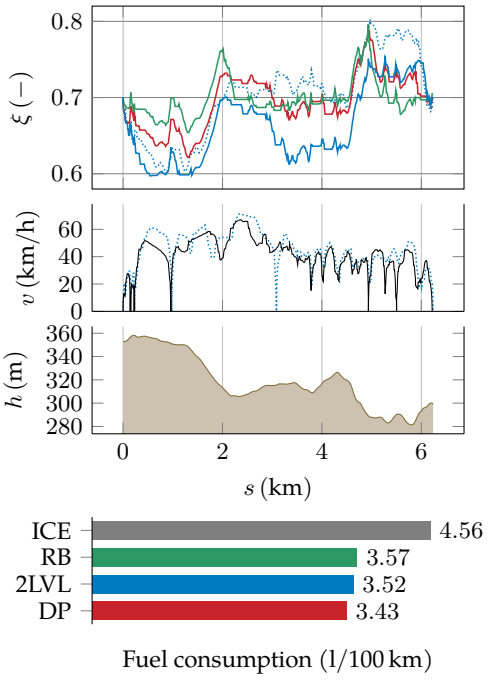

B Trip 1

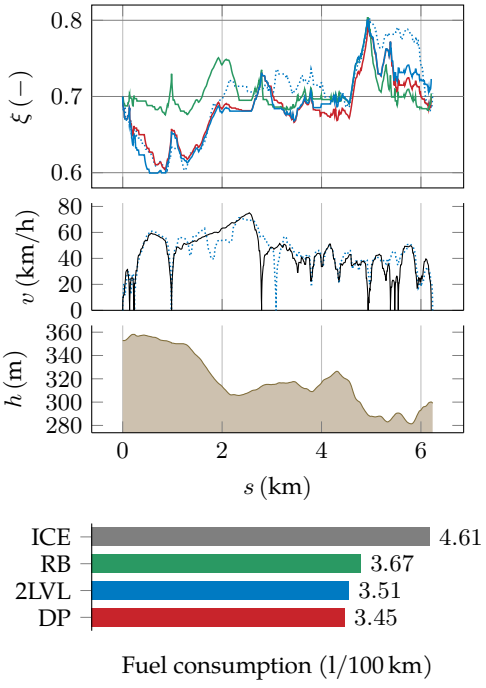

C Trip 2

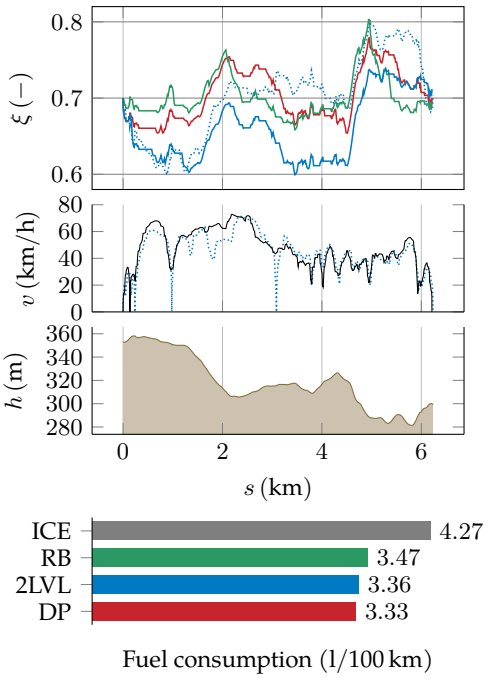

D Trip 3

Figure A.13 MHEV Route 4 (City 2 Return) results

Route 5 (Extra-urban)

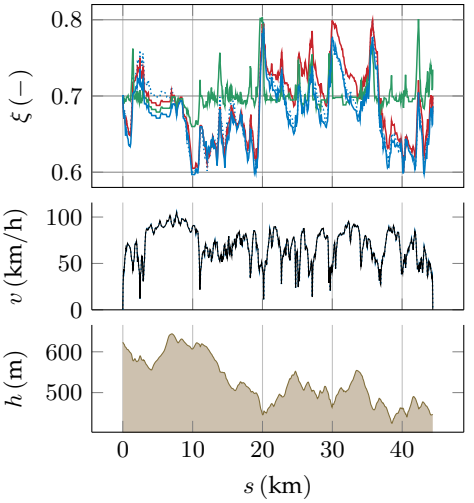

Fuel consumption (l/100 km)

A Trip 0; prediction speed = actual speed

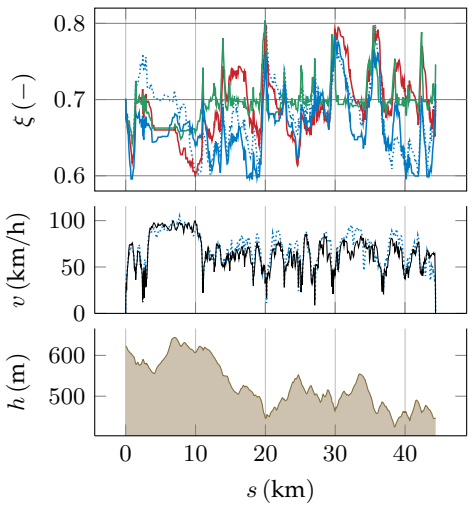

Fuel consumption (l/100 km)

B Trip 1

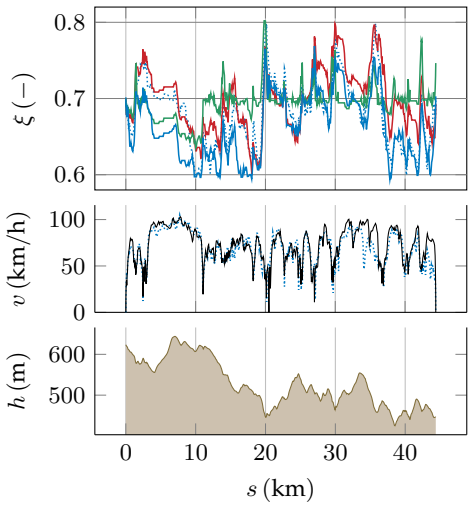

Fuel consumption (l/100 km)

C Trip 2

Figure A.14 MHEV Route 5 (Extra-urban) results

Route 6 (Highway/City)

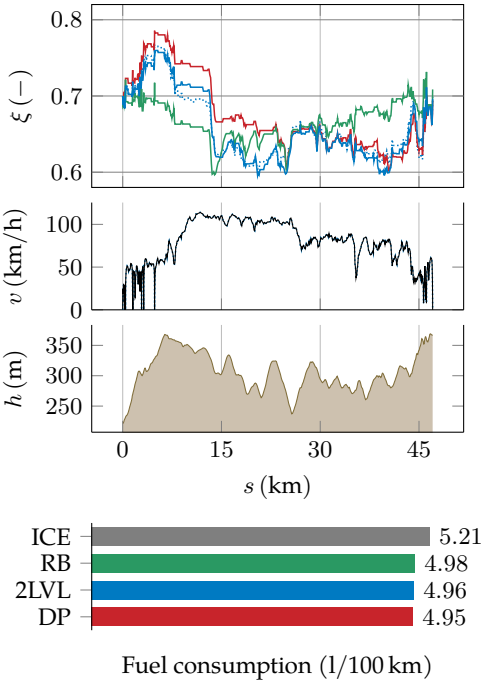

A Trip 0; prediction speed = actual speed

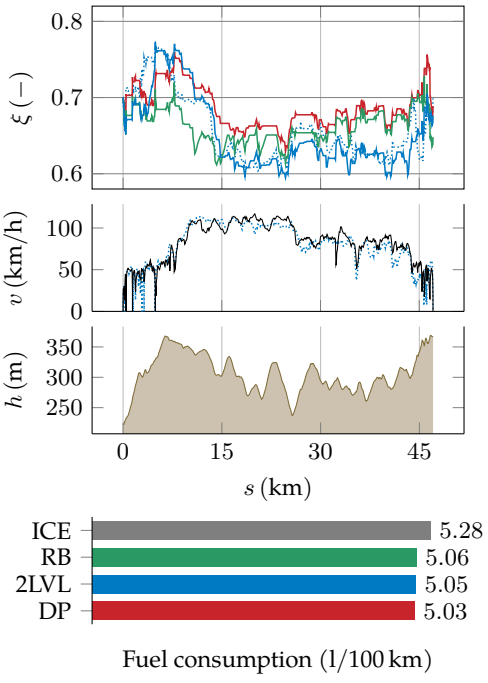

B Trip 1

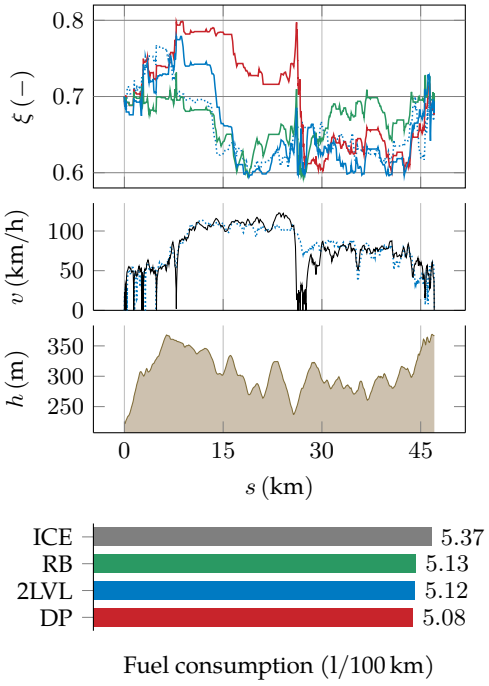

C Trip 2

Figure A.15 MHEV Route 6 (Highway/City) results

Route 7 (Highway/City Return)

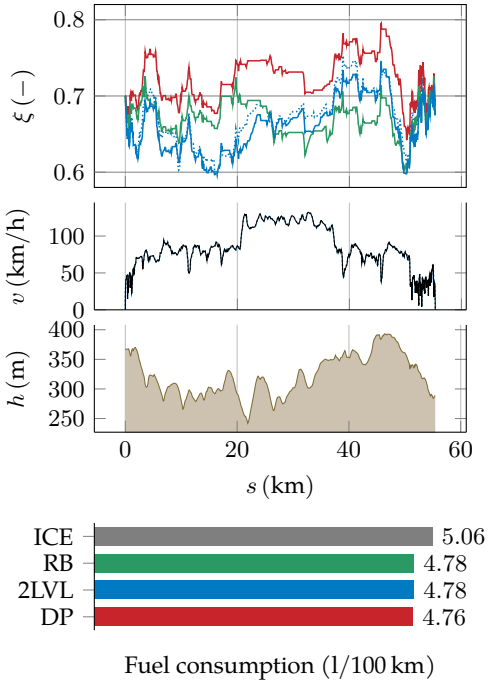

A Trip 0; prediction speed = actual speed

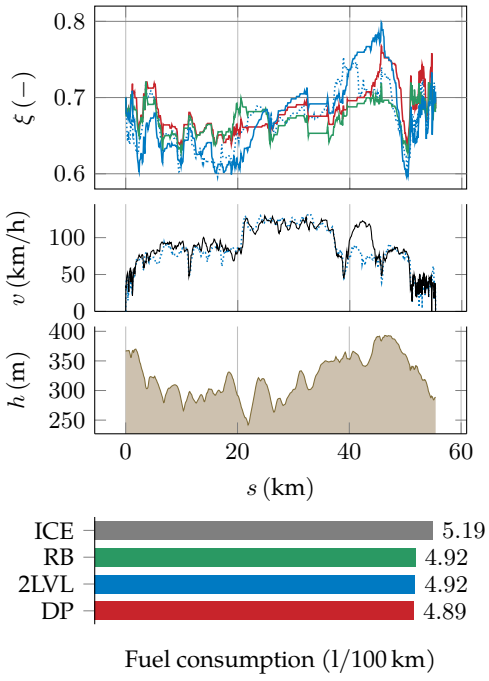

B Trip 1

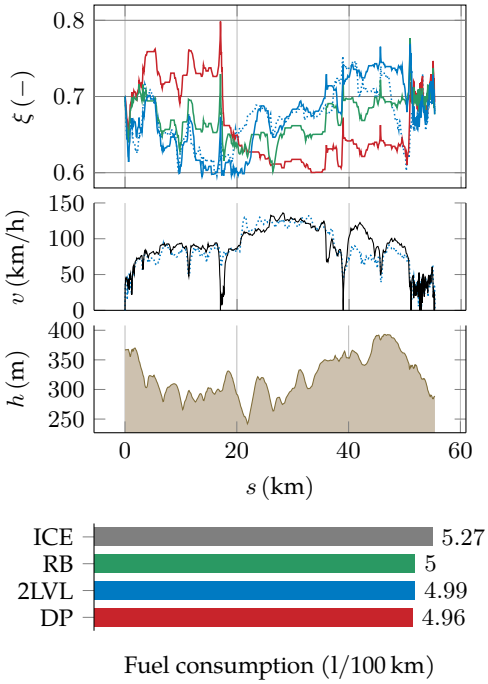

C Trip 2

Figure A.16 MHEV Route 7 (Highway/City Return) results

Route 8 (Highway/Extra-urban)

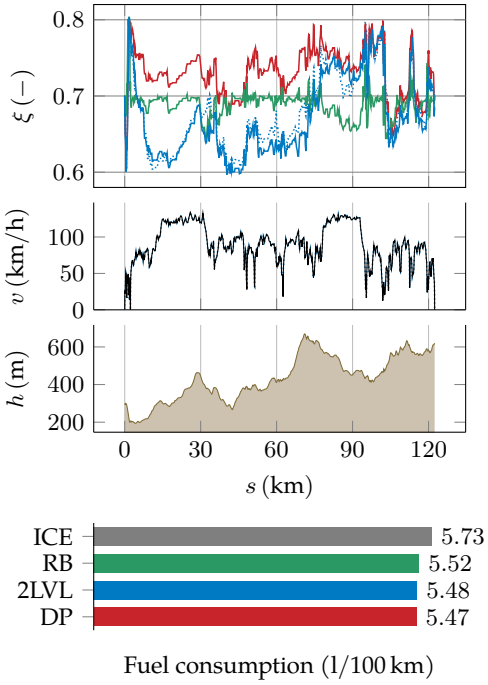

A Trip 0; prediction speed = actual speed

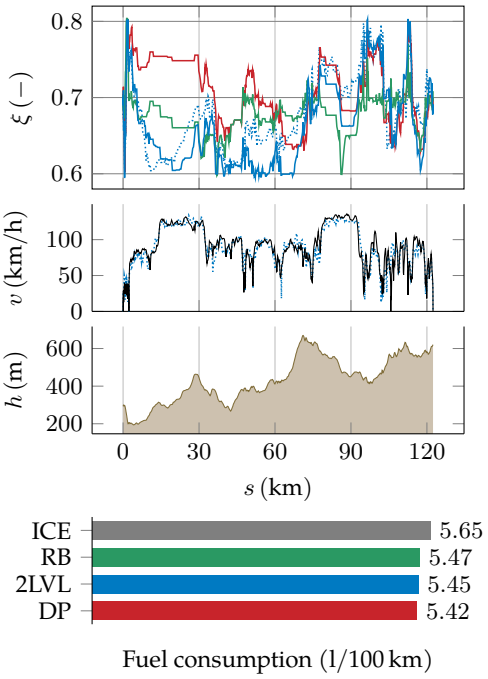

B Trip 1

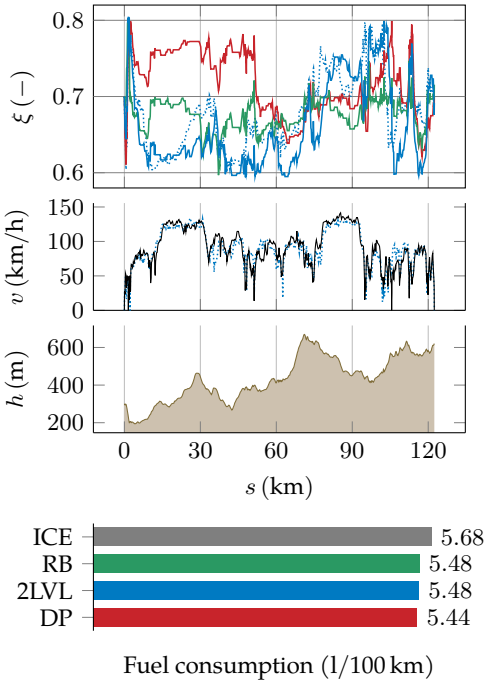

C Trip 2

Figure A.17 MHEV Route 8 (Highway/Extra-urban) results

Route 9 (Highway/Extra-urban Return)

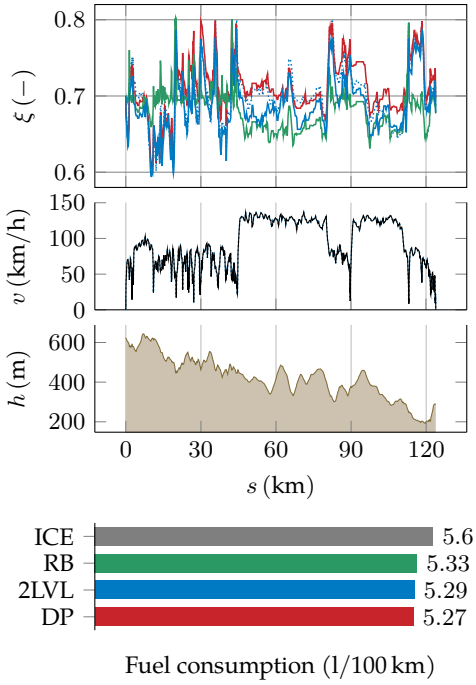

A Trip 0; prediction speed = actual speed

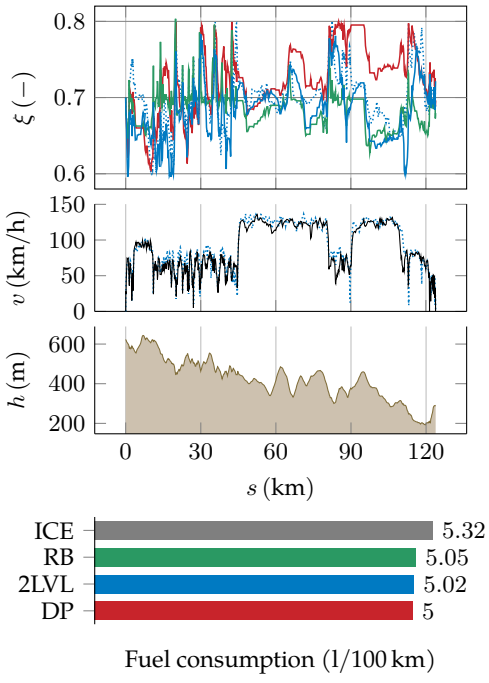

B Trip 1

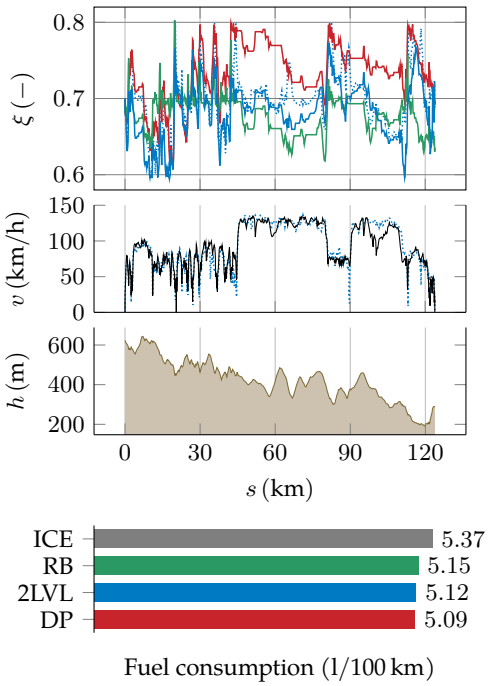

C Trip 2

Figure A.18 MHEV Route 9 (Highway/Extra-urban Return) results

A.3 PHEV

Route 6+7 (Highway/City & Return)

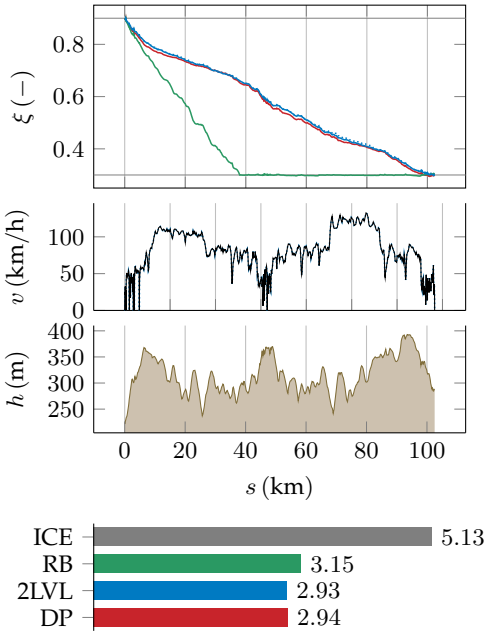

A Trip 0; prediction speed = actual speed

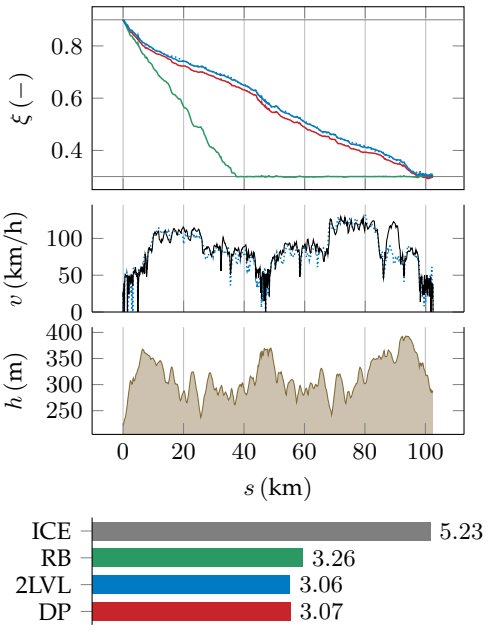

B Trip 1

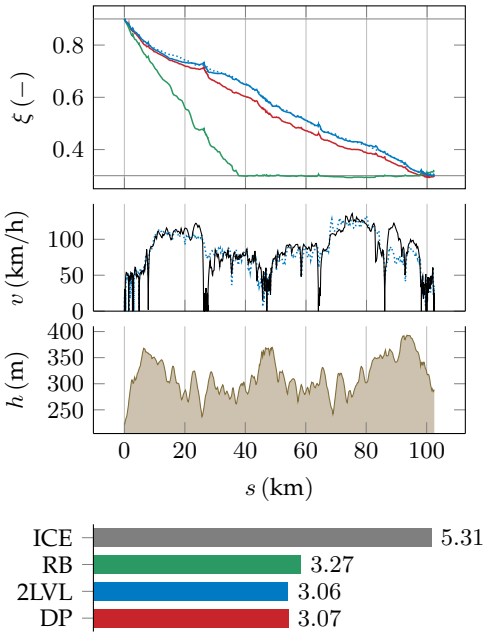

C Trip 2

Figure A.19 PHEV Route 6+7 (Highway/City & Return) results

Route 8 (Highway/Extra-urban)

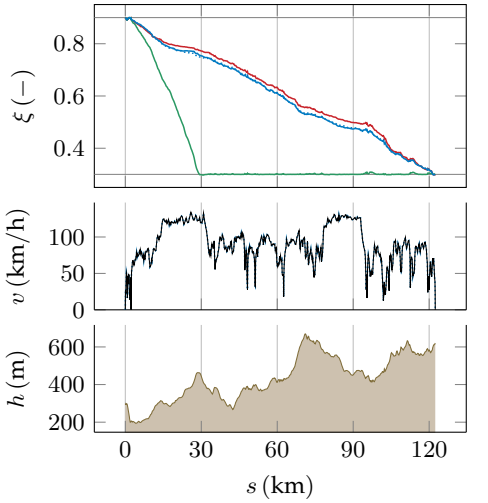

A Trip 0; prediction speed = actual speed

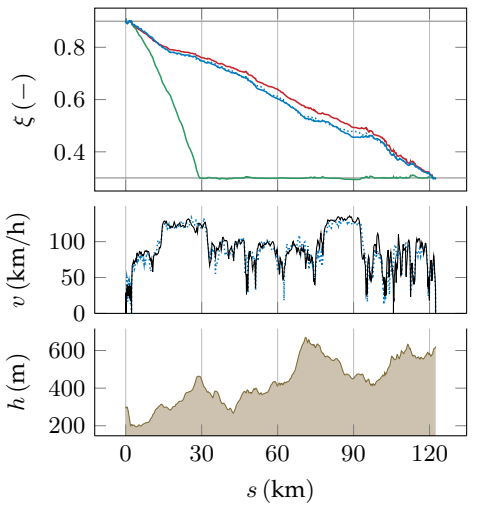

B Trip 1

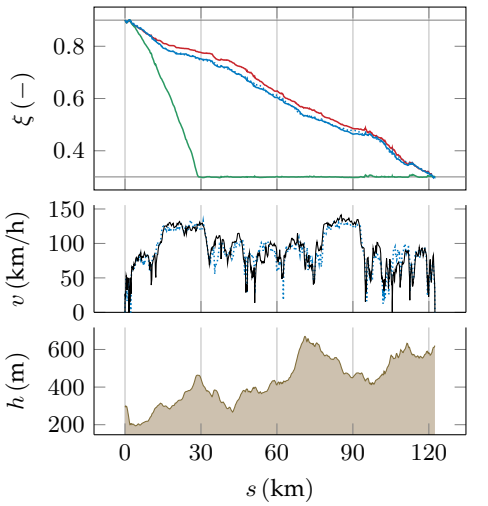

C Trip 2

Figure A.20 PHEV Route 8 (Highway/Extra-urban) results

Route 9 (Highway/Extra-urban Return)

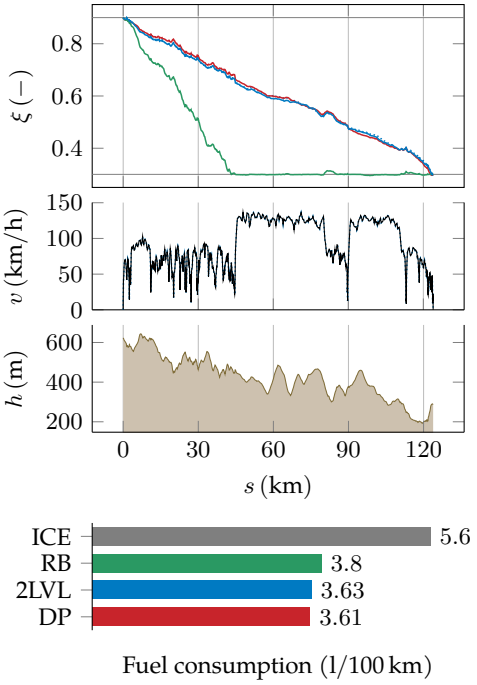

A Trip 0; prediction speed = actual speed

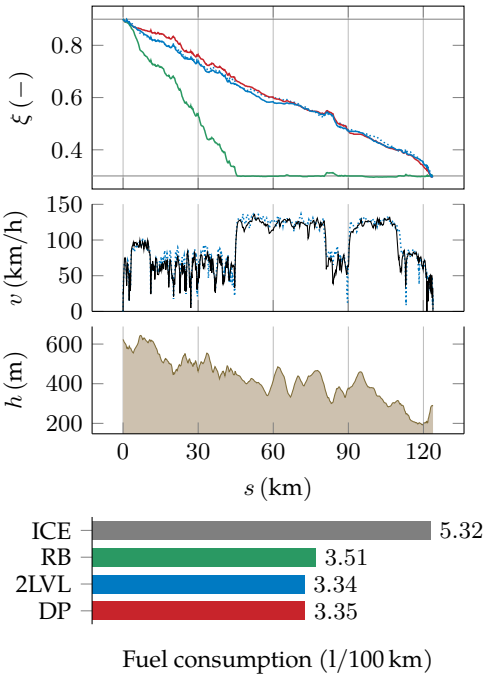

B Trip 1

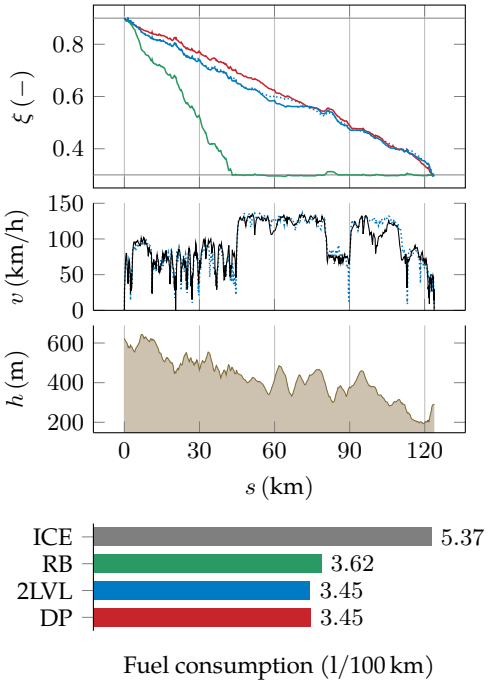

C Trip 2

Figure A.21 PHEV Route 9 (Highway/Extra-urban Return) results

Appendix B

PYTHON SIMULATION FILES

In a *.zip* file in the electronic version and on a CD in the physical version, simulation files written in Python are attached. This includes

- `simulation.py`, which is a simulation containing the algorithm for the proposed strategy, optimal solution using dynamic programming and for the rule-based strategy,
- `analysis.py`, which loads and plots results from the simulation,
- `hev_data.py`, which contains parameters of the hybrid vehicle configurations,
- `BSFC.py`, which contains the BSFC map for the ICE used in all tested vehicles.

All of the above was created and run by *Python v3.7.9*.

Appendix C

ROUTE AND TRIP DATA

All of the route and trip data is included in *.csv* files, as well as discretised *.p* files containing one-dimensional speed, time, distance and elevation arrays, that are the input to the simulation files from Appendix B.

Each route is characterised by elevation h dependent on distance s and each trip (drive) on a route by speed v dependent on time t.